(12) INTERNATIONAL APPLICATION PUBLISHED UNDER THE PATENT COOPERATION TREATY (PCT)

(19) World Intellectual Property Organization
International Bureau

(43) International Publication Date
2 February 2017 (02.02.2017)

WIPO | PCT

(10) International Publication Number
WO 2017/019577 A1

(51) International Patent Classification:
B01J 23/48 (2006.01) ***B01J 23/50*** (2006.01)
B01J 8/00 (2006.01) ***B01J 23/52*** (2006.01)
B01J 21/02 (2006.01) ***B01J 38/04*** (2006.01)

(21) International Application Number:
PCT/US2016/043783

(22) International Filing Date:
24 July 2016 (24.07.2016)

(25) Filing Language: English

(26) Publication Language: English

(30) Priority Data:
62/196,353 24 July 2015 (24.07.2015) US

(72) Inventors; and
(71) Applicants : **CHANDLER, Bert, D.** [US/US]; 157 Davis Ct., San Antonio, TX 78209 (US). **SAAVEDRA, Johnny** [US/US]; 701 NW 19th St. #411, Fort Lauderdale, FL 33311 (US). **PURSELL, Christopher, J.** [US/US]; 2211 Orange Blossom, San Antonio, TX 78247 (US).

(74) Agent: **NEVRIVY, Daniel, J.**; Nevrivy Patent Law Group P. L. L. C., 1000 Potomac Street, NW, Suite 200, Washington, DC 20007 (US).

(81) Designated States *(unless otherwise indicated, for every kind of national protection available)*: AE, AG, AL, AM, AO, AT, AU, AZ, BA, BB, BG, BH, BN, BR, BW, BY, BZ, CA, CH, CL, CN, CO, CR, CU, CZ, DE, DK, DM, DO, DZ, EC, EE, EG, ES, FI, GB, GD, GE, GH, GM, GT, HN, HR, HU, ID, IL, IN, IR, IS, JP, KE, KG, KN, KP, KR, KZ, LA, LC, LK, LR, LS, LU, LY, MA, MD, ME, MG, MK, MN, MW, MX, MY, MZ, NA, NG, NI, NO, NZ, OM, PA, PE, PG, PH, PL, PT, QA, RO, RS, RU, RW, SA, SC, SD, SE, SG, SK, SL, SM, ST, SV, SY, TH, TJ, TM, TN, TR, TT, TZ, UA, UG, US, UZ, VC, VN, ZA, ZM, ZW.

(84) Designated States *(unless otherwise indicated, for every kind of regional protection available)*: ARIPO (BW, GH, GM, KE, LR, LS, MW, MZ, NA, RW, SD, SL, ST, SZ, TZ, UG, ZM, ZW), Eurasian (AM, AZ, BY, KG, KZ, RU, TJ, TM), European (AL, AT, BE, BG, CH, CY, CZ, DE, DK, EE, ES, FI, FR, GB, GR, HR, HU, IE, IS, IT, LT, LU, LV, MC, MK, MT, NL, NO, PL, PT, RO, RS, SE, SI, SK, SM, TR), OAPI (BF, BJ, CF, CG, CI, CM, GA, GN, GQ, GW, KM, ML, MR, NE, SN, TD, TG).

Published:

- *with international search report (Art. 21(3))*
- *before the expiration of the time limit for amending the claims and to be republished in the event of receipt of amendments (Rule 48.2(h))*

(54) Title: CATALYST, PROCESS AND SYSTEM FOR THE SELECTIVE OXIDATION OF CARBON MONOXIDE

FIG. 1

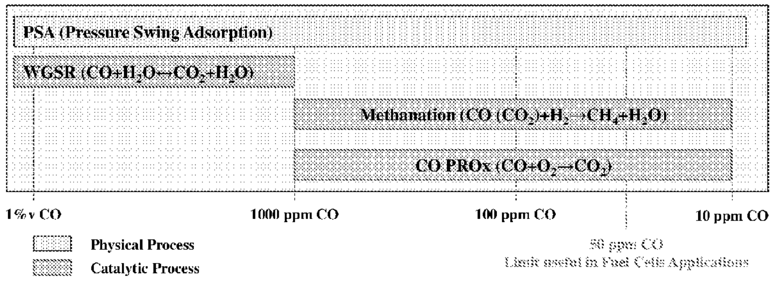

(57) Abstract: The present invention provides a preferential CO oxidation reaction (PROX) catalyst, comprising: a plurality of Au or Ag particles having a size ranging from about 0.5 to about 20 nm; a hydrophilic support in contact with the particles; and about 0.1 to about 10 monolayers of water on a surface of the support.

CATALYST, PROCESS AND SYSTEM FOR THE SELECTIVE OXIDATION OF CARBON MONOXIDE

STATEMENT OF FEDERALLY SPONSORED RESEARCH AND DEVELOPMENT

This invention was made with government support under grants CBET- 1160217 and CHE-1012395 awarded by the National Science Foundation. The government has certain rights in the invention.

FIELD OF THE INVENTION

The filed of the invention relates to purification of gases by CO oxidation, and catalysts and systems therefor.

BACKGROUND

The primary production method of hydrogen gas as an industrial feedstock is via steam reforming, wherein a mixture of methane and other light hydrocarbons is reacted with water at high temperature in the presence of a metal catalyst to produce H_2 and CO_2 according to reaction formula 1, shown below.

1) $CH_4 + 2\ H_2O \leftrightarrow CO_2 + 4H_2$

Incomplete reaction between the water and methane results in large amounts of CO in the initial reformate. This CO is further reacted with water by utilizing the water gas-shift (WGS) reaction shown in reaction formula 2, shown below, where CO and H_2O react to form CO_2 and H_2 in the presence of a catalyst. However, the WGS is an equilibrium reaction, and the best systems cannot lower the CO below 0.5-1.0% or 5,000-10,000 ppm, which is much higher than the <50 ppm concentration needed to prevent poisoning of the downstream catalysts.

2) $CO + H_2O \leftrightarrow CO_2 + H_2$

CO is also a common contaminant in other gas feedstocks, particularly those produced through partial oxidation chemistries. CO is a well-known poison for many industrial reactions, and as such must be removed from the gas prior to downstream processing. In particular, many catalytic processes are highly sensitive to CO. The CO strongly binds to the catalyst in place of the desired substrate resulting in partial or total deactivation of the reaction. Some processes that require CO-purified gaseous feedstocks include:

H_2/N_2 streams used in ammonia synthesis (Haber-Bosch Process)- 140 million tones NH_3 produced/year

Ethylene streams used in reactors containing Pt/Pd based catalysts (<2.5 ppm)

Hydrogen streams used in alkane reforming, hydrotreating, and hydroprocessing

Methane used in reforming processes

Preparation of UHP gases O_2, He, Ar, N_2, CH_4, H_2, etc.

Fuel Cells (10-50ppm)

As such, removal of CO from the presence of other gases, especially hydrogen is required for these processes and many others.

Current methods of CO purification include adsorption on solids, separation by membranes, liquid-gas scrubbers, and catalytic methods (Figure 1). Removal of CO from gases via adsorption utilizes the high binding affinity of CO on materials such as powder activated carbon (PAC) or other adsorbents to purify gas mixtures. Pressure swing adsorption (PSA) is the most common adsorption technique and is one of the most mature technologies for CO removal from gas streams.

However, adsorption separations require operating the process at high pressure (typically between 5 and 10 atm) to achieve high removal efficiencies. High pressure results in the physical attrition of the sorbent particles, which diminishes their adsorption capacity and necessitates the inclusion of additional beds in the process. PSA is a capital-intensive process and has low volume throughput, making it cost effective only in low volume, specialty gas separations. Further, PSA is a relatively slow process, which reduces hydrogen throughput and requires substantially higher capital expenditures for multiple large separation units.

Separation membranes have also been adapted to eliminate CO. Currently, the most viable membranes allow only one small chemical species, such as hydrogen through the membrane while all the other reformate gases are retained. Membranes are constructed of either inorganic ceramics or precious metal alloys of Pd. In comparison to PSA, these systems typically operate with 40 – 50 psi differential pressure at temperatures up to about 200 °C making them inefficient and/or expensive.

Scrubbers employ liquid – gas interactions to remove the contaminants. While proper selection of stripping agent allows these processes to be very selective, they are complicated systems that use specialty chemicals. Additionally, the units require multiple steps to transfer the contaminant from gas phase to liquid, then from liquid back to gas phase, which is ultimately vented. Scaled up processes have found limited applications in the hydrogen purification industry.

For purification after the WGS, the three physical separation methods discussed above can be used to selectively remove CO without impacting the H_2 yield of the reformate and WGS reactions. However, these methods are expensive and are often replaced by methanation units. Methanation removes CO by reacting with H_2 in the presence of a catalyst to form CH_4 and H_2O; this is the reverse process of steam reforming, as shown in reaction formula 3, shown below.

3) $CO + 3H_2 \leftrightarrow CH_4 + H_2O$

Methanation is commonly used to remove CO from the hydrogen feed in ammonia synthesis (e.g. the Haber-Bosch process). However, methanation requires relatively high temperatures (300° C) to be efficient and is unselective for CO, resulting in substantial reaction between hydrogen and the CO_2 that is also typically present in the feed. Most importantly, methanation consumes a substantial portion of the hydrogen that has been produced via the steam reforming and WGS reactions. The combination of all these factors typically results in loss of 3-10% of the produced hydrogen and requires this secondary methane to either be recycled or used as fuel for high temperature units. While methanation processes successfully remove CO, they result in substantial energy losses (nominally 5-15%) for the overall hydrogen production and purification process.

Another catalytic reaction with the potential for removing low concentrations of CO from gas streams is the preferential CO oxidation reaction (PROX) shown in reaction formula 4, shown below.

4) $CO + \frac{1}{2} O_2 \leftrightarrow CO_2$

However, the CO oxidation reaction is in competition with the hydrogen oxidation reaction shown in reaction formula 5, shown below.

5) $H_2 + \frac{1}{2} O_2 \leftrightarrow H_2O$

The primary advantage that PROX has over methanation is that the amount of oxygen introduced to the system can be controlled, thus limiting hydrogen losses. Typically 1% O_2 is added to a gas feed to remove 1% CO. This ratio can be adjusted to balance CO removal and H_2 losses (higher O_2 pressures result lower end amounts of CO, but greater H_2 losses. This results in a reaction that places strict performance demands on the PROX catalyst, which needs to maximize CO oxidation activity while limiting H_2 oxidation activity, even when H_2 concentrations are orders of magnitude higher than CO concentrations.

The ideal PROX catalyst must have high activity at low temperatures (<150 °C), preferably below 100 °C, and most preferably below 50 °C. The catalyst must also be highly selective for CO oxidation over H_2 oxidation, with at least 50% of the consumed oxygen used to oxidize CO, preferably more than 70% of the consumed oxygen used to oxidize CO, and most preferably more than 85% of the consumed oxygen used to oxidize CO. A reduction of the CO to below 10 ppm or below 1 ppm with high O_2 selectivity (> 50%) will make CO PROX catalysts viable for the purification of H_2 for fuel cells, ammonia synthesis, and other processes where CO presents problems in downstream feeds.

The ability to operate over a wide temperature range is desirable as well. For fuel cell applications, having high PROX activity at temperatures near the operating temperature of the fuel cell (70-90 °C) is highly desirable. In other applications, the PROX catalyst may be required to operate at approximately 20-30 °C. The ability to operate CO PROX over a wide range of temperatures, particularly temperatures close to the temperature required for either preceding or subsequent processing steps, may eliminate the necessity of cooling the gas streams and provide a substantial economic advantage.

These requirements exclude the use of most metal catalysts for the PROX reaction. Platinum, for example, requires temperatures greater than 200 °C in order to open surface sites for O_2 binding and activation required for CO oxidation. Another drawback is that most noble metal PROX catalysts are also excellent hydrogenation catalysts that bind and activate H_2 at low temperatures. Particularly in the presence of large amounts of H_2, the competitive reaction between O_2 and H_2 results in substantial H_2 loss and exceedingly poor selectivity at high CO conversions. Operating at lower temperatures typically requires much larger amounts of metal in the catalyst, which can further exacerbate these selectivity shortcomings.

As an alternative to noble metals, materials composed of mixed copper and cerium oxides have been examined as CO PROX catalysts; however, these materials are poisoned by CO_2 and H_2O, which are common impurities in the hydrogen and light hydrocarbon feeds. Carbon dioxide is also the reaction product and is therefore extremely difficult to remove as the reaction proceeds. In order to avoid catalyst poisoning and deactivation by H_2O/CO_2, the CuO_x/Ce_2O_3 catalysts must be operated in a very narrow temperature window. Achieving acceptable activity and selectivity in this temperature window remains a substantial technical challenge for these catalysts.

In contrast, gold based PROX catalysts have exceptional CO oxidation activity (high reaction rates) at low temperatures (<100 °C) and have exceedingly poor hydrogenation activity relative to traditional noble metal catalysts. This makes Au the most promising catalyst for the CO PROX reaction. Strategies to optimize Au catalysts used in CO PROX have included: adjusting metal particle size, incorporating heterometals in order to increase O_2 activation activity, modifying the metal oxide identity used as support by the combination of metal oxides with the primary goal to increase the selectivity towards CO oxidation compared to H_2 oxidation (using mixed/combined oxides), and varying the metal oxide morphology (porous/nanoscale metal oxides). Unfortunately, state of the art Au catalysts have not been able to consistently achieve the activity and selectivity necessary to achieve CO PROX performance adequate for industrial requirements.

In order to solve these problems, a highly active, highly selective PROX catalyst is desirable. Catalysts should desirably have sufficient activity and selectivity over a wide range of reaction conditions to compensate for various operating conditions and changes that occur during the catalyst and process lifetime.

This background information is provided for informational purposes only. No admission is necessarily intended, nor should it be construed, that any of the preceding information constitutes prior art against the present invention.

SUMMARY

It is to be understood that both the foregoing general description of the embodiments and the following detailed description are exemplary, and thus do not restrict the scope of the embodiments.

The inventors have carried out a careful study of process variables (experimental apparatus in Figure 2) and have found why existing PROX catalysts do not achieve the performance goals necessary for developing PROX as a viable method for CO removal systems. This will allow for PROX reactors to be used in a wide variety of commercial applications, some examples of which are shown in Figure 3. In one embodiment, the inventors have found that to best protect the downstream catalysts, a PROX catalyst should desirably achieve an outgoing CO concentration of 50 ppm or less (preferably 10 ppm or lower); this is a CO conversion of 99.5% or higher. Furthermore, changes in operating conditions that naturally occur under typical reaction conditions can be taken into consideration in designing PROX catalysts.

In one embodiment, a preferential CO oxidation reaction (PROX) catalyst is provided, comprising:

a plurality of Au or Ag particles having a size ranging from about 0.5 to about 20 nm;

a hydrophilic support in contact with the particles; and

about 0.1 to about 10 monolayers of water on a surface of the support.

In another embodiment, a preferential CO oxidation reaction (PROX) catalyst is provided, which is prepared by process comprising:

removing one or more of an adsorbed carbonate, bicarbonate, carboxylate, organic carbonate, adsorbed hydrocarbon, or a mixture of two or more thereof from a surface of a supported catalyst, the supported catalyst comprising a plurality of Au or Ag particles having a size ranging from about 0.5 to about 20 nm and a hydrophilic support in contact with the particles; and

simultaneously or thereafter adsorbing about 0.1 to about 10 monolayers of water on a surface of the support.

In one embodiment, a method for preparing or regenerating a preferential CO oxidation reaction (PROX) catalyst is provided, comprising:

removing one or more of adsorbed carbonate, bicarbonate, carboxylate, organic carbonate, adsorbed hydrocarbon, or a mixture of two or more thereof from a surface of a supported catalyst, the supported catalyst comprising a plurality of Au or Ag particles having a size ranging from about 0.5 to about 20 nm and a hydrophilic support in contact with the particles; and simultaneously or thereafter adsorbing about 0.1 to about 10 monolayers of water on a surface of the support.

In one embodiment, a process for oxidizing CO is provided, comprising:

contacting the catalyst and a feed gas comprising CO, O_2 and H_2O at a temperature ranging from about 0 to about 300 °C, to thereby oxidize the CO.

In one embodiment, a process for oxidizing CO is provided, comprising:

contacting the catalyst and a feed gas comprising CO, O_2 and H_2O at a temperature ranging from about 0 to about 300 °C, to thereby oxidize the CO and produce a first product gas comprising 1000 ppm or less of CO;

optionally, adding or removing one or more of O_2, H_2O, or both to or from the first product gas, to optionally form a second feed gas;

contacting the first product gas or second feed gas with a second catalyst at a temperature ranging from about 0 to about 300 °C, to thereby oxidize said CO.

In one embodiment, a process for oxidizing CO is provided, comprising:

contacting the catalyst and a feed gas comprising CO, O_2 and H_2O at a temperature ranging from about 0 to about 300 °C, to thereby oxidize the CO; wherein the catalyst is distributed along a catalyst bed having an upstream portion and a downstream portion, and wherein the temperature of the upstream portion is higher than the temperature of the downstream portion.

In one embodiment, a treatment method is provided for producing highly active Gold based catalysts to be used in the preferential CO oxidation reaction, improving the catalyst resistance to deactivation, and optimizing the use of catalytic metal by allowing for high gas throughput.

In one embodiment, a technology based on a dual-step process is provided for performing the CO oxidation reaction with increased activity (elevated throughput), more efficient use of the metal (high turnover rates), increased stability (resistance to deactivation over time), and increased selectivity (avoiding undesired side reactions, H_2 oxidation, methanation, WGS, etc).

In one embodiment, a process is provided for the flexible operation of the preferential CO oxidation reaction, allowing for high performance under a wide variety of process operating conditions, including temperature, feed content of water and CO_2.

In one embodiment, a process is provided that allows for the purification of a wide variety of gases including, but not limited to, hydrocarbon streams (C1-C10 alkanes, alkenes, and functionalized hydrocarbons) and permanent gases (N_2, O_2, H_2, Air, He, Ar, etc).

In some embodiments, provided are a composition of Au nanoparticles for CO oxidation, a process for synthesizing the same catalyst, and processes for using the same catalyst for purifying gas streams by converting CO to CO_2. In some embodiments, catalysts and processes are provided that are capable of selectively oxidizing CO in the presence of other gases including H_2, N_2, methane, ethane, and others for the purification of said gas streams under a variety of conditions.

In some embodiments, provided is a compositionally controlled catalyst capable of removing carbon monoxide (CO) from gas mixture via oxidation of CO to carbon dioxide (CO_2) by using supported gold nanoparticle catalysts with specific ratios of water content in the reactive gas mixture and on the surface of the catalyst. Careful control over the amount of water adsorbed on the catalysts generates a new composition of matter that allows for high CO oxidation activity while limiting the oxidation of hydrogen, hydrocarbons, and other molecules. This can be suitably applied to the purification of non-condensable hydrocarbon streams (C1-C3 alkanes and alkenes) and permanent gases (N_2, O_2, H_2, Air, He, Ar, etc). The resulting purified gases can be used in applications and processes that are sensitive to the amount of CO in the feed gas, such as fuel cells and processes employing metal catalysts. This can also be used in the purification of hydrogen and light hydrocarbons and may be used as a replacement for methanation processes in hydrogen production and purification, particularly for ammonia synthesis, petroleum refining, and the production of high purity gases.

In some embodiments, provided is a compositionally controlled catalyst capable of removing carbon monoxide (CO) and oxygen (O_2) from gas mixture via oxidation of CO to carbon dioxide (CO_2) by using supported gold nanoparticle catalysts with specific ratios of water content in the reactive gas mixture and on the surface of the catalyst, followed by a secondary catalyst bed containing a hydrogenation or oxidation catalyst for reacting the remaining O_2 with the feed gas (e.g. H_2). This can be suitably applied to the purification of non-condensable hydrocarbon streams (C1-C3 alkanes and alkenes) and reactive permanent gases (O_2, H_2, Air, etc). The resulting purified gases can be used in applications and processes that are sensitive to the amount of CO and O_2 in the feed gas, such as fuel cells and processes employing metal catalysts. This can also be used in the purification of hydrogen and light hydrocarbons and may be used as a replacement for methanation processes in hydrogen production and purification, particularly for ammonia synthesis, petroleum refining, and the production of high purity gases.

Other objects, features and advantages of the present invention will become apparent from the following detailed description. It should be understood, however, that the detailed description and the specific examples, while indicating specific embodiments of the invention, are given by way of illustration only, since various changes and modifications within the spirit and scope of the invention will become apparent to those skilled in the art from this detailed description.

BRIEF DESCRIPTION OF THE DRAWINGS

The skilled artisan will understand that the drawings, described below, are for illustration purposes only. The drawings are not intended to limit the scope of the present teachings in any way.

Fig 1. Process options and typical functional limits for reducing the concentration of CO in gaseous streams.

Fig 2. Experimental apparatus for catalyst testing. Reaction conditions: 5-120 mg of catalyst diluted in 1200 mg of SiC, total flow 140-180 mL/min, moisture content 0-4000 Pa. Mass flow controllers (MFC) allow for the mixing the gases (N_2, H_2, 5% CO/He, O_2) in various proportions.

Fig 3. Some potential applications of CO PROx in gas purification purification processes

Fig 4. Effect of thermal treatments and carbonate deposition during CO oxidation on the water adsorption capacity of a Au/TiO_2 catalyst. The H_2 treatment involved heating under flowing H_2 (100mL/min, 250 ºC, 16 h) (◍); regeneration refers to slowly cooling the catalyst immediately after the H_2 treatment under H_2O/N_2 (4000 Pa H_2O, 20 ºC, 12 hr, 100 mL/min N_2) (◍). The "carbonated" catalyst was operated under CO oxidation conditions (1% CO, 20% O_2, 20 ºC, 1 h, Dry gas) (■) and was again regenerated (○).

Fig 5. Dual step process for the preferential oxidation of CO in gas mixtures.

Key to Figure 5:

A: Inlet Feed

B, D: Drain

C: Humidity controlled inlet to upstream reaction bed

D: Effluent from upstream reaction bed (0-1000 ppm CO)

E: Drain

F: Humidity controlled inlet to downstream reaction bed

G: Process effluent (0-100 ppm CO)

32, 38: Heat exchanger

34, 40: Water saturator (humidifier / dryer)

36: Upstream reactor with catalyst bed

42: Downstream reactor with catalyst bed

Fig 6. PROX performance and deactivation of Au/Al_2O_3 with water in the feed (1% CO, 1.4% O_2, 60% H_2, balance He). (A) Performance comparison between Au/Al_2O_3 operated at 40 °C and 80 °C (various space velocities, 1-20 Torr H_2O, see Fig. 7) and literature reports (Table 8). When feed water content and space velocity are properly controlled, this Au/Al_2O_3 catalyst far surpasses literature reports for CO PROX performance, easily achieving literature benchmarks. (B) CO conversion and (C) O_2 selectivity during 10 hour experiments with Au/Al_2O_3 at 80 °C. When water is removed, selectivity immediately drops; CO oxidation activity also drops, but more slowly. Thus, maintaining sufficient water on the catalyst prevents deactivation over 10 hours, and is critical for optimum catalyst performance. CO conversion measurement errors are typically ± 0.02%; O_2 selectivity measurements are typically ± 5%.

Fig. 7. PROX reactivity over Au/Al_2O_3 at high conversion. Panel (A) shows CO slip versus P_{H2O} at several space velocity values; CO slip ≡ concentration of CO in the reactor outlet. At 40 °C, activity (low CO slip) and selectivity (~ 90%) are maximized at ~ 5 Torr added water; CO oxidation activity increased at 80°C, but the reaction was less sensitivity added water. Panel (B) shows CO slip versus SV for the data in panel A; panel (C) shows O_2 selectivity versus SV for the data in panel (A). The data demonstrate controlling space velocity can tune catalyst performance. When the space velocity is low, very low CO slips (~ 5ppm) are achieved, but at the expense of O_2 selectivity. Similarly, if the space velocity becomes too high, there is insufficient time for the CO to fully react and CO slip increases. This indicates that the two reactions are

essentially sequential: a majority of the CO reacts first, then the remaining O_2 begins to react with the available H_2. There appears to be a maximum O_2 selectivity of about 80 % at 80°C, suggesting there is insufficient added water.

Fig. 8. Effect of SV on CO PROX catalysis over Au/Al_2O_3. (A) CO conversion as a function of water content at several different values for the space velocity; (B) O_2 selectivity for CO_2 as a function of CO conversion at 20°C. These data show that CO conversion increases as the SV decreases while O_2 selectivity is essentially the same up to 99% CO conversion. Although there is a small amount of nascent H_2 oxidation at all conversions, the reaction is largely sequential – CO is oxidized first, then the catalyst begins oxidizing H_2. CO conversion measurement errors are typically ± 0.02%; O_2 selectivity measurements are typically ± 5%.\

Fig. 9. Effect of water and temperature on CO PROX catalysis over Au/Al_2O_3. (A) Normalized nominal activity and (B) O_2 selectivity for CO_2 as a function of P_{H2O} and temperature. As the reaction temperature increases, the water pressure required to reach maximum activity shifts to higher P_{H2O} and broadens substantially. This suggests that a certain water coverage on the support yields the highest activity. Additionally, the selectivity for CO_2 decreases somewhat as the reaction temperature increases. This is consistent with the mechanistic role of water as a co-catalyst in CO oxidation. Activity measurement errors are typically ± 0.02%; O_2 selectivity measurement errors are ± 5%.

Fig. 10. Gas adsorption data. (A) Volumetric water adsorption isotherms (20-50 °C) on the Au/Al_2O_3 catalyst. As the temperature increases, the amount of water adsorbed on the catalyst at a given pressure decreases substantially. The box indicates the range of θ_{H2O} that corresponds to the activity maxima in Figure 9A and Table 1. There is a relatively narrow range of water coverage enabling the highest CO oxidation activity, regardless of the reaction temperature. (B) CO adsorption isotherms (20°C) determined by infrared spectroscopy in the presence and absence of water. At pressures as low as 2.3 Torr, where total CO oxidation activity is maximized, roughly half of the CO adsorption sites are blocked by water. This is presumably due to physical blocking of the adsorption sites at the metal-support interface by water adsorbed on the support. Adsorption isotherm measurement errors are typically ± 5%.

Fig. 11. CO oxidation activity at 40 °C vs moisture content in the gas for Au/Al_2O_3 using two different heating protocols. Each point corresponds to steady state conditions after 30 min [60 mg of untreated Au/Al_2O_3 catalyst (space velocity= 2.33 $L/g_{cat}/min$, 1% CO, 1.4% O_2, 70% H_2)].

Fig. 12. Changes in FTIR spectra showing D_2O treatment of Au/TiO_2 and Au/Al_2O_3 (30 mg) wafers at 20°C. The top (blue) spectra were collected after H_2O saturation; the bottom (red) spectra were collected after D_2O interchange.

Fig. 13. Proposed reaction mechanism for CO oxidation over Au/TiO_2 in the presence of water. (A) Potential energy diagram; both pathways are limited by a combination of *COOH decomposition and the reaction between *CO and *O(H). (B) Schematic representation of the lower (green) pathway (* indicates an adsorbed species).

Fig. 14. CO oxidation activity at 20 °C vs water adsorbed on the catalysts. Each point corresponds to steady state conditions after 30 min. (5 mg of catalyst; SV = 36 $L/ g_{cat}/min$).

Fig. 15. Kinetic plots for the CO oxidation activity at 20 °C vs water content in the gas phase (▲blue data), and water adsorbed on the catalysts (◆ red data) on Au/TiO_2 (A-left) and Au/Al_2O_3 (B-right). Each point corresponds to steady-state conditions after 30 min. using 5 mg of catalyst (SV = 28 L/g_{cat} /min.).

Fig. 16. Kinetic Isotope Effect (KIE) for the CO oxidation activity at 20 °C versus time-on-stream. (blue line—), and water adsorbed on the catalysts (red line······) on Au/TiO_2 (A-left) and Au/Al_2O_3 (B-right). Each point corresponds to six measurements with 5 mg of catalyst (SV = 28 $L/g_{cat}/min$).

Fig. 17. CO oxidation kinetic dependence on CO concentration in the presence of added water (87, 260, 660, 1760 and 3800 Pa).

Fig. 18. Effects of added water on CO oxidation in the presence (PROX) and absence (CO Oxidation) of H_2 at 20 °C. Rates are normalized to the maximum observed conversion.

Fig. 19. Water adsorption isotherms for Au/Al_2O_3 at 20, 30, 40, and 50 °C.

Fig. 20. XPS data for the Au/Al_2O_3 catalyst.

Fig 21. XRD data for the Au/Al_2O_3 catalyst.

Fig. 22. Effects feed water content on CO oxidation activity by Au/TiO_2 and Au/Al_2O_3 catalysts shown through plots of (A) Activity vs. P_{H2O} (B) reaction order plots, and (C) reaction order based on the amount of weakly adsorbed water (wH_2O). Reaction conditions: 1% CO, 20% O_2, 22 °C.

Fig. 23. Adsorption isotherms (A) and linear Langmuir plots (B) at 20 °C for weak water adsorption on Au/Al_2O_3 and Au/TiO_2.

Fig. 24. Effects of added water on CO adsorption. (A) Au-CO peak area, measured via infrared spectroscopy, as a function of water pressure. (B) Au-CO peak area during drying with 1% CO/N_2 after saturating with water at several P_{H2O}.

Fig. 25. Infrared spectra of H_2O and D_2O exchanged (A) Au/TiO_2 and (B) Au/Al_2O_3.

Fig. 26. CO oxidation H(D) kinetic isotope effects experiments for Au/Al2O3. (A) average KIE for 7 experiments with H_2O and D_2O exchanged treated samples. (B) Effects of adding and removing 700 Pa H2O/D2O to co Au/Al_2O_3 catalytic activity. All testing was performed at (20 C with a 1% CO and 20 % O_2 feed.

Fig. 27. Kinetic parameters for Au/TiO_2 and Au/Al_2O_3 catalysts.

Fig. 28. CO oxidation in presence of 600 ppm of H_2O on Au/Al_2O_3.

Fig. 29. Removal of carbonates from Au/TiO_2 and Au/Al_2O_3 catalysts.

Fig. 30. Decrease in CO adsorption capacity on a Au/TiO_2 catalyst due to the presence of H_2O in the gas. The CO adsorption changes were monitored using the Au-CO integrated peak (~2100 cm^{-1} in the IR spectra). All spectra are referenced to the catalyst pellet (at 20°C) after drying at 120°C (N_2) for 1 hr.

Fig. 31. Variation in CO adsorption on the Au/TiO_2 catalyst with water adsorbed on the surface of the catalyst

Fig. 32. PROX catalysis showing CO slip and CO_2 selectivity as a function of water pressure for a Au/Al_2O_3 catalyst operating at 50 °C.

Fig 33. PROX catalysis showing CO slip and CO_2 selectivity as a function of water pressure for a Au/TiO_2 catalyst operating at 50 °C.

Fig. 34. Effects of heating protocol on Au/Al_2O_3 catalyst performance.

Fig. 35. PROX catalysis showing CO slip and CO_2 selectivity as a function of water pressure for a Au/ZnO catalyst operating at 80 °C.

Fig. 36. PROX catalysis showing CO slip and CO_2 selectivity as a function of water pressure for a Au/SiO_2 catalyst operating at 80 °C.

Fig. 37. PROX results for single-stage, dual-bed catalyst arrangement for removing CO and O_2 from a hydrogen stream.

DETAILED DESCRIPTION

For the purpose of interpreting this specification, the following definitions will apply and whenever appropriate, terms used in the singular will also include the plural and vice versa. In the event that any definition set forth below conflicts with the usage of that word in any other document, including any document incorporated herein by reference, the definition set forth below shall always control for purposes of interpreting this specification and its associated claims unless a contrary meaning is clearly intended (for example in the document where the term is originally used). The use of "or" means "and/or" unless stated otherwise. The use of “a” herein means “one or more” unless stated otherwise or where the use of “one or more” is clearly inappropriate. The use of “comprise,” “comprises,” “comprising,” “include,” “includes,” and “including” are interchangeable and not intended to be limiting. Furthermore, where the description of one or more embodiments uses the term “comprising,” those skilled in the art would understand that, in some specific instances, the embodiment or embodiments can be alternatively described using the language “consisting essentially of” and/or “consisting of.” As used herein, “about” encompasses a value that is ± 20% of the numerical value recited.

PROX catalysts

In one embodiment, the invention provides a preferential CO oxidation reaction (PROX) catalyst, comprising: a plurality of Au or Ag particles having a size ranging from about 0.5 to about 20 nm; a hydrophilic support in contact with the particles; and about 0.1 to about 10 monolayers of water on a surface of the support.

In one embodiment, the active catalyst is composed of gold nanoparticles interacting with a hydrophilic support with a thin layer of water adsorbed on the support. This thin layer of water is critical to the operation of the catalyst, and has not been previously described or employed. The gold nanoparticles can range in size from 0.5-20 nm, but preferably are smaller than 10 nm and most preferably smaller than 5 nm. Numerous supports can be used, including metal oxides (such as alumina, titania, silica, ceria, ZnO, iron oxides, manganese oxides, etc.), mixed metal oxides, metal hydroxides, zeolites, clays, etc. with the key feature being that the support adsorbs and retains water under the reaction conditions. The preferred support will vary based on the desired reaction conditions, with supports that bind water more strongly being preferred for higher temperature reactions and / or lower water content gas feeds and supports that bind water less strongly preferred for lower temperature reactions and / or higher water content gas feeds. The layer of adsorbed water can range from 0.1 monolayer to multiple monolayers, and can be adjusted to help control catalytic activity. The practical maximum height of the water layer is approximately 5 water monolayers higher than the height of the Au nanoparticles. The hydrophilic nature of the support allows the water layer to be controlled by adjusting the amount of water in the reactive gas. Additional promoters such as alkaline or alkaline earth metals and metal hydroxides may also be added to the catalyst.

In some embodiments, the Au or Ag particles have a size ranging from about 0.5 to about 15 nm. In some embodiments, the particles have a size ranging from about 0.5 to about 10 nm. In some embodiments, the particles have a size ranging from about 0.5 to about 5 nm. In some embodiments, the particles have a size ranging from about 0.5 nm to less than 5 nm.

In some embodiments, the hydrophilic support is metal oxide, mixed metal oxide, metal hydroxide, zeolite, vermiculite, clay, silica-alumina, mixed manganese oxide, MnO_2, Al_2O_3, $Ce_{10}AlO_x$, Ce_2AlO_x, Ce-Al-O_x, Ce-Co-O, Ce-Cu-O_x, $CeFeO_x$, Ce-Fe-O_x, Ce-Mn-O_x, CeO_2, CeO_2 nanocrystal, CeO_2 nanocube, CeO_2 nanorod, CeO_2 polyhedra, CeO_2/TiO_2, CeO_2-Co_2O_3, CeO_2-Fe_2O_3, $CeZnO_x$, $CeZrO_x$, Fe_2O_3, Fe-Ce-O_x, Mn-Ce-O_x, MnO_2-CeO_2, MnO_x-CeO_2, TiO_2, Zn-CeO_2, Zn-Ce-O_x, ZnO, ZnO-Fe_2O_3, or a mixture of two or more thereof. In some embodiments, the hydrophilic support is Al_2O_3.

In some embodiments, the support further comprises a promoter. In some embodiments, the promoter is selected from the group consisting of alkaline metal, alkaline earth metal, alkaline metal hydroxide, alkaline earth metal hydroxide, and a mixture of two or more thereof.

In some embodiments, the surface comprises an intersection of the support and one or more of the particles.

In some embodiments, the layer of adsorbed water comprises about 0.1 to about 5 monolayers of water on the surface of the support. In some embodiments, the layer of adsorbed water comprises about 0.1 to about 2.5 monolayers of water on the surface of the support. In some embodiments, the layer of adsorbed water comprises about 0.5 to about 2.5 monolayers of water on the surface of the support. In some embodiments, the layer of adsorbed water comprises about 1 to about 2 monolayers of water on the surface of the support.

In some embodiments, less than about 50% of the surface comprises a surface bound carbonate, bicarbonate, carboxylate, or organic carbonate. In some embodiments, less than about 25% of the surface comprises a surface bound carbonate, bicarbonate, carboxylate, or organic carbonate. In some embodiments, less than about 10% of the surface comprises a surface bound carbonate, bicarbonate, carboxylate, or organic carbonate. In some embodiments, less than about 5% of the surface comprises a surface bound carbonate, bicarbonate, carboxylate, or organic carbonate. In some embodiments, less than about 1% of the surface comprises a surface bound carbonate, bicarbonate, carboxylate, or organic carbonate. In some embodiments, the surface does not comprise a surface bound carbonate, bicarbonate, carboxylate, or organic carbonate.

In some embodiments, the particles are present in an amount ranging from about 0.1 to about 60% by weight of the catalyst. In some embodiments, the particles are present in an amount ranging from about 0.1 to about 30% by weight of the catalyst. In some embodiments, the particles are present in an amount ranging from about 0.1 to about 10% by weight of the catalyst. In some embodiments, the particles are present in an amount ranging from about 0.5 to about 10% by weight of the catalyst.

Method for preparing PROX catalysts

In some embodiments, the preferential CO oxidation reaction (PROX) catalyst is prepared by process comprising:

removing one or more of an adsorbed carbonate, bicarbonate, carboxylate, organic carbonate, or a mixture of two or more thereof from a surface of a supported catalyst, the supported catalyst comprising a plurality of Au or Ag particles having a size ranging from about 0.5 to about 20 nm and a hydrophilic support in contact with the particles; and simultaneously or thereafter adsorbing about 0.1 to about 10 monolayers of water on a surface of the support.

In some embodiments, the invention provides a method for preparing or regenerating a preferential CO oxidation reaction (PROX) catalyst, comprising: removing one or more of adsorbed carbonate, bicarbonate, carboxylate, organic carbonate, or a mixture of two or more thereof from a surface of a supported catalyst, the supported catalyst comprising a plurality of Au or Ag particles having a size ranging from about 0.5 to about 20 nm and a hydrophilic support in contact with the particles; and simultaneously or thereafter adsorbing about 0.1 to about 10 monolayers of water on a surface of the support.

In some embodiments, the removing comprises heating the supported catalyst to a temperature greater than about 150 °C for a time ranging from about 0 to about 16 hours.

In some embodiments, the adsorbing is carried out thereafter and comprises contacting the supported catalyst with liquid H_2O or an H_2O-containing inert gas or an H_2O-containing reactive gas.

In some embodiments, the removing comprises heating the supported catalyst to a temperature greater than about 150 °C, and wherein the adsorbing is carried out thereafter and comprises cooling the supported catalyst to a temperature of about 25 °C over a period of about 1 to about 24 hours while contacting the supported catalyst with an H_2O-containing inert gas.

In some embodiments, the removing comprises contacting the supported catalyst with a diluted mixture of H_2 and O_2 gases at a temperature ranging from about 20 to about 400 °C.

In some embodiments, the removing and simultaneous adsorbing comprise contacting the supported catalyst with a gaseous mixture of $O_2/N_2/He/H_2O/CO$ at a temperature ranging from about 20 to about 250 °C for a time ranging from about 0 to 5 hours.

In some embodiments, the removing and simultaneous adsorbing comprise contacting the supported catalyst with a gaseous mixture of $O_2/N_2/He/H_2O/CO$ at a temperature ranging from about 20 to about 100 °C for a time ranging from about 0 to 5 hours.

The active catalyst can be prepared in many ways and is not limiting. First, supported gold or silver nanoparticles must be prepared on a hydrophilic support. Numerous preparation methods are available in the literature; these methods include, but are not limited to, deposition-precipitation techniques (including urea deposition-precipitation), wetness impregnation techniques, strong electrostatic adsorption techniques, and colloid or nanoparticle deposition. We have used several methods to prepare the supported gold nanoparticles, but have primarily relied on deposition-precipitation and colloid deposition techniques. Commercially available catalysts can also be suitable precursors. We have used catalysts purchased from Strem Chemicals (Au/alumina, product number 79-0160; Au/titania, product number 79-0165; Au/zinc oxide, product number 79-0170) as well as catalysts provided by MinTek.

The preferred structural properties of the material are as described above: the gold nanoparticles can range in size from 0.5-20 nm, but preferably are smaller than 10 nm and most preferably smaller than 5 nm. Numerous supports can be used, including metal oxides (such as alumina, titania, silica, ceria, ZnO, iron oxides, manganese oxides etc.), mixed metal oxides, metal hydroxides, zeolites, clays, etc. with the key feature being that the support adsorbs and retains water under the reaction conditions.

Once the gold nanoparticles are prepared on the hydrophilic support, any adsorbed carbonates must be removed and the water layer must be added. Several methods can be used to prepare the active catalyst from the catalyst precursor, with the carbonate removal being the first critical step. This can be accomplished by heating to high temperatures under a flowing reactive or inert gas. A reactive mixture of H2 and O2 diluted in an inert carrier gas can also be passed over the catalyst at low to moderate temperatures to decompose the carbonates. After this treatment, the water layer can be added by passing liquid water over the catalyst and drying in an inert gas or by equilibrating the catalyst surface with a gas containing water in an inert carrier gas. Alternatively, water in an inert gas feed can be flowed over the catalyst at a low to moderate temperatures to decompose carbonates, hydroxylate the support surface, and deposit the water layer.

Below is one example of how the catalyst can be prepared from a suitable supported gold nanoparticle precursor. The thermal treatments used in catalyst preparation or regeneration often result in dehydroxylation of the catalyst surface and loss of adsorbed water. Therefore, the activation and pre-treatment typically performed immediately prior to contact with the reactive gas is particularly preferred in preparing the active composition of matter. This class of pretreatments, which generate the active composition of matter, enable the catalysts to generate high initial activity and can be used to regenerate a deactivated catalyst. This general activation method can be summarized by the following elements:

1- Immediately after high temperature thermal treatment (T > 150 °C) contacting the catalyst with moisture containing inert gas hydroxylates the surface of the support, preserving the water adsorption capacity of the catalyst. Figure 4 shows how regeneration under H_2O containing N_2 flow (4000 Pa of H_2O, 100 mL/min N_2, 20°C, 12hr,) restores the water adsorption capacity that is lost due to the CO oxidation reaction (▨).

2- A slow cooling of the catalyst for 1-24 hrs in presence of elevated amounts of moisture allows for re-hydroxylation of the catalyst surface.

3- When the catalyst has been stored for prolonged times, and prior to PROX catalysis, the catalyst should be contacted with a moisture containing gas (no CO) to prepare the active composition of matter.

4- Alternately, the catalyst may be contacted with a diluted mixture of H_2 and O_2 gases, at temperatures ranging from 20 – 400 °C.

5- Alternatively, the catalyst may be contacted with a diluted mixture of H_2, O_2, and H_2O gases, at temperatures ranging from 20 – 400 °C and cooled to the reaction temperature under a gas comprised of H_2O and an diluent gas (e.g. N_2, air, etc.)

6- In order to avoid carbonates build-up on the catalyst surface during initial CO PROX reaction, the pretreatment performed in points 1,2, 3, 4 and/or 5 should ensure that the water coverage is in the range to reach optimal catalytic activity before contacting the gas with CO containing gases (nominally 0.1-5 monolayers of water on the support).

7- The lack of water adsorbed on the catalyst or moisture in the gas, or when it is stored under dry atmospheres or containing CO/CO_2 will promote the formation carbonate-like species on the catalyst surface.

8- Carbonates formed on catalysts surfaces can be removed using mild treatments (at temperatures 20-100°C) for short times (0-5 hr) using mixtures of $O_2/N_2/He/H_2O/CO$ provided that enough water is preserved on catalyst surface (1-5 monolayers, Figure 4 line ○).

Depending on the relative strength of adsorption of the carbonates formed on a specific support, the temperature used in the treatment described in the point 1 should be changed accordingly. Supports that bind carbonates more strongly require the use of higher temperatures during catalyst pretreatment or regeneration.

Processes for carbon monoxide oxidation using PROX catalyst

In some embodiments, the invention provides a process for CO oxidation in the presence of other gases using a PROX catalyst as described herein. In some embodiments, the CO oxidation process is carried out during the production of hydrogen gas via steam reforming.

In some embodiments, the invention provides a process for oxidizing CO, comprising: contacting the PROX catalyst of the invention and a feed gas comprising CO, O_2 and H_2O at a temperature ranging from about 0 to about 300 °C, to thereby oxidize the CO.

In some embodiments, the process further comprises removing O_2 by contacting the gas with another catalyst. In some embodiments the O_2 removing catalyst is a hydrogenation catalyst. In some embodiments, the hydrogenation catalyst comprises a metal on an oxide support. In some embodiments, the metal comprises nickel, platinum, manganese, copper, iron, palladium or combinations thereof. In some embodiments, the oxide support comprises MnO_2, Al_2O_3, $Ce_{10}AlO_x$, Ce_2AlO_x, $Ce\text{-}Al\text{-}O_x$, Ce-Co-O, $Ce\text{-}Cu\text{-}O_x$, $CeFeO_x$, $Ce\text{-}Fe\text{-}O_x$, $Ce\text{-}Mn\text{-}O_x$, CeO_2, CeO_2 nanocrystal, CeO_2 nanocube, CeO_2 nanorod, CeO_2 polyhedra, CeO_2/TiO_2, $CeO_2\text{-}Co_2O_3$, $CeO_2\text{-}Fe_2O_3$, $CeZnO_x$, $CeZrO_x$, Fe_2O_3, $Fe\text{-}Ce\text{-}O_x$, $Mn\text{-}Ce\text{-}O_x$, $MnO_2\text{-}CeO_2$, $MnO_x\text{-}CeO_2$, TiO_2, $Zn\text{-}CeO_2$, $Zn\text{-}Ce\text{-}O_x$, ZnO, $ZnO\text{-}Fe_2O_3$, or a mixture of two or more thereof. In some embodiments, the oxide support is Al_2O_3. In some embodiments, the oxide support comprises SiO_2. In some embodiments, the hydrogenation catalyst is Ni/Al_2O_3. In some embodiments, the hydrogenation catalyst is Pt/SiO_2. In some embodiments, the process can utilize a single stage, dual-bed reactor system comprising the PROX catalyst and the second catalyst. In some embodiments, the process functions by having sufficiently high oxygen pressure to drive the CO oxidation reaction over the PROX catalyst to completion. The excess O_2 needed to drive the CO oxidation reaction can then be removed using the O_2 removing catalyst. In some embodiments, the second catalyst can be present at the bottom or the end of the reactor bed. In some embodiments, the O_2 removing catalyst removes 50%, 60%, 70%, 80%, 90%, 91%, 92%, 93%, 94%, 95%, 96%, 97%, 98%, 99%, or substantially 100% of the remaining oxygen. In some embodiments, the process results in a substantially pure hydrogen effluent. In some embodiments, only about 2% of the hydrogen is sacrificed.

In some embodiments, the feed gas comprises O_2 and CO in an O_2/CO molar ratio of about 1,000,000:1. In some embodiments, the feed gas comprises O_2 and CO in an O_2/CO molar ratio of about 100,000:1. In some embodiments, the feed gas comprises O_2 and CO in an O_2/CO molar ratio of about 10,000:1. In some embodiments, the feed gas comprises O_2 and CO in an O_2/CO molar ratio of about 1,000:1. In some embodiments, the feed gas comprises O_2 and CO in an O_2/CO molar ratio of about 100:1. In some embodiments, the feed gas comprises O_2 and CO in an O_2/CO molar ratio of about 75:1. In some embodiments, the feed gas comprises O_2 and CO in an O_2/CO molar ratio of about 50:1.

In some embodiments, the feed gas comprises O_2 and CO in an O_2/CO molar ratio of about 20:1. In some embodiments, the feed gas comprises O_2 and CO in an O_2/CO molar ratio of about 10:1. In some embodiments, the feed gas comprises O_2 and CO in an O_2/CO molar ratio of about 5:1. In some embodiments, the feed gas comprises O_2 and CO in an O_2/CO molar ratio of about 1:1. In some embodiments, the feed gas comprises O_2 and CO in an O_2/CO molar ratio ranging from about 0.2 to about 5.

In some embodiments, the feed gas comprises H_2O in an amount sufficient to maintain about 0.1 to about 10 monolayers of water on the surface of the support during said contacting.

In some embodiments, the process produces a product gas comprising 1000 ppm or less of CO. In some embodiments, the process produces a product gas comprising 100 ppm or less of CO. In some embodiments, the process produces a product gas comprising 10 ppm or less of CO. In some embodiments, the process produces a product gas comprising 1 ppm or less of CO. In some embodiments, the process produces a product gas comprising 0.1 ppm or less of CO.

In some embodiments, the process comprises an O_2 selectivity for CO_2 of 30% or greater. In some embodiments, the process comprises an O_2 selectivity for CO_2 of 40% or greater. In some embodiments, the process comprises an O_2 selectivity for CO_2 of 50% or greater. In some embodiments, the process comprises an O_2 selectivity for CO_2 of 60% or greater. In some embodiments, the process comprises an O_2 selectivity for CO_2 of 70% or greater. In some embodiments, the process comprises an O_2 selectivity for CO_2 of 80% or greater. In some embodiments, the process comprises an O_2 selectivity for CO_2 of 90% or greater.

In some embodiments, the temperature ranges from about 0 to about 200 °C. In some embodiments, the temperature ranges from about 0 to about 175 °C. In some embodiments, the temperature ranges from about 0 to about 150 °C. In some embodiments, the temperature ranges from about 10 to about 150 °C. In some embodiments, the temperature ranges from about 20 to about 150 °C. In some embodiments, the temperature ranges from about 20 to about 100 °C. In some embodiments, the temperature ranges from about 20 to about 50 °C.

In some embodiments, the feed gas further comprises one or more of non-condensable hydrocarbon, high dewpoint hydrocarbon, hydrocarbon, alkane, alkene, functionalized hydrocarbon, permanent gas, hydrogen, ammonia, N_2, H_2, air, He, Ar, C_1-C_{10} hydrocarbon, or a mixture of two or more thereof.

In some embodiments, the process produces a first product gas comprising 1000 ppm or less of CO; and which further comprises a second process for oxidizing said CO, the second process comprising:

optionally, adding or removing one or more of O_2, H_2O, or both to or from the first product gas, to optionally form a second feed gas;

contacting the first product gas or second feed gas with a second catalyst at a temperature ranging from about 0 to about 300 °C, to thereby oxidize said CO. In some embodiments, the second catalyst comprises the PROX catalyst as described herein.

In some embodiments, the catalyst is distributed along a catalyst bed having an upstream portion and a downstream portion, and wherein the temperature of the upstream portion is higher than the temperature of the downstream portion. In some embodiments, the temperature gradually decreases between the upstream portion and the downstream portion.

In another embodiment, the invention provides a dual stage process for using Au based catalysts to oxidize CO in non-condensable gas streams shown in Figure 5 (dew point > T36) comprising the steps of: decreasing initial CO concentration to 100 ppm, and finishing in a second stage until CO content is reduced to <10 ppm. In some embodiments, the catalytic activity and selectivity is tuned by the control of adsorbed water on the catalysts. In some embodiments, the temperature is gradually decreased between sequential operating units. In some embodiments, activity and selectivity is preserved in the range of 0-150 °C, and wherein water is adsorbed on the catalyst. In some embodiments, gas mixture is comprised by high dew point hydrocarbons. In some embodiments, gas mixture is comprised by permanent gases O_2, N_2, He, Ar, and their mixtures. In some embodiments, gas mixture is comprised of permanent gases and hydrocarbon mixtures. In some embodiments, gas mixture is comprised of high H_2 concentrations mixtures. In some embodiments, where the catalyst is pretreated with water vapor/O_2 mixtures to achieve high catalytic activity.

In another embodiment, the invention provides a single stage process for the preferential CO oxidation in gas streams using Au based catalysts exhibiting a gradual temperature decrease along the length of the bed.

In some embodiments, high selectivity is afforded by performing the reaction in two serial steps, in which the main components are:

1- An initial CO oxidation reactor (stage 1, unit 36 in Figure 5) using a near stoichiometric amount of O_2 (O_2/CO 0.2 – 5) from air in which the resulting CO concentration is reduced to a range of 1000- 1 ppm. The operating conditions for this reactor can be varied based on the specifics of the inlet feed and the requirements of the downstream process. Broad guidelines for this unit are as follows:

a. The unit (unit 36) is operated at a higher temperature, which can be close to the outlet temperature of the preceding unit (typically, but not exclusively, a water-gas shift reactor). These temperatures are typically in the range of (50-200 °C).

b. The moisture content of the feed stream is equilibrated at the temperature of saturator 34, where T34 corresponds to the temperature necessary to obtain the desired water pressure (and therefore water coverage - typically 0.5-2 monolayer equivalents of water on the support) on the catalyst in Stage 1 (36), operated at T36.

c. The amount of added O_2 can be varied based on the specifics of the feed and the operational requirements of the unit, but will typically have an O_2/CO ratio in the range of 0.2-5.

2- A second auxiliary stage (stage 2) in which CO content is lowered to <1000 ppm. The operation conditions in this stage are:

a. Operating temperature (in unit 42) either (a) a low temperature, particularly when high selectivity is desired or (b) close to the delivery temperature necessary for the next downstream unit in the processing This temperature (T42) can be varied according to the process requirements, but will typically range from 0 to 100 °C (Figure 5).

b. The moisture content necessary for stream F may differ from the moisture content of stream C based on differences in the operating temperatures and the properties of the catalysts employed. Consequently, the primary function of saturator 2 (40) is to adjust the water content to the value necessary to obtain the desired water coverage on the catalyst in Stage 2 (42), typically 0.5-2 monolayer equivalents of water on the support.

c. The amount of added O_2 can be varied based on the specifics of the feed and the operational requirements of the unit, but will typically have an O_2/CO ratio in the range of 0.2-5.

Two heat exchangers (32 and 38) are necessary to ensure that temperature values (TC, TF) and moisture contents (RHC and RHF) are adequate for stages 1(36) and 2 (42), respectively. Streams B and D can be used either to add water to the system or remove excess water, depending on the specifics of the inlet feed and the operating conditions.

By limiting CO slip after stage 1 to 1000 - 1 ppm, H_2 oxidation can be largely prevented, which improves the selectivity to values > 90%. High selectivity in stage 2 is attained due to two factors: (i) water adsorbed on the support physically blocks the H_2 binding sites at the metal-support interface, and (ii) H_2 binding is an activated process, so employing lower temperatures prevents H_2 adsorption / dissociation. Thus, the dual stage system takes advantage of the higher activity at higher temperatures, using a small amount of residual CO and water to prevent H_2 oxidation, and the higher intrinsic selectivity available at lower temperatures in stage 2. Using this system, CO conversions as high as 99.98% (CO slip < 2 ppm) can be achieved with overall process selectivity of 80% or higher.

Reducing the gas temperature stepwise through stages 1 and 2 (T36>T42) also allows for efficient heat management and assures that the polished gas can be delivered to downstream units at an appropriately low temperature, when required.

TA (~300 ºC) > TC > T36> TF > T42> TG (0-100 ºC)

The system can be operated under a variety of conditions and with a variety of catalysts.

The catalysts in stage 1 and stage 2 need not be identical, but certain qualities are required for high activity and selectivity:

1- The catalyst should consist of Au nanoparticles supported on a metal oxide or other material that can adsorb water.

2- The gold nanoparticles should be smaller than 10 nm in diameter, and preferably smaller than 5 nm in diameter. There should be sufficient remaining surface area on the support to adsorb water.

3- Supports may be either traditional amorphous supports or may consist of nanoscale support particles.

4- Micropore structures (<5 nm pore size) will favor capillary condensation, which may increase the amount of water adsorbed at a given humidity level.

5- Promotors, while not required, may be added (either to the support or to the Au) to improve catalyst performance. Bi-metallic and mixed (combined) oxides may also be used.

6- Many catalyst preparation methods are available, including those based on the deposition-precipitation of $HAuCl_4$.

7- A variety of catalyst pretreatments are available, although lower temperature oxidation and/or reduction steps are preferred. Au reduction can be performed at T<200 °C, where little or no sintering or support dehydroxylation is observed.

8- The catalyst used in stage 1 does not necessarily need to be the same as the catalyst used in stage 2. The catalyst and operating conditions used in Stage 1, particularly the water adsorption qualities, can be chosen based on the outlet conditions from the upstream unit. For relatively dry feeds and/or higher operating temperatures, the preferred catalyst will bind water strongly (or have a higher water adsorption capacity). For relatively wet feeds and/or lower operating temperatures, the preferred catalyst will bind water less strongly (or have a lower water adsorption capacity).

9- The catalyst and operating conditions used in stage 2, particularly the water adsorption qualities of the catalyst, can be chosen based on the outlet conditions from Stage 1, the overall process requirements (CO tolerance, selectivity), and downstream requirements (temperature, CO content, and humidity). Catalysts with higher intrinsic selectivity for CO oxidation (over H_2 oxidation) will generally be preferred and operated at temperatures that maximize selectivity and H_2 throughput. For lower operating temperatures, catalysts with lower water adsorption strength (or lower adsorption capacity) relative to stage 1 will generally be preferred.

10- Relatively hydrophilic catalysts are preferred for stage 1 (for example, alumina, silica-alumina, vermiculite, etc.), since higher operating temperatures of stage 1 will require greater adsorption strength by the support t maintain the optimum water coverage.

EMBODIMENT 1 – Two stages operated in such way that the CO slip in stream D (after stage 1) ranges from 1000-1 ppm. The specifics of the catalyst can be varied based on the humidity of the inlet feed. Alumina (better water sorbent) is preferred in the first stage and Titania is preferred in the second stage.

EMBODIMENT 2 – Two stages operated in such way that the CO slip in stream D (after stage 1) ranges from 1000-1 ppm. The specifics of the catalyst can be varied based on the humidity of the inlet feed. Alumina (better water sorbent) is preferred in the first stage and Titania is preferred in the second stage. At the end of the second stage, an additional H_2 or hydrocarbon oxidation catalyst can be placed to remove any remaining O2 from the process. The specifics of this secondary catalyst can be varied based on the humidity of the inlet feed and the oxygen tolerance of the downstream process. Typical oxidation catalysts are comprised of an active metal (e.g. Mn, Fe, Co, Ni, Cu, Zn, Ru, Rh, Pd, Ag, Cd, W, Re, Os, Ir, Pt, Au, Hg, etc.) supported on an oxide support (alumina, titania, silica, phosphate, etc.) or active carbon.

EMBODIMENT 3 – One stage process with a single catalyst where temperature gradually decreases along the catalytic bed. Temperature and moisture in the top of the bed can be chosen to reach high CO conversion while temperature in the bottom is chosen in order to reach the desired

CO slip. Excess of water in the bottom of the bed causes a under-optimal activity, but also limits H_2 oxidation. Weaker water sorbent support is preferred in this type of embodiment (e.g. TiO_2).

EMBODIMENT 4 – One stage process with a single catalyst where temperature gradually decreases along the catalytic bed. Temperature and moisture in the top of the bed can be chosen to reach high CO conversion while temperature in the bottom is chosen in order to reach the desired CO slip. Excess of water in the bottom of the bed causes a under-optimal activity, but also limits H_2 oxidation. Weaker water sorbent support is preferred in this type of embodiment (e.g. Al_2O_3 or TiO_2). At the end of the second stage, an additional H_2 or hydrocarbon oxidation catalyst can be placed to remove any remaining O2 from the process. The specifics of this secondary catalyst can be varied based on the humidity of the inlet feed and the oxygen tolerance of the downstream process. Typical oxidation catalysts are comprised of an active metal (e.g. Mn, Fe, Co, Ni, Cu, Zn, Ru, Rh, Pd, Ag, Cd, W, Re, Os, Ir, Pt, Au, Hg, etc.) supported on an oxide support (alumina, titania, silica, phosphate, etc.) or active carbon.

EXAMPLES

EXAMPLE 1: "Controlling Activity and Selectivity using Water in the Au-catalyzed Preferential Oxidation of CO in H_2"

A typical benchmark goal for the PROX reaction, arising primarily from PEM fuel cell requirements, is to reduce the CO concentration at the reactor outlet (hereafter referred to as the "CO slip") to 50 ppm with O_2 selectivity to $CO_2 \geq 50\%$.[1-3] We refer to this as the 50/50 goal. Supported Au nanoparticles are well-known to be highly active CO oxidation catalysts[4-6] and notoriously poor hydrogenation catalysts.[7] They should be excellent PROX catalysts, but 20 years of research has produced very few catalysts capable of achieving the 50/50 goal (Fig. 6A).[1,8] Numerous studies have searched for better catalysts, examining particle size effects,[6,9] metal oxide support effects,[10,11] mixed metal oxides,[9,12] and ordered mesoporous materials.[13] Bimetallic catalysts,[14] the inclusion of polyoxometallates in liquid phase media,[15] Au-ceria nanocomposites,[16] and embedded Au@CeO_2 catalysts[17] have also been examined with limited success.

A general lack of consensus on the CO oxidation mechanism has hampered catalyst development. Surface hydroxyl groups on the support are clearly necessary for the most active catalysts,[18-20] and we,[5] following work by the Haruta,[21,22] Davis,[20,23] Fujitani[24] and Iglesia[25] groups, have shown water greatly enhance reaction rates. Several groups have also suggested that oxygen vacancies on the support play in important mechanistic role.[26-28] More specific mechanistic PROX investigations by Widmann and Behm have shown H_2 promotes CO oxidation over Au and the same activated oxygen species is involved in both H_2 and CO oxidation.[29] There is fairly clear consensus that, for low temperature CO oxidation, the metal-support interface plays a critical role in the catalysis.[5,24,29-32]

We recently proposed a new mechanism for CO oxidation over Au/TiO_2 catalysts, in which water functions as a co-catalyst;[5] the study reported herein applies our newfound mechanistic understanding to CO PROX. Preliminary tests showed Au/Al_2O_3 catalysts have the same basic CO oxidation reaction kinetics, and therefore likely operate via the same mechanism as Au/TiO_2. The Au/Al_2O_3 catalysts were more selective for PROX in our initial testing, so we focused additional studies on this system. Although the promotional effects of water in PROX have been reported,[1,33] there is no systematic study seeking to control activity and selectivity by adjusting the feed water content. Herein, we show that carefully controlling the feed water content and space velocity leads to significant improvements in catalyst performance – far surpassing the 50/50 goal. We also show the catalyst functions best when the surface coverage of water on the support is ~ 1 monolayer (ML), and interpret the activity and selectivity gains in terms of our most recent mechanistic proposal.

Results and Discussion.

Influence of Water on Catalyst Performance. We studied a commercial Au/Al_2O_3 catalyst, controlling the water content in a model reformate gas stream (SI 2.1-3). Since catalysts are tested under a wide variety of conditions in various labs, we defined a figure of merit (FOM, SI 3.2) to efficiently compare key aspects of catalyst performance:

$$FOM = \frac{O_2\ selectivity\ (\%)}{CO\ slip\ (ppm)} \qquad (1)$$

For reference, a FOM value of 1 describes a catalyst and reaction conditions that meet the 50/50 goal.

Figure 6A plots several FOM values against the nominal activity for some of our experimental conditions. Approximately 60 literature reports are included (details in SI 3.3), most of which were collected at 80°C, the operating temperature of many fuel cell systems.[34] The literature results vary greatly, so nominal activities are normalized to the total amount of Au, making no adjustments for Au particle size. We are aware of only two reports that achieve the 50/50 goal, both using low space velocities and nominally dry feeds.[1,8] By controlling the amount of water added to the reaction (*vide infra*) and using higher space velocities, we far surpass the 50/50 goal, and do so at space velocities 1-2 orders of magnitude larger than literature reports (Fig. 6A, Table 8).

Catalyst deactivation is similarly important in PROX, and water may prevent the deposition of carbonates, which poison CO oxidation.[2,35,36] Long term activity and selectivity plots are shown in Figs. 6B and 6C, respectively. When water is added to the feed, there is no deactivation over the course of 10 hours, and O_2 selectivity remains both constant and high (~80%). When water is removed, O_2 selectivity immediately drops and the CO oxidation activity begins to degrade over time. These experiments, which employ an unoptimized catalyst, show that huge improvements in PROX performance are possible when the feed water content is carefully controlled. Further, the potential hydrogen production per unit time is increased 1-2 orders of magnitude over previous reports, with negligible catalyst deactivation over 10 hours.

Space Velocity Effect. Figure 7 shows CO slip and O_2 selectivity data for the experiments in Fig. 6A. The experimental protocol (SI 2.2-3) was critical to achieve high activity and selectivity, so catalysts were always equilibrated with 30 Torr water before initiating the reaction. The water pressure (P_{H2O}) was then systematically lowered, allowing the CO conversion to stabilize at each P_{H2O} (generally 30 min). Controlling the space velocity (SV), which is simply the flow rate normalized to the amount of catalyst, is critical to achieving high activity and selectivity. When both P_{H2O} and SV are properly controlled (Figs. 7B and 7C), the reaction can operate at very high conversions (99.9%, < 10 ppm CO slip) while maintaining high O_2 selectivity (> 80%); if the SV drops too low, O_2 selectivity suffers (Fig. 7C).

A space velocity study at 20°C (Fig. 8) demonstrated CO conversion increases as the SV decreases while O_2 selectivity is essentially the same up to 99% CO conversion. Similarly, when CO conversions are high (CO slip ~ 10 ppm), decreasing the SV only serves to decrease the O_2 selectivity (Figs. 7B and 2C; 80°C). These data indicate the PROX reaction is largely sequential, with CO reacting before H_2. This conclusion differs somewhat from the most popular literature mechanisms, which either require H_2 activation to generate the active oxidant[37] or utilize support O atoms.[29]

The trends in PROX activity and selectivity, both for our data and much of the PROX literature, can be readily understood in the context of our recently proposed CO oxidation mechanism for Au/TiO_2.[5] The key elements of this mechanism are (i) the facile generation of reactive Au-OOH from O_2 and a proton from water adsorbed at the metal-support interface, (ii) a very low reaction barrier between Au-OOH and Au-CO, and (iii) the rate limiting decomposition of Au-COOH.[5] The CO oxidation kinetics and H/D kinetic isotope effect for Au/Al_2O_3 are essentially identical to Au/TiO_2, indicating the same mechanism is likely at work (SI 3.1). Our results are largely consistent with the extensive PROX mechanistic work from the Behm[2,29] and Piccolo[37]; however, there are two important distinctions from their previous interpretations. First, H_2 activation is not required for CO oxidation activity since the active Au-OOH species is derived from O_2 and water. Second, our mechanism does not require the participation of support O, making it consistent with isotope labeling studies in the absence of H_2.[23,25]

Table 1. Estimated water content and coverage at maximum PROX activity.

Temperature	20 °C	30 °C	40 °C	50 °C
SV ($L/g_{cat}/min$)	2.3	3.5	4.7	9.3
P_{H2O} at max activity[a]	1.5 Torr	6.1 Torr	17.8 Torr	22.3 Torr
CO conversion	68%	70%	82%	68%
O_2 conversion	28%	30%	35%	30%
O_2 selectivity for CO_2	87%	84%	84%	83%
Total O_2 converted	3910 ppm	4170 ppm	4940 ppm	4100 ppm
O_2 lost to H_2 oxidation	508 ppm	667 ppm	840 ppm	696 ppm
H_2O produced in-situ	0.8 Torr	1.0 Torr	1.3 Torr	1.0 Torr
Estimated total P_{H2O}	2.3 Torr	7.1 Torr	19 Torr	23 Torr
Adsorbed H_2O[b]	2.4 mmol/g	3.1 mmol/g	3.5 mmol/g	2.7 mmol/g
θ_{H2O} ($molecules/nm^2$)[c]	6.1	7.6	8.9	7.1

[a] From Fig. 4A; Feed: 10,000 ppm (1%) CO, 14,000 ppm (1.4%) O_2, variable water, 60% H_2, balance He.
[b] Estimated from the total P_{H2O} and water adsorption isotherms (Fig. 5A).
[c] Based on the N_2 BET surface area.

Influence of Temperature and Water Coverage. To further explore the roles of water and temperature in PROX, we operated the catalyst under similar conversion at several temperatures. For each temperature, this necessitated adjusting the SV to achieve roughly 75% CO conversion at 30 Torr added water. The feed water content was then systematically decreased. To visualize the trends (Fig 9A), the nominal activity was normalized to the maximum CO conversion at that temperature; associated O_2 selectivity plots are in Fig. 9B. At 20°C, Fig. 9A shows a maximum activity at ~2 Torr of added water; this value is somewhat lower than the maximum found for CO oxidation in the absence of H_2 (~ 4-5 Torr, SI 3.4). This is readily explained by the O_2 selectivity data, which show that O_2 selectivity drops at low P_{H2O}. There are two sources of water in the system: water intentionally added to the inlet feed stream, and water produced in-situ from H_2 oxidation. As Table 1 shows, under the conditions yielding the maximum activity at 20°C, the water produced in-situ is important, accounting for about half of the total water in the system. This explains why so many literature catalysts have reported relatively low activity and O_2 selectivity using dry feeds – in the absence of sufficient surface water, the system oxidizes H_2 to generate the water co-catalyst necessary to oxidize CO. Since the amount of water on the support is governed by adsorption-desorption equilibrium, and the gas flow constantly removes water from the catalyst surface, the catalyst must constantly oxidize H_2 to maintain somewhat consistent water coverage on the support. Thus, with insufficient water in the feed, neither high activity nor selectivity is attainable.

The P_{H2O} range yielding the highest activity increases dramatically as the temperature increases, i.e. the peak in Fig 9A broadens with temperature. This is entirely consistent with the important mechanistic role of water adsorbed on the support since, as the water adsorption isotherms in Fig. 10A show, as the temperature increases, increasing P_{H2O} causes a small change in the amount of adsorbed water. To illustrate this, we used the activity and selectivity data from Fig. 9 to estimate the total amount of water in the system (*cf.* water intentionally added plus water formed by H_2 oxidation) at the activity maximum. This estimate was used along with the adsorption isotherms to estimate the water coverage (θ_{H2O}) at the activity maximum (Table 1). At each temperature, the maximum activity occurs at about the same θ_{H2O} (6-9 molecules/nm^2), which corresponds to roughly 1 ML of water on the support.[38] This range is illustrated by the box in Fig. 10A. This optimum water coverage is compellingly consistent, and is similar to the maximum value found for CO oxidation over Au/TiO_2 (~13 molecules/nm^2).[5]

As Figs. 8A and 9A show, if θ_{H2O} increases above the apparent maximum of approximately 1 ML, then catalytic activity drops. Water binds more strongly to itself than it does to Au;[39] indeed Au surfaces are considered hydrophobic, requiring cryogenic experiments to observe water adsorption.[40] This suggests the drop in activity is due water, which is adsorbed on the support at the metal-support interface, physically blocking CO from adsorbing on the Au particles. To test this, we measured CO adsorption isotherms in the presence of water (Fig. 10B) using infrared spectroscopy.[41] Even in the P_{H2O} regime where activity increases to the maximum value, CO adsorption decreases by 50% relative to the amount adsorbed in the absence of water. Nominal activities for CO oxidation are largely insensitive to CO pressure in this kinetic regime (SI 3.1), so physical blocking has little impact on CO oxidation activity until a very large fraction of the Au sites are blocked.

Beyond the influence on catalytic activity, Figs. 6C and 6B clearly show the addition of water also improves O_2 selectivity. This, too, can be understood in the context of our recently proposed CO oxidation reaction mechanism.[5] The P_{H2O} and SV studies indicate the reaction is largely sequential, such that most of the CO is consumed before H_2 is oxidized. This suggests catalyst selectivity is largely determined by the competition between adsorbed CO and H_2 for the Au-OOH intermediate. Spectroscopic evidence for peroxo- and superoxo- species stabilized on the support have been reported for Au/CeO_2 catalysts.[42] CO binds to Au much more strongly than does H_2, so the CO coverage is expected to be high relative to H_2 coverage, even under excess H_2. When the reaction is pushed to very high CO conversion (Fig. 7), there are sufficient Au sites available for H_2 to react towards the bottom of the catalyst bed. Thus, the SV, conversion, and water coverage control the fraction of Au sites available to catalyze H_2 oxidation.

There may also be kinetic influences on the high selectivity. Our previous DFT study found a very low reaction barrier (0.1 eV) for Au-CO reacting with Au-OOH.[5] Hydrogen chemisorption on Au is an activated process,[43] suggesting this may be slow relative to CO activation at low temperature. The general trend of decreasing O_2 selectivity as temperature increases (Fig. 9B) is also consistent with H_2 adsorption/reaction with Au-OOH having a larger activation barrier.

At all temperatures studied, PROX selectivity generally increased with P_{H2O} (Fig. 9B). Behm's group has shown CO and H_2 compete for a common reactive oxygen intermediate;[29] this indicates that water has a larger effect in blocking H_2 adsorption sites than it does in blocking CO sites (Fig 9B). Since water is adsorbed on the support, this is consistent with the conclusion that H_2 adsorption/activation sites are located at the metal-support interface.[29,30,37] This provides an interesting positive feedback loop – when water coverage is low, H_2 oxidation begins to produce water, which accelerates CO oxidation. This interpretation is largely consistent with the bulk of the PROX mechanistic literature, and explains why previous studies have not successfully achieved the 50/50 goal.

Our results show that an un-optimized catalyst can be a commercially viable H_2 purification catalyst provided the SV, θ_{H2O}, and reaction temperature are carefully controlled. Understanding the fundamental steps in the reaction mechanism essentially turns this from a catalyst optimization problem to one of reaction engineering. Controlling SV and θ_{H2O} essentially allows one to tune the number of available active sites, allowing adjustments for differing feeds. This is a substantial advantage, potentially allowing one to uncover additional active sites as a catalyst begins to deactivate over time (for example, due to sulfur poisoning). For wet feeds, this may be accomplished simply by cooling to a temperature where the water vapor pressure is close to the P_{H2O} required for maximum catalytic activity.

This is not to say that the catalyst cannot or should not be optimized; rather, the mechanistic understanding provides similarly clear directions to how the catalyst can be improved or tuned for specific conditions. Indeed, the basic needs of this process have been known: good catalysts must bind and activate CO far faster than they bind and activate H_2.[7] As we have now shown for the first time, balancing the water binding properties of the support with the feed water content is likely to be important in controlling both the CO and H_2 oxidation activity, as well as the water requirements in the process. Supports that bind water more tightly will be desirable for relatively dry feeds – this should reduce the need for adding water to the system; conversely, supports that bind water weakly will likely be better for wet feeds. Any electronic effects (e.g. support effects, particle size effects, or promoters) that increase the CO adsorption energy relative to the H_2 adsorption energy should provide for greater differentiation between the two reactants and higher selectivity.

EXAMPLE 2: Supporting Information for "Controlling Activity and Selectivity using Water in the Au-catalyzed Preferential Oxidation of CO in H_2"

2. Materials and Methods

2.1. Materials

The catalysts used in this study were commercial AUROlite™ samples (Au/Al_2O_3 and Au/TiO_2) purchased from AuTEK. These catalysts were pretreated by the manufacturer to ensure the particles were of appropriate size to be active for CO oxidation. The catalysts were crushed and stored in a dark refrigerator. Powdered silicon carbide (400 mesh) was purchased from

Aldrich. The Au particles on the Au/Al_2O_3 catalyst were too small to be imaged by TEM. A sintered catalyst (500 C under H_2 for 4 hours) showed an average particle size of 2.2 nm. Gases (N_2, He H_2, O_2, and 5% CO/He) were 5.0 grade supplied by Praxair and used with no additional purification. Water was purified to a resistivity of 18.6 Ω with a Barnstead Nanopure system.

2.2. Catalyst pretreatments

The catalysts are active with no further treatment; however, careful control of the reaction conditions is critical to maximize the resulting catalytic activity. This is due to the importance of surface water and carbonates:

- Au based catalysts are prone to deactivation by formation of carbonates on the surface [2,35,44-51].
- Carbonates formation is closely related to the lack of water adsorbed on the catalyst and/or in the gas mixture. In both cases, decomposition of –COOH intermediates (on Au or on the support) seems to be intimately related to the presence of water [5,22,25]. Additionally, higher temperature pretreatments result in catalysts that form greater amounts of surface carbonates under reaction conditions [35] resulting in lower catalytic activity [52].
- CO oxidation activity on Au based catalysts is greatly enhanced by the presence of H_2O and H_2 in the gas feed. The literature clearly shows that the addition of H_2O to the feed enhances CO oxidation activity on Au-based catalysts [5,22,25]. On the other hand, H_2 modifies the reaction pathway [2,44,53] with the resulting effect of an enhanced CO oxidation rate.

In typical literature reports, catalysts (20-200 mg) are diluted in an inert material (SiO_2, SiC, δ-Al_2O_3) and tested in a continuous bed reactor apparatus. A model gas reformate mixture (1-2% CO, 1-2% O_2, 50-60% H_2, and 0-5% CO_2, 20-200 mL/min) is passed through the catalyst bed. CO PROX experiments are typically performed in the 20-100°C temperature range. The heating rate is not always reported, but is normally low, and varies in the range 0.2-1°C/min [37,54].

Our preliminary experiments showed that slow heating of the catalyst has a negative effect on the resulting catalytic activity. Figure 11 plots the CO conversion for a Au/Al_2O_3 catalyst (60 mg) at 40°C when a slow heating ramp (2 °C/min (▨)) is used compared to the conversion when the reacting mixture is contacted with the catalyst at 40 °C with no ramping (▲). All other conditions were the same. This difference in activity for the same catalyst is attributable to two main causes: (i) carbonates deposited on the catalyst surface affect water binding properties of the support, and (ii) a fast formation of oxidation intermediates (-COOH, -OH, -OOH, -O) that occurs when no ramp is used accelerates the carbonates decomposition and/or avoids carbonates buildup on the catalyst surface.

We therefore developed an experimental protocol for the catalytic testing based on four main points:

1. The catalyst surface must have a high water coverage before and during the reaction.
2. Thermal pretreatments should be carried out at temperatures as low as possible.
3. Water must be co-fed at all times to avoid/inhibit the formation and buildup of carbonates.
4. Reaction temperature must be reached quickly by accelerating the heating ramp of the catalytic bed. This can be achieved by preheating the furnace before bringing the reactor on-line.

2.3. Catalysis experiments

CO oxidation catalysis. The CO oxidation reactor consisted of a home-built laboratory scale single pass plug-flow micro-reactor. The reaction zone consisted of finely ground fresh catalyst (5-100 mg) diluted in 1200 mg of silicon carbide. Gas flows were controlled with four electronic low-pressure mass flow controllers (Porter Instruments). The composition of the feed and reactor effluent (CO and CO_2) were determined using a Siemens Ultramat 23 IR gas analyzer, which included an electrochemical O_2 analyzer.

The reacting gas mixture (1% CO, 1.4% O_2, 60% H_2, balance He, 140 mL/min; SV = 1.4-28 L/g_{cat}/min) was saturated with a fixed moisture content (~30 Torr) using a water saturator that can be cooled with dry ice. No thermal pre-treatment was performed to the Au/Al_2O_3 catalyst. The reaction temperature (20-80 °C) was maintained with a water bath pumped through a dewar. The water bath was always heated to the reaction temperature before immersing the U-tube reactor in the dewar. The catalyst was then stabilized in the reactive atmosphere until steady-state conditions were reached (with no change in CO oxidation rate, ~ 30 min). The water pressure in the feed gas was changed by decreasing the temperature of the saturator; the lowest attainable value was approximately 1 mTorr (the equilibrium vapor pressure at the temperature of dry ice, -78.5 °C).

CO reaction order. CO kinetic dependence was performed using five CO concentrations (0.45, 0.73, 1.0, 1.24, and 1.46$\%_{vol}$) with variable concentration of water in the feed. O_2 content was held constant at 1.35%.

2.4. Isotope exchange on Au/Al_2O_3

OH and adsorbed H_2O on TiO_2 and Al_2O_3 can be interchanged *in-situ* under carefully controlled conditions. TiO_2 isotope exchange has been described in Ref [5]. Briefly, at 20°C, D_2O containing N_2 flow (100 mL/min) interchanges OH (to OD) and H_2O (to D_2O) from TiO_2 in a 30 min treatment. Additional treatment for 30 minutes under flowing N_2 eliminates excess D_2O. For Al_2O_3, the interchange process is slower compared to TiO_2 and requires either longer treatment times when interchange occurs at 20°C, or higher temperatures maintaining the same interchange time (30 min). In our case, we performed the interchange on Au/Al_2O_3 at 120°C for 30 min with saturated N_2 (700 Pa D_2O), followed by additional 30 min under N_2 at 20°C to eliminate the excess of D_2O.

FTIR evidence of the interchange process is summarized in Figure 12. Fresh catalysts (H-blue spectra in Fig 12) show the spectral features of OH stretching bands (2200-3800 cm^{-1}), including 'dangling' OH vibrations (3600-3800 cm^{-1}), and δHOH bending frequency at 1623 cm^{-1}. After the interchange process (red spectra), all the spectral features are red shifted to lower wavenumbers: OD stretching (1700-2800 cm^{-1}), 'dangling' OD (2600-2800 cm^{-1}), and δDOD (1212 cm^{-1}). Only a small residual amount of H remains on the surface, likely in the form of δHOD (symmetrical band centered at 3400 cm^{-1}), also evident by the bending vibration at ~1411 cm^{-1} [55].

2.5. CO adsorption on Au catalysts in presence of water

CO adsorption experiments on untreated catalysts were performed as described previously [41,56]. Briefly, approximately 25 mg of sample were pressed into a 30 × 30 Ti mesh (Unique Wire Weaving Co.). The mesh-supported pellet was mounted into a custom-built copper cell and vacuum chamber (International Cryogenics) with a gas-phase optical path length of 1.2 cm. The vacuum chamber was placed in the sample compartment of a Nicolet Magna 550 FTIR spectrometer and evacuated to a pressure of < 1 mTorr for 30-60 minutes. All measurements were made at ambient temperature and all spectra were referenced to a background spectrum of the catalyst pellet under vacuum prior to the addition of CO. Transmission spectra consisted of 100 scans collected with 8 cm^{-1} resolution (spectral data spacing = 4 cm^{-1}) and were reported in absorbance units.

The gas handling system consisted of a mechanical pump and liquid nitrogen trap, a glass line with stainless steel transfer lines to the sample apparatus, and a Baratron pressure gauge (P = 0 to 20 Torr). A liquid nitrogen trap was used to remove impurities from the CO tank (UHP Grade, from Air Products). The entire gas handling system was purged with CO three times before exposing the sample. After collecting a background spectrum, the sample was exposed to 20 Torr CO, and the surface was allowed to equilibrate for 5-10 minutes; previous work has shown this is ample time for CO equilibration on Au catalysts [41,56,57]. An infrared spectrum was recorded and the pressure in the cell was slowly decreased to the next pressure.

For the adsorption of CO in the presence of water, the sample was first dried under vacuum at room temperature. CO (20 Torr) was added to the cell and allowed to equilibrate for 5-10 minutes. Once at equilibrium, an IR spectrum was collected. The CO pressure was then incrementally decreased with IR spectra being collected at each equilibrated pressure of CO. Next, the cell was evacuated, 0.1 Torr of water was added to the chamber, and allowed to equilibrate. CO was then incrementally added to the chamber and IR spectra collected at each pressure of CO. This general procedure was repeated for higher pressures of added water.

2.6. Surface area measurements by volumetric adsorption

The total surface area of the Au/Al_2O_3 and Au/TiO_2 catalysts were measured by N_2 physisorption at 77 K using a Micromeritics ASAP 2020. Prior to the adsorption measurement, the catalysts were heated under vacuum at a ramp rate of 10°C/min to 120°C and held at this temperature under vacuum. After 3 h, the catalysts were cooled down to room temperature under vacuum. The complete adsorption and desorption isotherms were collected for both catalysts. The BET surface area was determined from adsorption data over the relative pressure range (P/P_0 = 0.05 – 0.3). The surface area determined for Au/Al_2O_3 and Au/TiO_2 was 238 m^2/g and 48 m^2/g, respectively.

2.7. Water adsorption isotherm measurements

Water adsorption isotherms were measured at four different temperatures (20, 30, 40 and 50 °C) using a Micromeritics 3Flex volumetric adsorption apparatus. Prior to measuring the isotherms, the catalyst (100 mg) was evacuated at a rate of 10 mm Hg/s to less than 0.01 μm Hg. The catalyst was first heated to 90°C at 5°C/min and held at that temperature for 30 minutes. A second temperature ramp was used to heat the samples (*in vacuo*) from 90 to 120°C using a rate of 5 °C/min. The catalyst was then held at 120°C for a minimum of eight hours; the pressure did not exceed 0.01 μm Hg during the second stage of the pretreatment. After 1 h, the catalyst was cooled to the adsorption experiment temperature under vacuum. The sample temperature was maintained using a Neslab recirculating bath coupled to a Cryofab dewar. The water source temperature was maintained at 43 ± 0.1°C and the instrument manifold was maintained at 45 ± 0.02 °C. During the measurements small doses of water (0.05 mmol/g) were equilibrated with the sample to develop the high resolution adsorption and desorption isotherms. Free-space was measured after the analysis to avoid any stray gas interference or exposure prior to the water adsorption.

3. Results

3.1 CO oxidation kinetics and reaction mechanism

Based on a kinetics and density functional theory (DFT) study, we recently proposed a new reaction mechanism for CO oxidation over Au/TiO_2 catalysts [5]. We include this material for two purposes: (i) to provide appropriate background on the CO oxidation reaction mechanism and (ii) to show that, since the reaction kinetics are essentially the same over Au/Al_2O_3, the reaction mechanisms are likely the same. We considered and investigated the PROX reaction in the context of this mechanism.

Our newly proposed reaction mechanism is shown schematically in Figure 13. The key steps in the mechanism (displayed in Fig. 13) are:

1. Fast O_2 binding to Au, accompanied by a barrierless proton transfer from water adsorbed on the support, generating Au-OOH at the interface.
2. Fast reaction between Au-OOH and Au-CO, generating Au-COOH and Au-O.
3. Fast proton transfer between Au-COOH and Au-O, yielding Au-OH and accompanied by liberation of CO_2.

4. Reaction between Au-OH and Au-CO, yielding Au-COOH
5. Rate-determining decomposition of Au-COOH, accompanied by a proton transfer from Au-COOH to water adsorbed on the support.

Table 2. CO oxidation parameters for over Au/Al_2O_3 and Au/TiO_2.

Paramater	Reaction Order	
	Au/TiO_2	Au/Al_2O_3
CO rxn order[1]	~0	~0
O_2 rxn order[2]	0.1-0.3	0.3-0.4
H_2O (gas) rxn order[3]	0.30	0.28
ML wH_2O at activity maximum[3]	1.3	1.8
KIE (k_H/k_D)	1.84	1.81
K_{wH2O}	0.036[4]	0.029[4]

[1] Reaction conditions: 20 °C, 20% O_2, no added H_2O
[2] Reaction conditions: 20 °C, 1% CO, 50-300 Pa H_2O
[3] Reaction conditions: 20 °C, 1% CO, 20% O_2
[4] Equilibrium constant value determined from water adsorption data

A more detailed comparison of the reaction kinetics data is found below; for convenience, we have compiled the key kinetic parameters in Table 2. The overall reaction kinetics are essentially the same for both catalysts, indicating that both materials catalyze CO oxidation via the same, or very similar, reaction mechanisms.

A. Reaction orders. In order to determine the effect of adsorbed water on catalytic activity, a series of samples (5 mg) of each catalyst (Au/TiO_2 and Au/Al_2O_3) was equilibrated with a N_2 flow saturated with different amounts of moisture. Prior to catalysis experiments, weakly bound water was removed from the catalysts with flowing N_2 (100 mL/min) for 1 h at 120 °C. After drying, the catalysts were equilibrated with water saturated N_2 for 4 h.

This experimental procedure yields catalysts with controlled amounts of adsorbed water. The effect of adsorbed water on the resulting catalytic activity is shown in Fig. 14. Each point in Figure 14 was collected from a separate fresh catalyst sample and measured after the CO oxidation reached steady state (30 minutes).

The water reaction order was studied in a separate set of experiments. Maintaining constant O_2 and CO concentrations, as well as total flow (140 mL/min), the water content in the system was adjusted by changing the moisture content of the feed gas.

Figure 15 shows that reaction rate correlates extremely well with the amount of water adsorbed on the catalysts; additionally, the reaction orders for adsorbed water are substantially larger than the reaction orders for the water in the gas phase.

B. Kinetic isotope effect. As we have described previously, surface hydroxyls and adsorbed water on the catalysts can be deuterated *in-situ* with flowing D_2O/N_2 prior to a catalysis experiment (details in Section 2.4) [5]. The isotope exchange allows comparison of the catalytic activity of interchanged samples (D) with the fresh samples (H). The resulting ratio of the catalytic rates (k_H/k_D) is interpreted as the kinetic isotope effect (KIE).

Figure 16 shows the results for the KIE experiment for CO oxidation on Au/TiO_2 (A-left) and Au/Al_2O_3 (B-right). Six separate experiments were performed and averaged with H_2O saturated (▲ blue data, H) and D_2O saturated (◆ red data, D) samples. The measured KIE values (1.84 and 1.81 for TiO_2 and Al_2O_3, respectively) are essentially the same for the two catalysts. The magnitude is consistent with a primary KIE, indicating that O-H(D) bond cleavage is involved in a kinetically important step. Although KIE values are the same for both catalysts, some differences are apparent. First, the catalytic rate for Au/TiO_2 is roughly three times faster than for Au/Al_2O_3 after 60 min time-on-stream (TOS). This difference is also apparent in the different scales in the y-axes of Fig. 16. Second, the deactivation rate is more pronounced for Al_2O_3; these two elements could be related and are likely attributable to greater carbonates formation on Al_2O_3 at the very first moments of catalysis.

C. CO reaction order in the presence of water. Table 2 shows that under low CO conversion conditions (20 °C, 20% O_2, no H_2) the reaction is largely independent of the CO concentration. Under CO PROX conditions, Behm and co-workers showed the presence of H_2 increases the CO reaction order from 0.24 to 0.82 [2]. They further showed that the reaction order for O_2 remains unchanged under CO PROX conditions (0.32 and 0.36 under CO oxidation and CO PROX conditions, respectively).

In order to maintain low conversion (< 15%), 5 mg of Au/Al_2O_3 were used in CO PROX at 40 °C with a total gas flow of 140 mL/min. The CO reaction order was studied using five CO concentrations (0.45, 0.73, 1.0, 1.24, and 1.46%; Section 2.3), at five different feed moisture contents (87, 260, 660, 1760 and 3800 Pa). The O_2 concentration was held constant at 1.35%. Results are shown in Fig. 17. The reaction has a relatively small but complicated dependence on CO. The rate reaches a maximum value at about 1.1 % CO; for higher CO contents the catalytic rates decrease (Fig. S7A). Although the reaction rate increased with added moisture, the overall CO dependence was essentially similar at all the moisture contents (between 87 and 3800 Pa).

Figure 17 shows that higher CO concentrations (> 1%) decrease the overall reaction rate; consequently, the apparent reaction orders are negative. On CO oxidation over Pt, there is an inverse relationship between the reaction rate and CO partial pressure resulting also in negative reaction orders [58,59]. In the context of CO PROX reaction, slightly negative reaction orders can be interpreted as the saturation of the metal surface by adsorbed CO causing a 'poisoning' of the oxygen activation sites. Surprisingly, while the water pressure increases the overall reaction rate substantially, it has a minimal effect on the CO reaction order.

3.2. Water coverage during catalysis

Water is a co-catalyst for oxygen activation, so understanding the factors that affect the amount of water on the catalyst is necessary. For CO oxidation in the absence of H_2, this is relatively straightforward in that we can assume that the water coverage on the support is equilibrated with the water in the feed. We note that the surface water coverage in flow catalysis experiments is likely to be somewhat lower than in equilibrium adsorption experiments, due to local changes in temperature and to the more complicated dynamics of the flowing system. CO oxidation during PROX is further complicated by the unselective oxidation of H_2, which also produces water.

Figure 18 illustrates the effect of water produced from H_2 oxidation on the CO oxidation reaction during PROX. In the absence of H_2 (blue data), CO oxidation activity drops precipitously when water is removed from the system and reaches a maximum at about 4 Torr. In PROX (with H_2, red data), the maximum CO oxidation activity occurs at much lower added P_{H2O} (ca. 1.5 Torr) and does not decrease substantially when water is removed. These differences are readily attributed to the unselective oxidation of H_2, which produces water.

Table 1 estimates the actual support water coverage (θ_{H2O}) by accounting for the water produced by the unselective oxidation of H_2. For simplicity and clarity, we evaluated the total water on the surface at the CO oxidation activity maximum. This value was estimated as follows:

- The O_2 conversion and selectivity data were used to calculate the total O_2 converted.
- The O_2 converted to CO_2 was subtracted from the total O_2 conversion to determine the O_2 lost to H_2 oxidation, and thus the amount of H_2O produced by this reaction.
- Using the adsorption isotherm data (Fig. 9A; full isotherms in Fig. 19), the total P_{H2O} was used to estimate the amount of H_2O adsorbed on the catalyst.

3.3. PROX Data Tables (data from this work)

Since the PROX literature has largely focused on catalyst screening, particularly the search for better catalyst supports, it is extremely varied in terms of the catalysts and operating conditions employed. This makes comparing catalysts difficult; however, the goals of < 50 ppm CO slip with high (> 50%) O_2 selectivity are widely recognized as the desired performance goals [1-3]. To assist in comparing catalysts and conditions, we developed a simple figure of merit (FOM) defined by these goals:

$$FOM = \frac{O_2\ selectivity\ (\%)}{CO\ slip\ (ppm)} \tag{1}$$

The FOM is a nominal measure of both activity and selectivity; high selectivity and high CO oxidation activity (represented by a low CO slip) result in larger values for the FOM. Since the FOM describes performance under a given set of conditions (space velocity, temperature, feed composition, etc.) a single catalyst will have a FOM value for every set of conditions tested.

The FOM formally has units of %/ppm due to the activity definition in terms of CO slip which, in this case, is more useful than a unitless measure, such as CO conversion. Although the FOM is formally boundless, in practice it is limited by the precision in the CO slip measurement, which is about 1 ppm CO for our experiments. The lower limit approaches 0; thus the practical range of the FOM, at least for our experiments and those we have found in the literature, is 0-100 %/ppm.

The data in Tables 3-7 were collected using our system and the Au/Al_2O_3 catalyst described above. Table 8 compiles numerous reports from the literature.

Table 3. PROX data for Au/Al_2O_3 at 40 °C with SV = 140,000 mL/g/hr (2.3 $L/g_{cat}/min$)[a]

P_{H2O} (Torr)	CO slip (ppm)	CO conversion	O_2 slip (ppm)	O_2 selectivity	Nominal Activity ($mol_{CO}/mol_{Au}/min$)	FOM (%/ppm)

30	29	99.71%	9302	100%	15.8	3.7
19	24	99.76%	9230	100%	15.8	4.4
15	20	99.80%	9157	100%	15.8	5.2
12	15	99.85%	9157	100%	15.8	6.9
7.8	12	99.88%	9157	100%	15.8	8.6
5.0	7	99.93%	8721	95%	15.9	14
2.9	14	99.86%	8576	92%	15.8	6.6
1.8	16	99.84%	8503	91%	15.8	5.7
1.3	26	99.74%	8430	90%	15.8	3.4
0.72	39	99.61%	8358	88%	15.8	2.3
0.35	49	99.51%	8358	88%	15.8	1.8
0.19	62	99.38%	8285	87%	15.8	1.4
0.07	80	99.20%	8285	87%	15.7	1.1
0.02	96	99.04%	8285	87%	15.7	0.9
0.00	134	98.66%	8358	87%	15.6	0.7

[a]Feed: 10,000 ppm (1%) CO, 14,000 ppm (1.4%) O_2, water, 60% H_2, balance He

Table 4. PROX data for Au/Al_2O_3 at 80 °C with SV = 210,000 mL/g/hr (3.5 $L/g_{cat}/min$)[a]

P_{H2O} (Torr)	CO slip (ppm)	CO conversion	O_2 slip (ppm)	O_2 selectivity	Nominal Activity ($mol_{CO}/mol_{Au}/min$)	FOM (%/ppm)
30	5	99.95%	4797	54%	23.8	10.9
21	3	99.97%	3634	48%	23.8	16.1
13	3	99.97%	3343	47%	23.8	15.6
8.7	2	99.98%	3198	46%	23.8	23.1
4.9	2	99.98%	2980	45%	23.8	22.7
3.2	1	99.99%	2907	45%	23.8	45.1
1.4	1	99.99%	2834	45%	23.8	44.8
0.62	1	99.99%	2834	45%	23.8	44.8
0.20	1	99.99%	2907	45%	23.8	45.1

[a]Feed: 10,000 ppm (1%) CO, 14,000 ppm (1.4%) O_2, water, 60% H_2, balance He

Table 5. PROX data for Au/Al_2O_3 at 80 °C with SV = 280,000 mL/g/hr (4.7 $L/g_{cat}/min$)[a]

P_{H2O} (Torr)	CO slip (ppm)	CO conversion	O_2 slip (ppm)	O_2 selectivity	Nominal Activity ($mol_{CO}/mol_{Au}/min$)	FOM (%/ppm)
30	6	99.94%	6686	68%	31.7	11
20	2	99.98%	6395	66%	31.7	33
13	3	99.97%	5669	60%	31.7	20
8.2	2	99.98%	5378	58%	31.7	29
5.0	3	99.97%	5087	56%	31.7	19

2.5	1	99.99%	4942	55%	31.7	55
1.2	1	99.99%	4724	54%	31.7	54
0.53	1	99.99%	4651	53%	31.7	53
0.14	1	99.99%	4578	53%	31.7	53
0.00	3	99.97%	4506	53%	31.7	18

[a] Feed: 10,000 ppm (1%) CO, 14,000 ppm (1.4%) O_2, water, 60% H_2, balance He

Table 6. PROX data for Au/Al_2O_3 at 80 °C with SV = 420,000 mL/g/hr (7.0 L/g_{cat}/min)[a]

P_{H2O} (Torr)	CO slip (ppm)	CO conversion	O_2 slip (ppm)	O_2 selectivity	Nominal Activity (mol_{CO}/mol_{Au}/min)	FOM (%/ppm)
30	14	99.86%	7994	83%	47.5	5.9
21	7	99.93%	7994	83%	47.6	12
15	6	99.94%	7849	81%	47.6	14
10	8	99.92%	7776	80%	47.5	10
7.0	6	99.94%	7703	79%	47.6	13
5.2	9	99.91%	7631	78%	47.5	8.7
3.1	4	99.96%	6977	71%	47.6	18
2.3	6	99.94%	6831	70%	47.6	12
1.5	5	99.95%	6686	68%	47.6	14
1.0	5	99.95%	6613	68%	47.6	14
0.68	8	99.92%	6541	67%	47.5	8.4
0.38	9	99.91%	6468	66%	47.5	7.4
0.13	10	99.90%	6468	66%	47.5	6.6
0.05	9	99.91%	6468	66%	47.5	7.4
0	12	99.88%	6468	66%	47.5	5.5

[a] Feed: 10,000 ppm (1%) CO, 14,000 ppm (1.4%) O_2, water, 60% H_2, balance He

Table 7. PROX data for Au/Al_2O_3 at 80 °C with SV = 560,000 mL/g/hr (9.3 L/g_{cat}/min)[a]

P_{H2O} (Torr)	CO slip (ppm)	CO conversion	O_2 slip (ppm)	O_2 selectivity	Nominal Activity (mol_{CO}/mol_{Au}/min)	FOM (%/ppm)
30	108	98.92%	7994	82%	62.8	0.76
21	133	98.67%	7994	82%	62.6	0.62
15	153	98.47%	7849	80%	62.5	0.52
10	173	98.27%	7776	79%	62.3	0.46
7.0	190	98.10%	7703	78%	62.2	0.41
5.2	205	97.95%	7631	77%	62.1	0.38
3.1	239	97.61%	6977	69%	61.9	0.29
2.3	265	97.35%	6831	68%	61.8	0.26
1.5	291	97.09%	6686	66%	61.6	0.23

[a] Feed: 10,000 ppm (1%) CO, 14,000 ppm (1.4%) O_2, water, 60% H_2, balance He

3.4. Literature PROX data

Table 8. Literature data for supported Au PROX catalysts. In order to calculate the FOM, we were limited to literature that clearly reported both the CO slip (or CO % conversion to at least one decimal place, eg. 99.5%) and the O_2 selectivity.

Catalyst	Temp °C	GHSV		Feed CO (ppm)	Feed O_2 (ppm)	CO % Conv	CO slip (ppm)	O_2 selectivity	Nominal Activity ($mol_{CO}/mol_{Au}/min$)	FOM %/ppm	ref
		($mL/g_{cat}/hr$)	($L/g_{cat}/min$)								
5% Au/Fe_2O_3	80	12000	0.20	9000	9000	99.8%	18	51.0%	0.2	2.83	1
1% Au/Fe_2O_3	100	25000	0.42	10000	12500	99.5%	50	54.5%	2.4	1.09	8
Au/TiO_2	80	39600	0.66	10000	20000	99.5%	50	22.0%	5.8	0.44	60
Au/Zn-Ce-O_x	67	120000	2.00	10000	12500	98.0%	200	65.0%	17.6	0.33	61
1% Au/$Ce_{10}AlO_x$	50	60000	1.00	20000	20000	98.0%	200	63.0%	13.6	0.32	62
Au /Ce-AI-O_x	55	60000	1.00	20000	20000	99.0%	200	63.0%	17.6	0.32	62
Au /Ce-Co-O_x	40	30000	0.50	10000	10000	98.0%	200	60.0%	4.4	0.30	13
Au /Ce-Fe-O_x	75	60000	1.00	10000	10000	98.0%	200	50.0%	8.8	0.25	63
Au/Zn-CeO_2	80	25000	0.42	10000	10000	98.0%	200	42.0%	3.7	0.21	8
Au/ZnO	80	30000	0.50	10000	10000	97.0%	300	58.0%	4.4	0.19	64
Au/Zn-CeO_2	80	120000	2.00	10000	10000	98.0%	200	38.0%	17.6	0.19	8
Au/CeO_2	80	120000	2.00	10000	12500	98.0%	200	37.0%	17.6	0.19	65
Au /Ce-Mn-O_x	80	30000	0.50	13300	13300	97.8%	292.6	49.0%	5.8	0.17	66
Au/Ce-Cu-O_x	120	60000	1.00	20000	10000	98.0%	400	60.0%	17.6	0.15	67
1% Au/CeO_2	90	60000	1.00	20000	20000	98.0%	400	49.0%	13.6	0.12	62
1% Au/CeO_2	90	60000	1.00	20000	20000	98.0%	400	49.0%	17.6	0.12	62
1% Au/CeO_2 nanorods	57	30000	0.50	10000	10000	95.0%	500	50.0%	4.4	0.10	68
1% Au/CeO_2	132	30000	0.50	10000	10000	95.0%	500	50.0%	4.4	0.10	69
3 %Au/CeO_2	90	120000	2.00	10000	12500	96.0%	400	39.0%	5.9	0.10	65
1% Au/Ce_2AlO_x	60	60000	1.00	20000	20000	97.0%	600	52.0%	13.6	0.09	62
Au/CeO_2-Co_2O_3	80	30000	0.50	10000	10000	94.0%	600	52.0%	4.4	0.09	70
1.6 %Au/CeO_2	120	18000	0.30	10000	20000	98.0%	200	15.0%	1.6	0.07	71

Catalyst	Temp °C	GHSV ($mL/g_{cat}/hr$)	GHSV ($L/g_{cat}/min$)	Feed CO (ppm)	Feed O_2 (ppm)	CO % Conv	CO slip (ppm)	O_2 selectivity	Nominal Activity ($mol_{CO}/mol_{Au}/min$)	FOM %/ppm	ref
$Au/CeO_2/TiO_2$	80	30000	0.50	10000	10000	93.0%	700	52.0%	4.4	0.07	72
5% Au/Fe_2O_3	80	12000	0.20	9000	9000	92.0%	720	47.0%	0.2	0.07	1
4.3 % Au/CeO_2	40	96000	1.60	10000	10000	90.0%	1000	58.0%	3.3	0.06	73
Au /Ce-Co-O	80	30000	0.50	10000	10000	91.0%	900	51.0%	4.4	0.06	74
Au/MnO_2-CeO_2	80	30000	0.50	13300	13300	92.0%	1064	60.0%	5.8	0.06	66
Au /Fe-Ce-O_x	75	60000	1.00	20000	10000	95.0%	1000	56.0%	17.6	0.06	75
1% Au-Pt/CeO_2	90	30000	0.50	10000	10000	90.0%	1000	50.0%	4.4	0.05	76
1% Au/CeO_2 nanocubes	57	30000	0.50	10000	10000	90.0%	1000	48.0%	4.4	0.05	68
Au/ZnO-Fe_2O_3	80	30000	0.50	10000	10000	90.0%	1000	42.0%	4.4	0.04	77
2.1 %Au/CeO_2	120	240000	4.00	10000	10000	90.0%	1000	40.0%	16.7	0.04	78
3% Au/CeO_2	80	30000	0.50	10000	10000	84.7%	1530	57.4%	4.4	0.04	13
Au /Mn-Ce-O_x	120	12000	0.20	15000	15000	90.0%	1500	55.0%	2.6	0.04	79
Au/TiO_2	80	57300	0.96	10000	10000	85.0%	1500	55.0%	8.4	0.04	44
2.8% Au/CeO_2 nanocrystals	20	n/a	n/a	8000	4000	65.0%	2800	99.7%	0.0	0.04	16
2.8% Au/CeO_2 nanocrystals	30	n/a	n/a	8000	4000	64.0%	2880	99.7%	0.0	0.03	16
2.8% Au/CeO_2 nanocrystals	40	n/a	n/a	8000	4000	63.0%	2960	99.7%	0.0	0.03	16
2.8% Au/CeO_2 nanocrystals	60	n/a	n/a	8000	4000	60.0%	3200	99.7%	0.0	0.03	16
2.8 % Au/CeO_2	25	150,000	2.50	8000	4000	60.0%	3200	99.0%	6.3	0.03	16
1% Au/Ce_2AlO_x	60	60000	1.00	20000	20000		1800	49.0%	13.6	0.03	62
1% Au/CeO_2	25	30000	0.50	13000	13000	80.0%	2600	65.0%	5.7	0.03	66
Au/CeO_2	60	165000	2.75	10000	40000	60.0%	4000	99.7%	16.1	0.02	1
3 %Au/CeO_2	75	30000	0.50	10000	10000	80.0%	2000	38.0%	1.5	0.02	13
1% Au/Al_2O_3	70	60000	1.00	20000	20000	85.0%	3000	52.0%	13.6	0.02	62
1% Au/Fe_2O_3	80	25000	0.42	10000	12500	65.0%	3500	60.0%	2.4	0.02	8

Catalyst	Temp °C	GHSV (mL/g_{cat}/hr)	GHSV (L/g_{cat}/min)	Feed CO (ppm)	Feed O_2 (ppm)	CO % Conv	CO slip (ppm)	O_2 selectivity	Nominal Activity (mol_{CO}/mol_{Au}/min)	FOM %/ppm	ref
3 %Au/CeO_2	75	30000	0.50	10000	10000	80.0%	2000	38.0%	1.5	0.02	13
1% Au/Al_2O_3	70	60000	1.00	20000	20000	85.0%	3000	52.0%	13.6	0.02	62
1% Au/Fe_2O_3	80	25000	0.42	10000	12500	65.0%	3500	60.0%	2.4	0.02	8
1.4 % Au/CeO_2	100	60000	1.00	10000	10000	76.0%	2400	40.0%	6.3	0.02	80
Au/CeO2-Fe_2O_3	80	120000	2.00	10000	12500	80.0%	2000	33.0%	17.6	0.02	81
Au/MnO_x-CeO_2	80	12000	0.20	15000	15000	74.0%	3900	63.0%	2.6	0.02	79
Au /Ce-Fe-O_x	107	120000	2.00	10000	12500	70.0%	3000	38.0%	17.6	0.01	81
Au/$CeZnO_x$	80	18000	0.30	20000	10000	70.0%	6000	73.0%	5.3	0.01	75
1% Au/CeO_2	80	12000	0.20	9000	9000	68.0%	2880	35.0%	0.8	0.01	1
1% Au/CeO_2	162	75000	1.25	10000	10000	65.0%	3500	40.0%	11.0	0.01	17
Au/$CeFeO_x$	80	18000	0.30	20000	10000	70.0%	6000	67.0%	5.3	0.01	75
1% Au/CeO_2 polyhedra	57	30000	0.50	10000	10000	65.0%	3500	38.0%	4.4	0.01	68
1% Au/CeO_2	150	30000	0.50	10000	10000	70.0%	3000	30.0%	4.4	0.01	82
Au/$CeZrO_x$	80	18000	0.30	20000	10000	65.0%	7000	66.0%	5.3	0.01	75
Au/CeO_2	90	110000	1.83	10000	15000	20.0%	8000	20.0%	10.7	0.00	83

4. Additional Characterization Data

4.1. **XPS Data.** XPS spectra were collected on a Kratos Analytical Axis Ultra DLD spectrometer, equipped with a monochromatic Al-Kα excitation source (hv = 1486.6 eV), a delay-line detector system, and a hemispherical sector analyzer. The powdered catalysts were finely ground using a mortar and pestle. Powder mounting substrates were prepared by fastening a 5mm x 5mm square of 3M double-sided tape to a piece of Si wafer with dimensions of about 1 x 1 cm. The catalyst powder was pressed into the surface of the 3M tape in a manner that completely covered the adhesive. Each powder sample was individually mounted. Loose particles were removed from each sample mount by blowing the surface off with a jet of dry nitrogen. Four or five powder mounts were placed on the sample bar for analysis. Each mount was secured to the sample bar with a 5mm x 5 mm piece of 3M double-sided tape, so the individual mounts are electrically insulated from the sample bar. All spectra were acquired with the charge neutralizer on. Analytical chamber pressures were in the mid 10-8 torr range. The x-ray gun anode voltage and current were 14 keV and 20 mA respectively. Survey scans were acquired at a pass energy of 80 eV, a step size of 0.5 eV, and dwell time of 150 ms. High-resolution Au 4f spectra were acquired at a pass energy of 20 eV, a step size of 0.5 eV, and a dwell time of 2500 ms.

Carbon levels on the sample were too low to provide reliable charge referencing, so the binding energy scale was calibrated by setting the Al2p peak at 74 eV. All spectra were analyzed using CasaXPS software. The Au peaks in the raw data were difficult to see due to the presence of the Al2p energy loss feature, so the spectra have been plotted with the (linear) background subtracted.

4.2. X-ray Diffraction (XRD) Data. The X-ray diffraction (XRD) pattern was collected on a PANalytical Empyrean diffractometer with Cu Kα radiation at 45 kV and 40 mA. Fixed slit para-focusing geometry was utilized with 0.04 radians soller slits, 10 mm beam mask, a 0.25° divergence and a 0.5° anti-scatter slit on the incidence side. Divergent optics included a 0.25° anti-scatter slit, 0.04 radians soller slits, and a nickel filter. A PIXcel detector in 1D scanning mode with PSD length of 3.35° was used.

Based on the background subtracted spectrum, the alumina is most consistent with the γ-phase (cubic), as shown by the fit of red lines above.

EXAMPLE 3: Evidence for common mechanism on Au/TiO_2 and Au/Al_2O_3.

To better understand the factors that control CO oxidation catalysis over supported Au nanoparticles, we performed a detailed comparison between a Au/TiO_2 and a Au/Al_2O_3 catalyst. Support effects have long been reported as being important in this reaction, and our choices here allow us to compare reducible (TiO_2) and non-reducible (Al_2O_3) supports. This comparison is particularly important given the lore associated with gold catalysts, and the potential role of reducing the support during the catalysis. Figure 22 shows the CO oxidation activity at low conversions (< 12%) for both catalysts plotted against the feed water content. Both catalysts show similar trends in activity, reaching a maximum around 300-600 Pa water. The Au/TiO_2 catalyst is substantially more active at the lowest water contents, but is only about 2.5 more active at this maximum.

Water adsorption studies. Figure 22 shows that the catalytic behavior of Au/Al_2O_3 and Au/TiO_2 are generally very similar with respect to water, particularly the reaction orders. Our previous work, and that of others, has shown that water is a key co-catalyst in CO oxidation over Au.*refs In particular, our work showed that weakly adsorbed water on the support was the key catalytic species on Au/TiO_2. This weakly adsorbed water, which we hereafter refer to simply as "wH_2O", is somewhat arbitrarily defined as water that can be removed with flowing N_2 at 120 °C. To better characterize this water, we followed the adsorption of this water onto the dried catalysts using infrared spectroscopy. Following the δ(HOH) bending vibration centered around 1640 cm^{-1} ensured that we only monitored changes in the amount of surface water, and not any potential changes in the surface hydroxyl groups.

Figure 23A shows the adsorption isotherms for wH_2O on the two catalysts. The isotherms are well described by the Langmuir adsorption model; linear Langmuir plots and extracted equilibrium constants for wH_2O binding to the catalysts (K_{wH2O}) are shown in Figure 23B. The equilibrium constants are essentially the same; the small differences between the two measured values are unlikely to account for the differences in catalytic activity. Further, Au is widely considered to be hydrophilic *ref and control experiments indicate that the observed adsorption is consistent with adsorption on the support and not on Au.

Although water is a key co-catalyst, having too much water in the feed is clearly detrimental to catalytic activity.[5] We therefore examined the effect of added water on CO adsorption using infrared spectroscopy in a transmission flow cell. Figure 24 shows the results of two studies. First, we flowed a 1% CO/N2 gas feed over a dried Au/TiO2 sample to allow the CO to adsorb onto the catalyst. The feed was then passed through a water saturator and the saturator temperature was adjusted to yield several different water pressures. The sample was equilibrated at each water pressure, and an infrared spectrum was recorded. The plot in figure 24A clearly shows that the Au-CO peak, which was normalized to the original Au-CO peak area, significantly drops as water was added to the system. At 720 Pa water, which is where catalytic activity begins to drop, about 35% of the CO adsorption sites have been lost. We note that the CO reaction order is still close to 0 at these water pressures.

The second experiment similarly shows the important relationship between the Au-CO binding and the amount of water on the support. In this set of experiments, the catalyst was first saturated with a 1% CO + H2O/ N2 gas feed. The water was then removed from the feed and the catalyst was dried in flowing 1% CO/N2. Infrared spectra were collected during drying and both the νCO and δHOH peaks were monitored over time. As Figure 24B clearly shows, there is an essentially linear relationship between the amount of water adsorbed on the support and the amount of CO adsorbed on the gold.

Gold is widely considered to be hydrophilic, and we see no evidence to support the conclusion that water adsorbs directly onto the Au. Rather, we believe that these results are consistent with a physical blocking of CO adsorption sites at or near the metal-support interface. As greater amounts of water are adsorbed onto the support, more of these sites are blocked, and fewer CO adsorption sites remain. In a sense, this can be thought of as a wetting of the catalyst surface and, at high enough water pressures, the water layer can become deep enough that the Au nanoparticles are “flooded” with water and can no longer readily adsorb CO. As we will discuss later, this indicates that two types of adsorption sites are important for the catalysis: CO adsorption sites on the top of the nanoparticles and O_2 adsorption sites that have access to protons from the water adsorbed on the support.
at several P_{H2O}.

Reaction kinetics. Table 2 shows the results from a study of the reaction kinetics over both catalysts. The reaction orders vary within reasonable experimental errors for different amounts of water in the feed. Both catalysts show small fractional oxygen reaction orders; the Au/Al_2O_3 oxygen order is slightly larger, but not markedly so. Similarly, the reaction order based on the amount of surface water is only slightly larger for Au/Al_2O_3. Thus, the basic reaction kinetics are essentially the same for the two catalysts.

We previously showed a substantial O-H(D) kinetic isotope effect in CO oxidation over Au/TiO_2. To measure this, we exchanged the surface water and hydroxyl groups by flowing D2O over the catalyst at ambient temperature. The reaction occurred quickly on Au/TiO_2, and the exchange was complete in 30 minutes. For Au/Al_2O_3, however, the exchange was much less facile, requiring higher temperatures (120 °C) or longer times. This is likely due, at least in part, to the much higher surface area and therefore total amount of water adsorbed on the Au/Al_2O_3 catalyst. Infrared spectra of the two catalysts after the exchange (Figure 23) showed essentially complete exchange of the OH groups for OD groups after these treatments.

After completing the H/D exchange, we measured an O-H(D) kinetic isotope effect of 1.8 ± 0.3 over the Au/Al_2O_3 (Figure 26); this is the same value as we previously reported for Au/TiO_2.[5] When 600 Pa H_2O/D_2O was added to the feed, the activity increased and the KIE value dropped to 1.4 (Figure 26). When the H_2O/D_2O was removed, the activity decreased, and the KIE increased, approaching the original value. This is consistent with the behavior we observed for Au/TiO_2[5] and consistent with the small KIE values under similar pressures of water measured by other research groups.[25]

Using the Au/TiO_2 kinetic data coupled with a DFT study, we recently proposed a new mechanism for the low temperature CO oxidation over Au/TiO_2 catalysts.[5] Scheme 1 shows a simplified schematic of the key mechanistic steps from the DFT calculations. This mechanism is consistent with the vast majority of the literature studies, especially isotope labeling studies reported by the Iglesia and Davis groups. Further, this mechanism is readily understandable in terms of simple electron pushing mechanisms, and is consistent with what one might expect using low temperature organic chemistry principles.

Scheme 1. Proposed mechanism for CO oxidation over supported gold nanoparticles with the water cocatalyst adsorbed on the support at the metal-support interface.

$$(1)\quad 2\left(Au' + CO \overset{K_1}{\leftrightarrow} Au' - CO\right)$$

$$(2)\quad Au + (H_2O)_{MSI} \overset{K_2}{\leftrightarrow} Au^*(H_2O)_{MSI}$$

$$(3)\quad Au^*(H_2O)_{MSI} + O_2 \overset{K_3}{\leftrightarrow} Au^* - OOH + (OH^-)_{MSI}$$

$$(4)\quad Au^* - OOH + Au' - CO \overset{K_4}{\leftrightarrow} Au' - COOH + Au^* - O$$

$$(5)\quad Au' - COOH + (H_2O)_{MSI} \overset{k_5}{\rightarrow} Au' + CO_2 + (H_3O^+)_{MSI} \qquad RDS$$

$$(6)\quad Au^* - O + Au' - CO \overset{k_6}{\rightarrow} Au + Au' + CO_2 \qquad very\,fast\,step$$

$$(7)\quad \boldsymbol{overall\,reaction}\text{:}\ 2\,CO + O_2 \rightarrow 2\,CO_2$$

Since the reaction kinetics (water, CO, and O_2 reaction orders; KIE) are essentially the same for Au/Al_2O_3 and Au/TiO_2, the two catalysts almost certainly operate with essentially the same reaction mechanism. This has important implications for other mechanisms suggested in the literature, primarily mechanisms that invoke a reduction of the titania support. In essence, the reaction kinetics indicate that, while titania is a reducible support, that reducibility (which leads to O vacancies on the surface) does not appear to play an important role in CO oxidation catalysis under the reaction conditions that we have studied. The logic behind this conclusion is as follows: Alumina cannot be reduced under the reaction conditions we have studied; therefore, oxygen vacancies cannot be invoked in the reaction mechanism for Au/Al_2O_3. Since the reaction kinetics are essentially identical for Au/Al_2O_3 and Au/TiO_2, the two catalysts almost certainly operate via the same reaction mechanism. Therefore, oxygen vacancies and the reducibility of titania should not be invoked to explain the catalysis on Au/TiO_2 under these reaction conditions.

The strong positive effect of water on the catalysis is also inconsistent with O vacancies playing an important role, as water would be expected to rapidly block these sites. Similarly, there is little evidence for oxygen activation on alumina, which would be necessary for a Mars-Van Krevelen type mechanism. Therefore, it is unlikely that this is an important pathway for Au/TiO_2, at least under our reaction conditions (near room temperature, in the presence of water), where the catalysis is fastest. We note that other mechanisms may well be possible under other conditions, particularly low temperature and high vacuum studies in the absence of water. Indeed, the mechanism recently proposed by Neurock and Yates, which invokes a Ti-O-O-Au intermediate under low temperature UHV conditions, goes through fundamentally very similar O_2 activation chemistry as the mechanism that we propose.

There may be other reaction conditions where the reducibility of titania plays a more important role in catalytic activity. Since water plays a critical role as a co-catalyst (Scheme 1), studies performed in the absence of water may provide insight into these processes. Similarly, we cannot comment directly on mechanisms that might be available on other supports beyond suggesting that it would be prudent to investigate the possible mechanistic role(s) of water in the catalysis, since water is extremely difficult to exclude from oxide supports, even when using UHP gasses. Once this possibility is evaluated, the reducibility of the support may indeed be important for some metal oxide supports. However, based on the reaction kinetics of Au/Al_2O_3 and Au/TiO_2, and contrary to many reports in the literature, the reducibility of titania does not appear to play a significant role in the fast room temperature catalytic activity.

The importance of the metal-support interface is well recognized in the literature, and our previous work suggested that the number of active sites depended on the amount of water adsorbed on the support.[5] Similarly, this reaction is well recognized to be controlled by O_2 binding, which DFT calculations have shown to be a perimeter or near-perimeter Au sites that have access to water adsorbed on the support.[5] Our previous work[5,35,57,84,85] has shown that an "active site" model for the catalysis, which employs some of the core ideas of Michaelis-Menten kinetics, can be useful in evaluating and comparing catalysts. These treatments have been particularly useful in identifying changes to catalytic activity that result from changes in the number of active sites[5,35,57,84] versus to changes to the inherent reactivity of the active site.[85]

Our previous kinetic model did not include a role for water in the reaction mechanism; we therefore developed a new kinetic treatment based on the mechanism proposed in Scheme 1.

We therefore considered the number of active sites to be Au atoms in close proximity to water molecules adsorbed on the support. (Eq. XX). Using this information, we derived the following rate expression:

Based on these mechanistic elements, we derived the following rate expression:

$$(X) \quad Rate = k_5\, K_4'\, [(H_2O)_{MSI}][Au_T'] \left\{ \frac{K_3'\, P_{O_2}}{1 + K_3'\, P_{O_2}} [Au_T^*] \right\}$$

Inverting this rate expression creates a double-inverse expression,

$$(X) \quad \frac{1}{Rate} = \frac{K_3' k_5\, K_4'\, [(H_2O)_{MSI}][Au_T'][Au_T^*]}{k_5\, K_4'\, [(H_2O)_{MSI}][Au_T'][Au_T^*]} \left(\frac{1}{P_{O_2}} \right) + \frac{1}{k_5\, K_4'\, [(H_2O)_{MSI}][Au_T'][Au_T^*]}$$

This expression can be simplified to

$$(X) \quad \frac{1}{Rate} = \frac{K_R}{v_{max}} \left(\frac{1}{P_{O_2}} \right) + \frac{1}{v_{max}}$$

When defining the v_{max} and K_R terms as

$$(X) \quad v_{max} = k_5\, K_4'\, [(H_2O)_{MSI}][Au_T'][Au_T^*]$$

$$(X) \quad K_R = v_{max} K_3'$$

Which has the corresponding double reciprocal form:

Double reciprocal plots of O_2 dependence data collected at various pressures of added water (see SI) can then be used to extract K_R and υ_{max} kinetic parameters that describe the catalysts under those specific conditions. These parameters are plotted as a function of the added water content in (expressed in terms of the coverage of weakly bound water) in Figure 27, and allow for a number of conclusions regarding each catalyst. First, the K_R values are relatively constant for each catalyst, suggesting that added water has little effect on the electronics of the active site. This is consistent with the proposed mechanism, and indicates water's primary role as a proton donor and acceptor.

The active site kinetic treatment indicates that the Au/Al2O3 and Au/TiO2 catalysts have very similar intrinsic reactivity for CO oxidation. The primary difference between the two catalysts is in the number of active sites. This difference is clearly tied to the amount of weakly adsorbed water on the catalyst; however, the strength of adsorption of water on the catalysts is identical (Figure 23). The only significant difference we have observed between the two catalysts that might be tied to the difference in activity is the much slower rate of H/D exchange over Au/Al2O3. This suggests that the differences in activity might be indirectly tied to the reactivity of either the surface hydroxyl groups, or some other adsorbed surface species.

We,[5] and others[22,25,47], have shown that weakly adsorbed water is critical for achieving high activity, and functions as a co-catalyst during CO oxidation.[5,25] Therefore, differences in catalytic activity might be attributable to differences in water adsorption. The distinction between the weakly adsorbed water and all water adsorption is an important one. Our previously reported kinetic correlations, as well as the correlations reported above, relate catalytic activity to the amount of weakly adsorbed water. The weakly adsorbed water was defined as water that readsorbs after drying at 120 °C. However, water can adsorb as an in-tact molecular species or at a bridging Ti-O-Ti site, creating two surface hydroxyls. By monitoring the δ(HOH) bending vibration at ~1640 cm^{-1} as a function of water pressure, which can only be due to molecular water, the IR spectra allow us to readily distinguish between these two possible adsorption modes.

Figure 23 shows adsorption isotherms for weakly adsorbed water measured by infrared spectroscopy. Although there are large differences in the total amount of water adsorbed, these are largely attributed to the differences in the support surface area. Linear Langmuir plots of the data show that the adsorption thermodynamics are essentially identical for the two catalysts. This is perhaps not surprising – the adsorption energy for water adsorbing as a molecular species on surface hydroxyls, which is dominated by hydrogen bonding interactions, might be expected to be relatively insensitive to the underlying metal oxide structure.

We previously investigated pretreatment effects on the catalytic activity of Au/TiO2, and found that surface carbonates appeared to play an important role in the catalytic activity.[35] To briefly recap this study, we showed that the CO oxidation reaction produces surface carbonates adsorbed on the support. Although these species do not affect CO adsorption on Au, CO oxidation activity was inversely proportional to the amount of carbonates generated. The observed carbonates were not reaction intermediates, and could not be removed at near-ambient temperatures. Based on our current understanding of the role of water in the reaction mechanism, it now seems likely that the carbonates likely poison the reaction either by excluding water from the active sites at the metal-support interface or by physically blocking those interface sites (Figure 28). This suggests an intimate relationship between surface water, carbonates, and catalytic activity.

We have also found that the surface carbonates bind more strongly to titania than to aluminia. Figure 29 shows that higher temperatures are required to remove carbonates from alumina. Table 9, Figure 4, and Figure 30 show that the presence of surface carbonates reduces the water adsorption capacity of the catalyst. Water also blocks some CO adsorption sites, as shown in Figure 31.

Table 9. Effects of catalyst treatment on water adsorption capacity

Treatment	S_{max}
None	936
H_2 250°C 16 hr	715
20C 16hr (reg 1)	887
With carbonates	632
H_2&O_2 2hr + 20C 16 hr (reg 2)	854

EXAMPLE 4: Oxidation of 1% CO in presence of 60% H_2 at 50 °C using Au/Al_2O_3 catalyst.

Using the experimental setup shown in Figure 5, 30 mg of Au/Al_2O_3 catalyst was diluted in 1200 mg of inert Silicon Carbide and loaded to the plug flow reactor. 140 mL/min of a 1% CO, 1.3% O_2, 60% H_2 and 4000 Pa of water (approx. 4%) was fed to the reactor (SV=3.5L/g_{cat}/min). After 30 minutes stabilization at 50 °C, the water content in the gas is reduced by decreasing the temperature of the saturator (Fig 5). The example (Figure 32) shows that CO slip of about 100 ppm can be reached with appropriate water coverage on the catalyst, while simultaneously achieving very high O_2 selectivity.

EXAMPLE 5: Oxidation of 1% CO in presence of 60% H_2 at 80 °C using Au/TiO_2 catalyst.

This example shows that the system can be operated as a single stage reactor. Low CO slips can be achieved; however, O_2 selectivity, while good, is not as high as when the system is operated with a second stage catalyst at lower temperature.

EXAMPLE 6: Oxidation of 1% CO in presence of 60% H_2 at 40 °C using Au/Al_2O_3 catalyst. Effect of pretreatment of the catalysts.

The example shows CO oxidation activity at 40 °C vs moisture content in the gas for Au/Al_2O_3 using two different heating protocols: fast heating under a flow of water and slow heating under the reaction mixture. Each point corresponds to steady state conditions after 30 min [60 mg of untreated Au/Al_2O_3 catalyst (space velocity= 2.33 L/g_{cat}·min, 1% CO, 1.4% O_2, 70% H_2)].

EXAMPLE 7: PROx data for several catalysts

Catalyst	Preparation	Pretreatment	CO slip (ppm)	O2 selectivity (%)	Temp (C)	SV (L/gAu/s)
1% Au/Al2O3	WGC	H2O, 1 hr @ 120 °C	56	56	60	5.2
2% Au/Al2O3	Urea DP	10% H2, 10% O2, 1 hr @ 100 °C	12	65	40	1.9
2% Au/TiO2	Urea DP	1 hr @ 100 °C 10% H2, 10% O2	5500	62	40	1.9
2% Au/Fe2O3	Urea DP	H2O, 1 hr @ 120 °C	6300	65	40	1.9
1.98% Au/TiO2	NaOH DP	10% H2, 10% O2, 1 hr @ 100 °C	550	58	40	2.0
2.28% Au/Al2O3	NaOH DP	10% H2, 10% O2, 1 hr @ 100 °C	1900	64	40	1.7
3.15% Au/Al2O3	NaOH DP	2 hr @ 300 °C + 20% O2 followed by 1 hr @ 120 °C + H2O	130	62	40	4.9

** all experiments done with 1.4% O2, 1% CO, 60% H2 and balance N2/He. Water content was constant at 20 Torr. H2O **

EXAMPLE 8: Oxidation of 1% CO in presence of 60% H_2 at 50 °C using Au/ZnO catalyst

Using the experimental setup shown in Figure 5, 20 mg of Au/ZnO catalyst was diluted in 1200 mg of inert Silicon Carbide and loaded to the plug flow reactor. 140 mL/min of a 1% CO, 1.3% O_2, 60% H_2 and 4000 Pa of water (approx. 4%) was fed to the reactor (SV=3.5L/g_{cat}/min). After 30 minutes stabilization at 80 °C, the water content in the gas is reduced by decreasing the temperature of the saturator (Fig 5). The example (Figure 35) shows that CO slip of about 100 ppm can be reached with appropriate water coverage on the catalyst, while simultaneously achieving very high O_2 selectivity.

EXAMPLE 9: Oxidation of 1% CO in presence of 60% H_2 at 50 °C using Au/SiO_2 catalyst

Using the experimental setup shown in Figure 5, 20 mg of Au/SiO_2 catalyst was diluted in 1200 mg of inert Silicon Carbide and loaded to the plug flow reactor. 140 mL/min of a 1% CO, 1.3% O_2, 60% H_2 and 4000 Pa of water (approx. 4%) was fed to the reactor (SV=3.5L/g_{cat}/min). After 30 minutes stabilization at 80 °C, the water content in the gas is reduced by decreasing the temperature of the saturator (Fig 5). The example (Figure 36) shows that CO slip of about 100 ppm can be reached with appropriate water coverage on the catalyst, while simultaneously achieving very high O_2 selectivity.

EXAMPLE 10: PROX catalysis with hydrogen oxidation catalyst at the bottom of the bed.

Using the experimental setup shown in Figure 5, 10 mg of 10% Ni/Al_2O_3 catalyst was diluted in 300 mg of inert silicon carbide and loaded to the plug flow reactor. Additionally 70 mg of Au/Al_2O_3 catalyst was diluted in 1200 mg of inert Silicon Carbide and loaded into the plug flow reactor on top of the Ni/Al_2O_3 catalyst. A feed of 1% CO,1-1.4% O_2, 60% H_2 and 20 torr of water (approx. 3 %) was fed to the reactor. After 30 minutes stabilization at 60 °C, the space velocity was varied (SV=1.5-2.6 L/g_{Au}/s). Figure 37 shows that under these conditions, both the CO and O_2 can be removed to the detection limit of the experimental apparatus. This single-stage, dual-bed reactor functions by having sufficiently high oxygen pressure to drive the CO oxidation reaction over the Au and water catalyst to completion. The Ni catalyst at the bottom of the bed removes the remaining oxygen, leaving a pure hydrogen effluent while sacrificing only 2% of the hydrogen.

The entire contents of each of the below-cited literature are hereby incorporated by reference.

Cited Literature

(1) Landon, P.; Ferguson, J.; Solsona, B. E.; Garcia, T.; Al-Sayari, S.; Carley, A. F.; Herzing, A. A.; Kiely, C. J.; Makkee, M.; Moulijn, J. A.; Overweg, A.; Golunski, S. E.; Hutchings, G. J. *J. Mater. Chem.* **2006**, *16*, 199.

(2) Schumacher, B.; Denkwitz, Y.; Plzak, V.; Kinne, M.; Behm, R. J. *J. Catal.* **2004**, *224*, 449.

(3) Lakshmanan, P.; Park, J.; Park, E. *Catal. Surv. Asia* **2014**, *18*, 75.

(4) Green, I. X.; Tang, W.; Neurock, M.; Yates, J. T., Jr. *Science* **2011**, *333*, 736.

(5) Saavedra, J.; Doan, H. A.; Pursell, C. J.; Grabow, L. C.; Chandler, B. D. *Science* **2014**, *345*, 1599.

(6) Valden, M.; Lai, X.; Goodman, D. W. *Science* **1998**, *281*, 1647.

(7) Bond, G. C.; Louis, C.; Thompson, D. T. *Catalysis by Gold* Imperial College Press: London, 2006; Vol. 6.

(8) Avgouropoulos, G.; Ioannides, T.; Papadopoulou, C.; Batista, J.; Hocevar, S.; Matralis, H. K. *Catal. Today* **2002**, *75*, 157.

(9) Grisel, R. J. H.; Nieuwenhuys, B. E. *J. Catal.* **2001**, *199*, 48.

(10) Ivanova, S.; Pitchon, V.; Petit, C.; Caps, V. *ChemCatChem* **2010**, *2*, 556.

(11) Widmann, D.; Liu, Y.; Schueth, F.; Behm, R. J. *J. Catal.* **2010**, *276*, 292.

(12) Tompos, A.; Margitfalvi, J. L.; Szabo, E. G.; Paszti, Z.; Sajo, I.; Radnoczi, G. *J. Catal.* **2009**, *266*, 207.

(13) Liu, Y.; Liu, B.; Wang, Q.; Li, C.; Hu, W.; Liu, Y.; Jing, P.; Zhao, W.; Zhang, J. *J. Catal.* **2012**, *296*, 65.

(14) Li, X.; Fang, S. S. S.; Teo, J.; Foo, Y. L.; Borgna, A.; Lin, M.; Zhong, Z. *ACS Catal.* **2012**, *2*, 360.

(15) Kim, W. B.; Voitl, T.; Rodriguez-Rivera, G. J.; Evans, S. T.; Dumesic, J. A. *Angew. Chem., Int. Ed.* **2005**, *44*, 778.

(16) Carrettin, S.; Concepcion, P.; Corma, A.; Lopez Nieto, J. M.; Puntes, V. F. *Angew. Chem., Int. Ed.* **2004**, *43*, 2538.

(17) Cargnello, M.; Gentilini, C.; Montini, T.; Fonda, E.; Mehraeen, S.; Chi, M.; Herrera-Collado, M.; Browning, N. D.; Polizzi, S.; Pasquato, L.; Fornasiero, P. *Chem. Mater.* **2010**, *22*, 4335.

(18) Singh, J. A.; Overbury, S. H.; Dudney, N. J.; Li, M.; Veith, G. M. *ACS Catal.* **2012**, *2*, 1138.

(19) Ketchie, W. C.; Murayama, M.; Davis, R. J. *Top. Catal.* **2007**, *44*, 307.

(20) Ide, M. S.; Davis, R. J. *Acc. Chem. Res.* **2014**, *47*, 825.

(21) Date, M.; Haruta, M. *J. Catal.* **2001**, *201*, 221.

(22) Date, M.; Okumura, M.; Tsubota, S.; Haruta, M. *Angew. Chem., Int. Ed.* **2004**, *43*, 2129.

(23) Calla, J. T.; Davis, R. J. *J. Catal.* **2006**, *241*, 407.

(24) Fujitani, T.; Nakamura, I. *Angewandte Chemie International Edition* **2011**, *50*, 10144.

(25) Ojeda, M.; Zhan, B.-Z.; Iglesia, E. *J. Catal.* **2012**, *285*, 92.

(26) Widmann, D.; Behm, R. J. *Acc. Chem. Res.* **2014**, *47*, 740.

(27) Kung, M. C.; Davis, R. J.; Kung, H. H. *J. Phys. Chem. C* **2007**, *111*, 11767.

(28) Haruta, M. *Faraday Discuss.* **2011**, *152*, 11.

(29) Widmann, D.; Hocking, E.; Behm, R. J. *J. Catal.* **2014**, *317*, 272.

(30) Fujitani, T.; Nakamura, I.; Akita, T.; Okumura, M.; Haruta, M. *Angewandte Chemie International Edition* **2009**, *48*, 9515.

(31) Cargnello, M.; Doan-Nguyen, V. V. T.; Gordon, T. R.; Diaz, R. E.; Stach, E. A.; Gorte, R. J.; Fornasiero, P.; Murray, C. B. *Science* **2013**, *341*, 771.

(32) Kotobuki, M.; Leppelt, R.; Hansgen, D. A.; Widmann, D.; Behm, R. J. *Journal of Catalysis* **2009**, *264*, 67.

(33) Schubert, M. M.; Venugopal, A.; Kahlich, M. J.; Plzak, V.; Behm, R. J. *J. Catal.* **2004**, *222*, 32.

(34) Ghenciu, A. F. In *Fuel Cells Compendium*; Brandon, N., Thompsett, D., Eds.; Elsevier: Oxford, UK, 2005, p 91.

(35) Saavedra, J.; Powell, C.; Panthi, B.; Pursell, C. J.; Chandler, B. D. *J. Catal.* **2013**, *307*, 37.

(36) Denkwitz, Y.; Zhao, Z.; Hoermann, U.; Kaiser, U.; Plzak, V.; Behm, R. J. *J. Catal.* **2007**, *251*, 363.

(37) Quinet, E.; Piccolo, L.; Morfin, F.; Avenier, P.; Diehl, F.; Caps, V.; Rousset, J.-L. *J. Catal.* **2009**, *268*, 384.

(38) Carrasco, J.; Hodgson, A.; Michaelides, A. *Nat. Mater.* **2012**, *11*, 667.

(39) Gong, J. *Chem. Rev.* **2011**, *112*, 2987.

(40) Ikemiya, N.; Gewirth, A. A. *J. Am. Chem. Soc.* **1997**, *119*, 9919.

(41) Pursell, C. J.; Hartshorn, H.; Ward, T.; Chandler, B. D.; Boccuzzi, F. *J. Phys. Chem. C* **2011**, *115*, 23880.

(42) Guzman, J.; Carrettin, S.; Corma, A. *J. Am. Chem. Soc.* **2005**, *127*, 3286.

(43) Bus, E.; Miller, J. T.; van Bokhoven, J. A. *J. Phys. Chem. B* **2005**, *109*, 14581.

(44) Denkwitz, Y.; Schumacher, B.; Kucerova, G.; Behm, R. J. *J. Catal.* **2009**, *267*, 78.

(45) Konova, P.; Naydenov, A.; Venkov, C.; Mehandjiev, D.; Andreeva, D.; Tabakova, T. *J. Mol. Catal. A: Chem.* **2004**, *213*, 235.

(46) Schubert, M. M.; Plzak, V.; Garche, J.; Behm, R. J. *Catal. Lett.* **2001**, *76*, 143.

(47) Costello, C. K.; Yang, J. H.; Law, H. Y.; Wang, Y.; Lin, J. N.; Marks, L. D.; Kung, M. C.; Kung, H. H. *Appl. Catal., A* **2003**, *243*, 15.

(48) Boccuzzi, F.; Chiorino, A.; Tsubota, S.; Haruta, M. *J. Phys. Chem.* **1996**, *100*, 3625.

(49) Costello, C. K.; Kung, M. C.; Oh, H. S.; Wang, Y.; Kung, H. H. *Appl. Catal., A* **2002**, *232*, 159.

(50) Gao, F.; Wood, T. E.; Goodman, D. W. *Catal. Lett.* **2010**, *134*, 9.

(51) Kim, C. H.; Thompson, L. T. *J. Catal.* **2005**, *230*, 66.

(52) Landon, P.; Ferguson, J.; Solsona, B. E.; Garcia, T.; Carley, A. F.; Herzing, A. A.; Kiely, C. J.; Golunski, S. E.; Hutchings, G. J. *Chem. Commun.* **2005**, 3385.

(53) Rossignol, C.; Arrii, S.; Morfin, F.; Piccolo, L.; Caps, V.; Rousset, J.-L. *J. Catal.* **2005**, *230*, 476.

(54) Shodiya, T.; Schmidt, O.; Peng, W.; Hotz, N. *J. Catal.* **2013**, *300*, 63.

(55) Auer, B.; Kumar, R.; Schmidt, J. R.; Skinner, J. L. *PNAS* **2007**, *104*, 14215.

(56) Hartshorn, H.; Pursell, C. J.; Chandler, B. D. *J. Phys. Chem. C* **2009**, *113*, 10718.

(57) Chandler, B. D.; Kendell, S.; Doan, H.; Korkosz, R.; Grabow, L. C.; Pursell, C. J. *ACS Catalysis* **2012**, *2*, 684.

(58) Manasilp, A.; Gulari, E. *Appl. Catal., B* **2002**, *37*, 17.

(59) Kim, D. H.; Lim, M. S. *Appl. Catal., A* **2002**, *224*, 27.

(60) Galletti, C.; Fiorot, S.; Specchia, S.; Saracco, G.; Specchia, V. *Chem. Eng. J. (Amsterdam, Neth.)* **2007**, *134*, 45.

(61) Avgouropoulos, G.; Manzoli, M.; Boccuzzi, F.; Tabakova, T.; Papavasiliou, J.; Ioannides, T.; Idakiev, V. *J. Catal.* **2008**, *256*, 237.

(62) Fonseca, J.; Royer, S.; Bion, N.; Pirault-Roy, L.; Rangel, M. d. C.; Duprez, D.; Epron, F. *Appl. Catal., B* **2012**, *128*, 10.

(63) Arzamendi, G.; Uriz, I.; Dieguez, P. M.; Laguna, O. H.; Hernandez, W. Y.; Alvarez, A.; Centeno, M. A.; Odriozola, J. A.; Montes, M.; Gandia, L. M. *Chem. Eng. J.* **2011**, *167*, 588.

(64) Naknam, P.; Luengnaruemitchai, A.; Wongkasemjit, S. *Energy Fuels* **2009**, *23*, 5084.

(65) Avgouropoulos, G.; Papavasiliou, J.; Tabakova, T.; Idakiev, V.; Ioannides, T. *Chem. Eng. J.* **2006**, *124*, 41.

(66) Chang, L.-H.; Sasirekha, N.; Chen, Y.-W.; Wang, W.-J. *Ind. Eng. Chem. Res.* **2006**, *45*, 4927.

(67) Laguna, O. H.; Hernandez, W. Y.; Arzamendi, G.; Gandia, L. M.; Centeno, M. A.; Odriozola, J. A. *Fuel* **2014**, *118*, 176.

(68) Yi, G.; Xu, Z.; Guo, G.; Tanaka, K.-i.; Yuan, Y. *Chem. Phys. Lett.* **2009**, *479*, 128.

(69) Luengnaruemitchai, A.; Osuwan, S.; Gulari, E. *Int. J. Hydrogen Energy* **2004**, *29*, 429.

(70) Wang, H.; Zhu, H.; Qin, Z.; Liang, F.; Wang, G.; Wang, J. *J. Catal.* **2009**, *264*, 154.

(71) Liao, X.; Chu, W.; Dai, X.; Pitchon, V. *Appl. Catal., A* **2012**, *449*, 131.

(72) Sangeetha, P.; Chen, Y.-W. *Int. J. Hydrogen Energy* **2009**, *34*, 7342.

(73) Scire, S.; Crisafulli, C.; Riccobene, P. M.; Patane, G.; Pistone, A. *Appl. Catal., A* **2012**, *417-418*, 66.

(74) Wang, H.; Zhu, H.; Qin, Z.; Wang, G.; Liang, F.; Wang, J. *Catal. Commun.* **2008**, *9*, 1487.

(75) Laguna, O. H.; Romero, S. F.; Centeno, M. A.; Odriozola, J. A. *J. Catal.* **2010**, *276*, 360.

(76) Monyanon, S.; Pongstabodee, S.; Luengnaruemitchai, A. *J. Chin. Inst. Chem. Eng.* **2007**, *38*, 435.

(77) Naknam, P.; Luengnaruemitchai, A.; Wongkasemjit, S. *Int. J. Hydrogen Energy* **2009**, *34*, 9838.

(78) Liao, X.; Chu, W.; Dai, X.; Pitchon, V. *Appl. Catal., B* **2013**, *142-143*, 25.

(79) Tu, Y.-B.; Luo, J.-Y.; Meng, M.; Wang, G.; He, J.-J. *Int. J. Hydrogen Energy* **2009**, *34*, 3743.

(80) Liotta, L. F.; Di Carlo, G.; Pantaleo, G.; Venezia, A. M. *Catal. Today* **2010**, *158*, 56.

(81) Tabakova, T.; Avgouropoulos, G.; Papavasiliou, J.; Manzoli, M.; Boccuzzi, F.; Tenchev, K.; Vindigni, F.; Ioannides, T. *Appl. Catal., B* **2011**, *101*, 256.

(82) Monyanon, S.; Pongstabodee, S.; Luengnaruemitchai, A. *Journal of Power Sources* **2006**, *163*, 547.

(83) Panzera, G.; Modafferi, V.; Candamano, S.; Donato, A.; Frusteri, F.; Antonucci, P. L. *J. Power Sources* **2004**, *135*, 177.

(84) Long, C. G.; Gilbertson, J. D.; Vijayaraghavan, G.; Stevenson, K. J.; Pursell, C. J.; Chandler, B. D. *J. Am. Chem. Soc.* **2008**, *130*, 10103.

(85) Chandler, B. D.; Long, C. G.; Gilbertson, J. D.; Vijayaraghavan, G.; Stevenson, K. J.; Pursell, C. J. *The Journal of Physical Chemistry C* **2010**, *114*, 11498.

While there have been shown and described what are presently believed to be the preferred embodiments of the present invention, those skilled in the art will realize that other and further embodiments can be made without departing from the spirit and scope of the invention described in this application, and this application includes all such modifications that are within the intended scope of the claims set forth herein.

CLAIMS

What is claimed is:

1. A preferential CO oxidation reaction (PROX) catalyst, comprising:

a plurality of Au or Ag particles having a size ranging from about 0.5 to about 20 nm;

a hydrophilic support in contact with the particles; and

about 0.1 to about 10 monolayers of water on a surface of the support.

2. The catalyst of claim 1, which comprises a plurality of Au particles.

3. The catalyst of claim 1, which comprises a plurality of Ag particles.

4. The catalyst of any of claims 1-3, wherein the particles have a size ranging from about 0.5 to about 15 nm.

5. The catalyst of any of claims 1-4, wherein the particles have a size ranging from about 0.5 to about 10 nm.

6. The catalyst of any of claims 1-5, wherein the particles have a size ranging from about 0.5 to about 5 nm.

7. The catalyst of any of claims 1-6, wherein the particles have a size ranging from about 0.5 nm to less than 5 nm.

8. The catalyst of any of claims 1-7, wherein the hydrophilic support is metal oxide, mixed metal oxide, metal hydroxide, zeolite, vermiculite, clay, silica-alumina, mixed manganese oxide, MnO_2, Al_2O_3, $Ce_{10}AlO_x$, Ce_2AlO_x, Ce-Al-O_x, Ce-Co-O, Ce-Cu-O_x, $CeFeO_x$, Ce-Fe-O_x, Ce-Mn-O_x, CeO_2, CeO_2 nanocrystal, CeO_2 nanocube, CeO_2 nanorod, CeO_2 polyhedra, CeO_2/TiO_2, CeO_2-Co_2O_3, CeO_2-Fe_2O_3, $CeZnO_x$, $CeZrO_x$, Fe_2O_3, Fe-Ce-O_x, Mn-Ce-O_x, MnO_2-CeO_2, MnO_x-CeO_2, TiO_2, Zn-CeO_2, Zn-Ce-O_x, ZnO, ZnO-Fe_2O_3, or a mixture of two or more thereof.

9. The catalyst of any of claims 1-8, wherein the hydrophilic support is Al_2O_3.

10. The catalyst of any of claims 1-9, wherein the support further comprises a promoter.

11. The catalyst of any of claims 1-10, wherein the support further comprises a promoter selected from the group consisting of alkaline metal, alkaline earth metal, alkaline metal hydroxide, alkaline earth metal hydroxide, and a mixture of two or more thereof.

12. The catalyst of any of claims 1-11, wherein the surface comprises an intersection of the support and one or more of the particles.

13. The catalyst of any of claims 1-12, which comprises about 0.1 to about 5 monolayers of water on the surface of the support.

14. The catalyst of any of claims 1-13, which comprises about 0.1 to about 2.5 monolayers of water on the surface of the support.

15. The catalyst of any of claims 1-14, which comprises about 0.5 to about 2.5 monolayers of water on the surface of the support.

16. The catalyst of any of claims 1-15, which comprises about 1 to about 2 monolayers of water on the surface of the support.

17. The catalyst of any of claims 1-16, wherein less than about 50% of the surface comprises a surface bound carbonate, bicarbonate, carboxylate, or organic carbonate.

18. The catalyst of any of claims 1-17, wherein less than about 25% of the surface comprises a surface bound carbonate, bicarbonate, carboxylate, or organic carbonate.

19. The catalyst of any of claims 1-18, wherein less than about 10% of the surface comprises a surface bound carbonate, bicarbonate, carboxylate, or organic carbonate.

20. The catalyst of any of claims 1-19, wherein less than about 5% of the surface comprises a surface bound carbonate, bicarbonate, carboxylate, or organic carbonate.

21. The catalyst of any of claims 1-20, wherein less than about 1% of the surface comprises a surface bound carbonate, bicarbonate, carboxylate, or organic carbonate.

22. The catalyst of any of claims 1-21, wherein the surface does not comprise a surface bound carbonate, bicarbonate, carboxylate, or organic carbonate.

23. The catalyst of any of claims 1-22, wherein the particles are present in an amount ranging from about 0.1 to about 60% by weight of the catalyst.

24. The catalyst of any of claims 1-23, wherein the particles are present in an amount ranging from about 0.1 to about 30% by weight of the catalyst.

25. The catalyst of any of claims 1-24, wherein the particles are present in an amount ranging from about 0.1 to about 10% by weight of the catalyst.

26. The catalyst of any of claims 1-25, wherein the particles are present in an amount ranging from about 0.5 to about 10% by weight of the catalyst.

27. A preferential CO oxidation reaction (PROX) catalyst, prepared by process comprising:

removing one or more of an adsorbed carbonate, bicarbonate, carboxylate, organic carbonate, or a mixture of two or more thereof from a surface of a supported catalyst, the supported catalyst comprising a plurality of Au or Ag particles having a size ranging from about 0.5 to about 20 nm and a hydrophilic support in contact with the particles; and

simultaneously or thereafter adsorbing about 0.1 to about 10 monolayers of water on a surface of the support.

28. A method for preparing or regenerating a preferential CO oxidation reaction (PROX) catalyst, comprising:

removing one or more of adsorbed carbonate, bicarbonate, carboxylate, organic carbonate, or a mixture of two or more thereof from a surface of a supported catalyst, the supported catalyst comprising a plurality of Au or Ag particles having a size ranging from about 0.5 to about 20 nm and a hydrophilic support in contact with the particles; and

simultaneously or thereafter adsorbing about 0.1 to about 10 monolayers of water on a surface of the support.

29. The catalyst or method of claims 27 or 28, wherein the removing comprises heating the supported catalyst to a temperature greater than about 150 °C for a time ranging from about 0 to about 16 hours.

30. The catalyst or method of claims 27 or 28, wherein the adsorbing is carried out thereafter and comprises contacting the supported catalyst with liquid H_2O or an H_2O-containing inert gas.

31. The catalyst or method of claims 27 or 28, wherein the removing comprises heating the supported catalyst to a temperature greater than about 150 °C, and wherein the adsorbing is carried out thereafter and comprises cooling the supported catalyst to a temperature of about 25 °C over a period of about 1 to about 24 hours while contacting the supported catalyst with an H_2O-containing inert gas.

32. The catalyst or method of claims 27 or 28, wherein the removing comprises contacting the supported catalyst with a diluted mixture of H_2 and O_2 gases at a temperature ranging from about 20 to about 400 °C.

33. The catalyst or method of claims 27 or 28, wherein the removing and simultaneous adsorbing comprise contacting the supported catalyst with a gaseous mixture of $O_2/N_2/He/H_2O/CO$ at a temperature ranging from about 20 to about 250 °C for a time ranging from about 0 to 5 hours.

34. The catalyst or method of claims 27 or 28, wherein the removing and simultaneous adsorbing comprise contacting the supported catalyst with a gaseous mixture of $O_2/N_2/He/H_2O/CO$ at a temperature ranging from about 20 to about 100 °C for a time ranging from about 0 to 5 hours.

35. The catalyst or method of claims 27 or 28, wherein the catalyst comprises a plurality of Au particles.

36. The catalyst or method of claims 27 or 28, wherein the catalyst comprises a plurality of Ag particles.

37. The catalyst or method of claims 27 or 28, wherein the particles have a size ranging from about 0.5 to about 15 nm.

38. The catalyst or method of claims 27 or 28, wherein the particles have a size ranging from about 0.5 to about 10 nm.

39. The catalyst or method of claims 27 or 28, wherein the particles have a size ranging from about 0.5 to about 5 nm.

40. The catalyst or method of claims 27 or 28, wherein the particles have a size ranging from about 0.5 nm to less than 5 nm.

41. The catalyst or method of claims 27 or 28, wherein the hydrophilic support is metal oxide, mixed metal oxide, metal hydroxide, zeolite, vermiculite, clay, silica-alumina, Al_2O_3, $Ce_{10}AlO_x$, Ce_2AlO_x, Ce-Al-O_x, Ce-Co-O, Ce-Cu-O_x, $CeFeO_x$, Ce-Fe-O_x, Ce-Mn-O_x, CeO_2, CeO_2 nanocrystal, CeO_2 nanocube, CeO_2 nanorod, CeO_2 polyhedra, CeO_2/TiO_2, CeO_2-Co_2O_3, CeO_2-Fe_2O_3, $CeZnO_x$, $CeZrO_x$, Fe_2O_3, Fe-Ce-O_x, Mn-Ce-O_x, MnO_2-CeO_2, MnO_x-CeO_2, TiO_2, Zn-CeO_2, Zn-Ce-O_x, ZnO, ZnO-Fe_2O_3, or a mixture of two or more thereof.

42. The catalyst or method of claims 27 or 28, wherein the hydrophilic support is Al_2O_3.

43. The catalyst or method of claims 27 or 28, wherein the support further comprises a promoter.

44. The catalyst or method of claims 27 or 28, wherein the support further comprises a promoter selected from the group consisting of alkaline metal, alkaline earth metal, alkaline metal hydroxide, alkaline earth metal hydroxide, and a mixture of two or more thereof.

45. The catalyst or method of claims 27 or 28, wherein the surface comprises an intersection of the support and one or more of the particles.

46. The catalyst or method of claims 27 or 28, wherein said adsorbing comprises adsorbing about 0.1 to about 5 monolayers of water on the surface of the support.

47. The catalyst or method of claims 27 or 28, wherein said adsorbing comprises adsorbing about 0.1 to about 2.5 monolayers of water on the surface of the support.

48. The catalyst or method of claims 27 or 28, wherein said adsorbing comprises adsorbing about 0.5 to about 2.5 monolayers of water on the surface of the support.

49. The catalyst or method of claims 27 or 28, wherein said adsorbing comprises adsorbing about 1 to about 2 monolayers of water on the surface of the support.

50. The catalyst or method of claims 27 or 28, wherein, after said removing, less than about 50% of the surface comprises a surface bound carbonate, bicarbonate, carboxylate, or organic carbonate.

51. The catalyst or method of claims 27 or 28, wherein, after said removing, less than about 25% of the surface comprises a surface bound carbonate, bicarbonate, carboxylate, or organic carbonate.

52. The catalyst or method of claims 27 or 28, wherein, after said removing, less than about 10% of the surface comprises a surface bound carbonate, bicarbonate, carboxylate, or organic carbonate.

53. The catalyst or method of claims 27 or 28, wherein, after said removing, less than about 5% of the surface comprises a surface bound carbonate, bicarbonate, carboxylate, or organic carbonate.

54. The catalyst or method of claims 27 or 28, wherein, after said removing, less than about 1% of the surface comprises a surface bound carbonate, bicarbonate, carboxylate, or organic carbonate.

55. The catalyst or method of claims 27 or 28, wherein, after said removing, the surface does not comprise a surface bound carbonate, bicarbonate, carboxylate, or organic carbonate.

56. The catalyst or method of claims 27 or 28, wherein the particles are present in an amount ranging from about 0.1 to about 60% by weight of the catalyst.

57. The catalyst or method of claims 27 or 28, wherein the particles are present in an amount ranging from about 0.1 to about 30% by weight of the catalyst.

58. The catalyst or method of claims 27 or 28, wherein the particles are present in an amount ranging from about 0.1 to about 10% by weight of the catalyst.

59. The catalyst or method of claims 27 or 28, wherein the particles are present in an amount ranging from about 0.5 to about 10% by weight of the catalyst.

60. The method of claim 28, further comprising contacting the catalyst and a feed gas comprising CO, O_2 and H_2O at a temperature ranging from about 0 to about 300 °C, to oxidize the CO.

61. A process for oxidizing CO, comprising:

contacting the catalyst of claims 1 or 27 and a feed gas comprising CO, O_2 and H_2O at a temperature ranging from about 0 to about 300 °C, to thereby oxidize the CO.

62. The process of claim 61, further comprising contacting the gas with a catalyst that removes O_2.

63. The process of claim 62, wherein the catalyst that removes O_2 is a hydrogenation catalyst.

64. The process of claim 63, wherein the hydrogenation catalyst comprises a metal on an oxide support.

65. The process of claim 64, wherein the hydrogenation catalyst comprises Ni/Al_2O_3.

66. The process of any of claims 62-65, wherein the process is performed in a dual-bed reactor system.

67. The process of any of claims 61-66, wherein the feed gas comprises O_2 and CO in an O_2/CO molar ratio of about 1,000,000:1.

68. The process of any of claims 61-67, wherein the feed gas comprises O_2 and CO in an O_2/CO molar ratio of about 100,000:1.

69. The process of any of claims 61-68, wherein the feed gas comprises O_2 and CO in an O_2/CO molar ratio of about 10,000:1.

70. The process of any of claims 61-69, wherein the feed gas comprises O_2 and CO in an O_2/CO molar ratio of about 1,000:1.

71. The process of any of claims 61-70, wherein the feed gas comprises O_2 and CO in an O_2/CO molar ratio of about 100:1.

72. The process of any of claims 61-71, wherein the feed gas comprises O_2 and CO in an O_2/CO molar ratio of about 75:1.

73. The process of any of claims 61-72, wherein the feed gas comprises O_2 and CO in an O_2/CO molar ratio of about 50:1.

74. The process of any of claims 61-73, wherein the feed gas comprises O_2 and CO in an O_2/CO molar ratio of about 20:1.

75. The process of any of claims 61-74, wherein the feed gas comprises O_2 and CO in an O_2/CO molar ratio of about 10:1.

76. The process of any of claims 61-75, wherein the feed gas comprises O_2 and CO in an O_2/CO molar ratio of about 5:1.

77. The process of any of claims 61-76, wherein the feed gas comprises O_2 and CO in an O_2/CO molar ratio of about 1:1.

78. The process of any of claims 61-77, wherein the feed gas comprises O_2 and CO in an O_2/CO molar ratio ranging from about 0.2 to about 5.

79. The process of any of claims 61-78, wherein the feed gas comprises H_2O in an amount sufficient to maintain about 0.1 to about 10 monolayers of water on the surface of the support during said contacting.

80. The process of any of claims 61-79, which produces a product gas comprising 1000 ppm or less of CO.

81. The process of any of claims 61-80, which produces a product gas comprising 100 ppm or less of CO.

82. The process of any of claims 61-81, which produces a product gas comprising 10 ppm or less of CO.

83. The process of any of claims 61-82, which produces a product gas comprising 1 ppm or less of CO.

84. The process of any of claims 61-83, which produces a product gas comprising 0.1 ppm or less of CO.

85. The process of any of claims 61-84, which comprises an O_2 selectivity for CO_2 of 30% or greater.

86. The process of any of claims 61-85, which comprises an O_2 selectivity for CO_2 of 40% or greater.

87. The process of any of claims 61-86, which comprises an O_2 selectivity for CO_2 of 50% or greater.

88. The process of any of claims 61-87, which comprises an O_2 selectivity for CO_2 of 60% or greater.

89. The process of any of claims 61-88, which comprises an O_2 selectivity for CO_2 of 70% or greater.

90. The process of any of claims 61-89, which comprises an O_2 selectivity for CO_2 of 80% or greater.

91. The process of any of claims 61-90, which comprises an O_2 selectivity for CO_2 of 90% or greater.

92. The process of any of claims 61-91, wherein the temperature ranges from about 0 to about 200 °C.

93. The process of any of claims 61-92, wherein the temperature ranges from about 0 to about 175 °C.

94. The process of any of claims 61-93, wherein the temperature ranges from about 0 to about 150 °C.

95. The process of any of claims 61-94, wherein the temperature ranges from about 10 to about 150 °C.

96. The process of any of claims 61-95, wherein the temperature ranges from about 20 to about 150 °C.

97. The process of any of claims 61-96, wherein the temperature ranges from about 20 to about 100 °C.

98. The process of any of claims 61-97, wherein the temperature ranges from about 20 to about 50 °C.

99. The process of any of claims 61-98, wherein the feed gas further comprises one or more of non-condensable hydrocarbon, high dewpoint hydrocarbon, hydrocarbon, alkane, alkene, functionalized hydrocarbon, permanent gas, hydrogen, ammonia, N_2, H_2, air, He, Ar, C_1-C_{10} hydrocarbon, or a mixture of two or more thereof.

100. The process of any of claims 61-99, which produces a first product gas comprising 1000 ppm or less of CO; and which further comprises a second process for oxidizing said CO, the second process comprising:

optionally, adding or removing one or more of O_2, H_2O, or both to or from the first product gas, to optionally form a second feed gas;

contacting the first product gas or second feed gas with a second catalyst at a temperature ranging from about 0 to about 300 °C, to thereby oxidize said CO.

101. The process of claim 100, wherein the second catalyst comprises the catalyst of claims 1 or 27.

102. The process of claim 100, wherein the process of any of claims 61-99 and the second process are carried out in separate catalyst beds.

103. The process of claim 100, wherein the temperature of the second process is lower than the temperature in the process of claim 61.

104. The process of any of claims 61-99, wherein the catalyst is distributed along a catalyst bed having an upstream portion and a downstream portion, and wherein the temperature of the upstream portion is higher than the temperature of the downstream portion.

105. The process of claim 104, wherein the temperature gradually decreases between the upstream portion and the downstream portion.

106. A dual stage process for using Au based catalysts to oxidize CO in non-condensable gas streams shown in Figure 5 (dew point > T36) comprising the steps of: decreasing initial CO concentration to 100 ppm, and finishing in a second stage until CO content is reduced to <10 ppm.

107. The method of claim 106 where the catalytic activity and selectivity is tuned by the control of adsorbed water on the catalysts.

108. A dual stage method of claim 106 where the temperature is gradually decreased between sequential operating units.

109. The method of claim 106 where activity and selectivity is preserved in the range of 0-150 ℃, and wherein water is adsorbed on the catalyst.

110. The method of claim 106 where gas mixture is comprised by high dew point hydrocarbons.

111. The method of claim 106 where gas mixture is comprised by permanent gases O_2, N_2, He, Ar, and their mixtures.

112. The method of claim 106 where gas mixture is comprised of permanent gases and hydrocarbon mixtures.

113. The method of claim 106 where gas mixture is comprised of high H_2 concentrations mixtures.

114. The method of claim 106 where the catalyst is pretreated with water vapor/O_2 mixtures to achieve high catalytic activity.

115. A single stage process for the preferential CO oxidation in gas streams using Au based catalysts where the gradual temperature decrease along the length of the bed.

116. A water based pretreatment for the Au catalysts to maximize catalytic activity.

117. A method for catalyst regeneration using a variety of gas mixtures $O_2/H_2O/N_2/CO$ that allows carbonates decomposition under mild temperatures (0-150 ℃).

FIG. 1

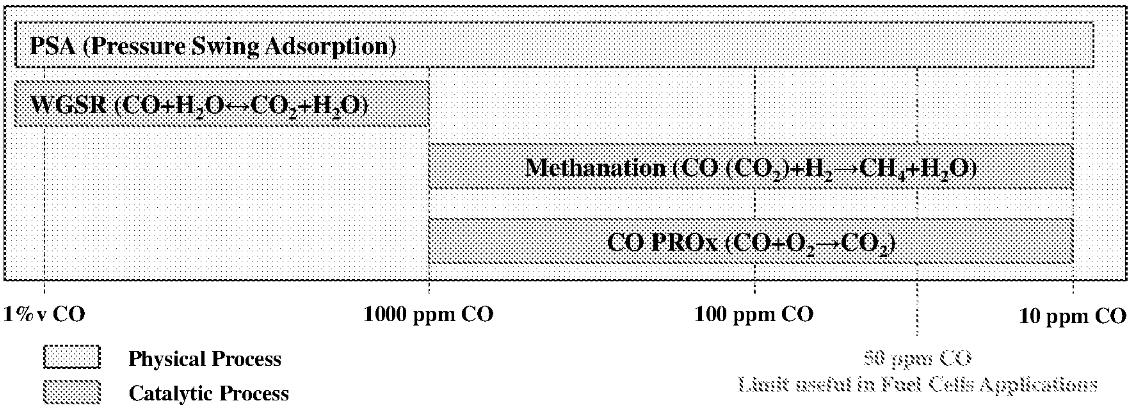
PSA (Pressure Swing Adsorption)
WGSR ($CO+H_2O \leftrightarrow CO_2+H_2O$)
Methanation (CO (CO_2)+$H_2 \rightarrow CH_4+H_2O$)
CO PROx ($CO+O_2 \rightarrow CO_2$)
1%v CO
1000 ppm CO
100 ppm CO
10 ppm CO
Physical Process
Catalytic Process
50 ppm CO
Limit useful in Fuel Cells Applications

FIG. 2

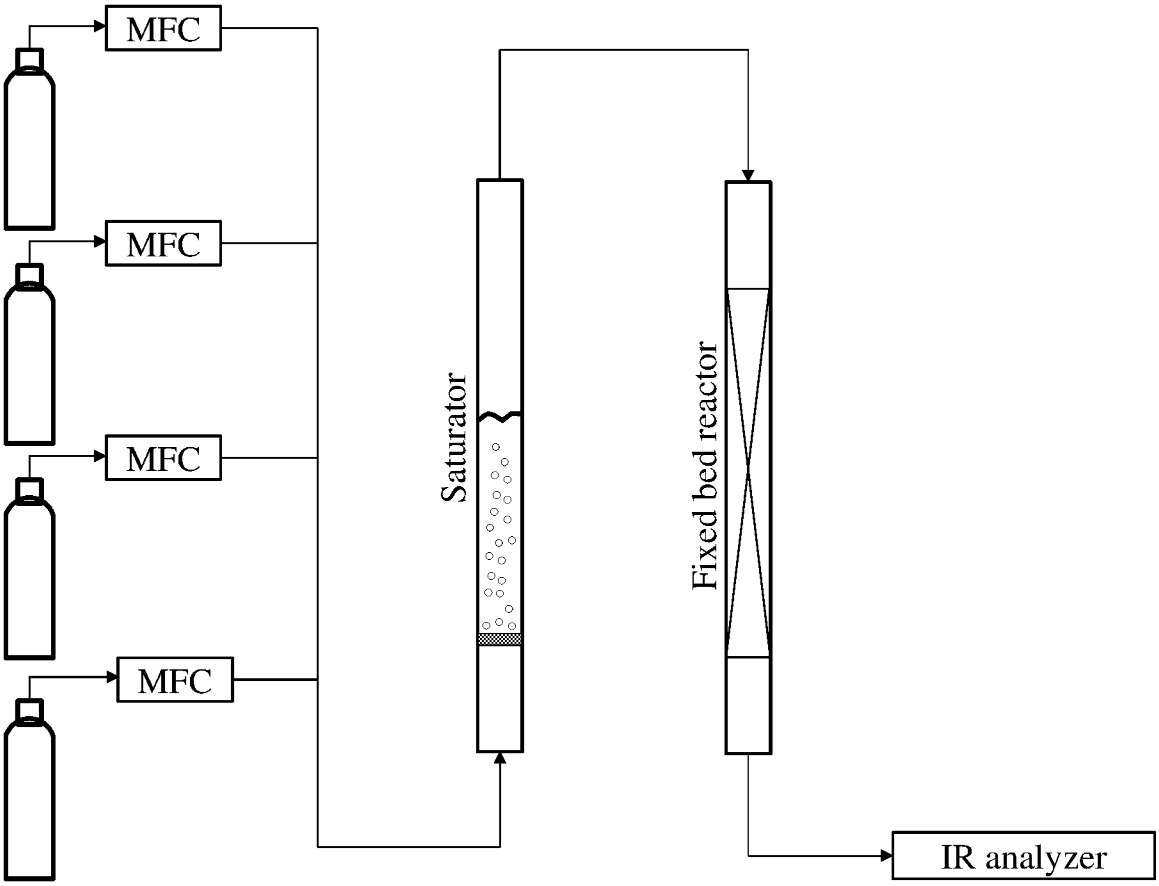
MFC
MFC
MFC
MFC
Saturator
Fixed bed reactor
IR analyzer

FIG. 3

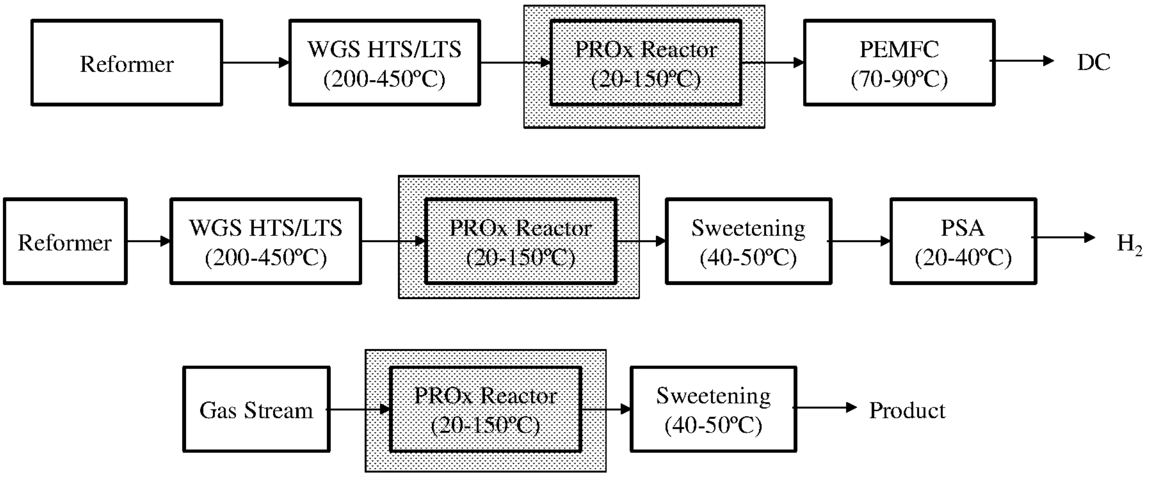
Reformer
WGS HTS/LTS (200-450°C)
PROx Reactor (20-150°C)
PEMFC (70-90°C)
DC
Reformer
WGS HTS/LTS (200-450°C)
PROx Reactor (20-150°C)
Sweetening (40-50°C)
PSA (20-40°C)
H_2
Gas Stream
PROx Reactor (20-150°C)
Sweetening (40-50°C)
Product

FIG. 4

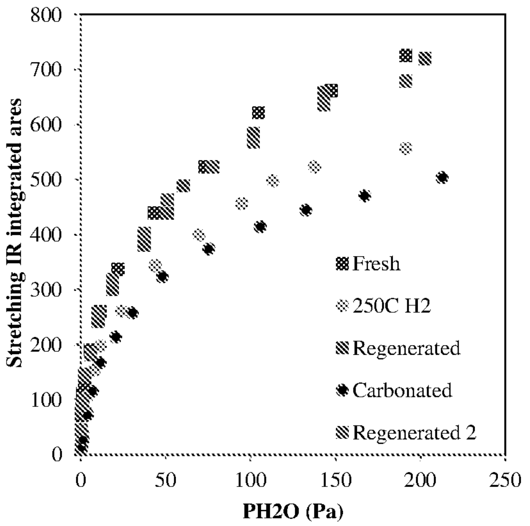
Stretching IR integrated ares
800
700
600
500
400
300
200
100
0
0
50
100
150
200
250
PH2O (Pa)
Fresh
250C H2
Regenerated
Carbonated
Regenerated 2

FIG. 5

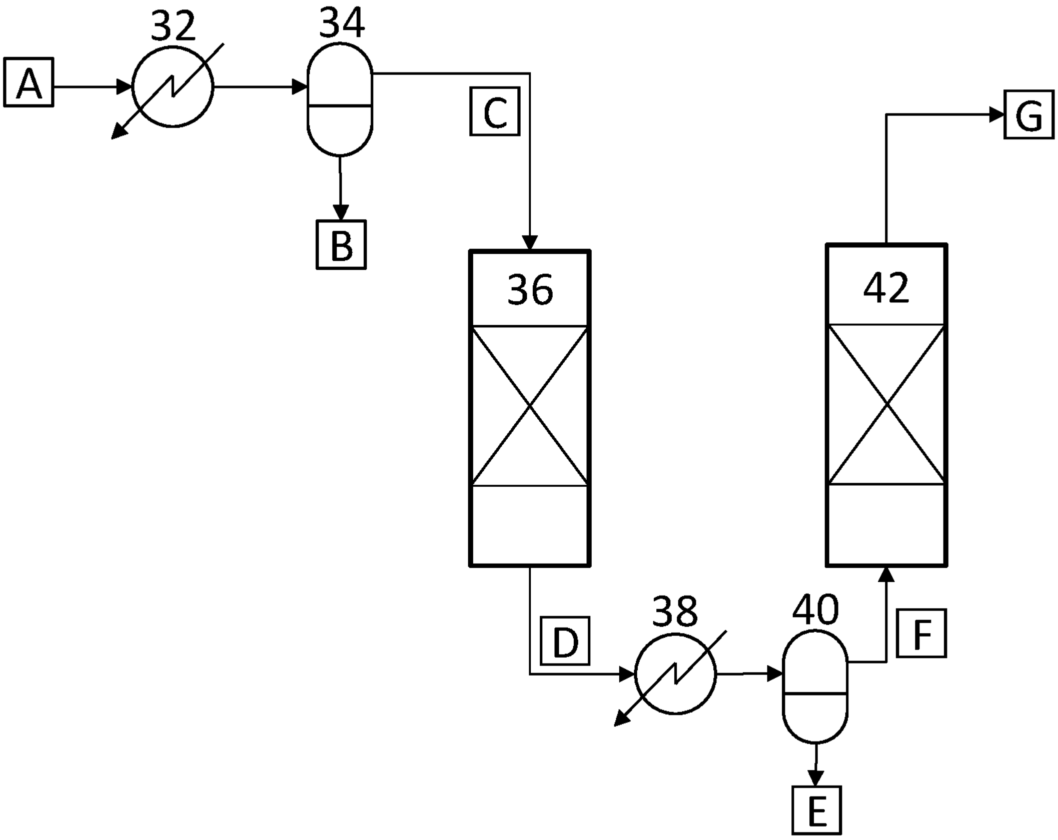

FIG. 6

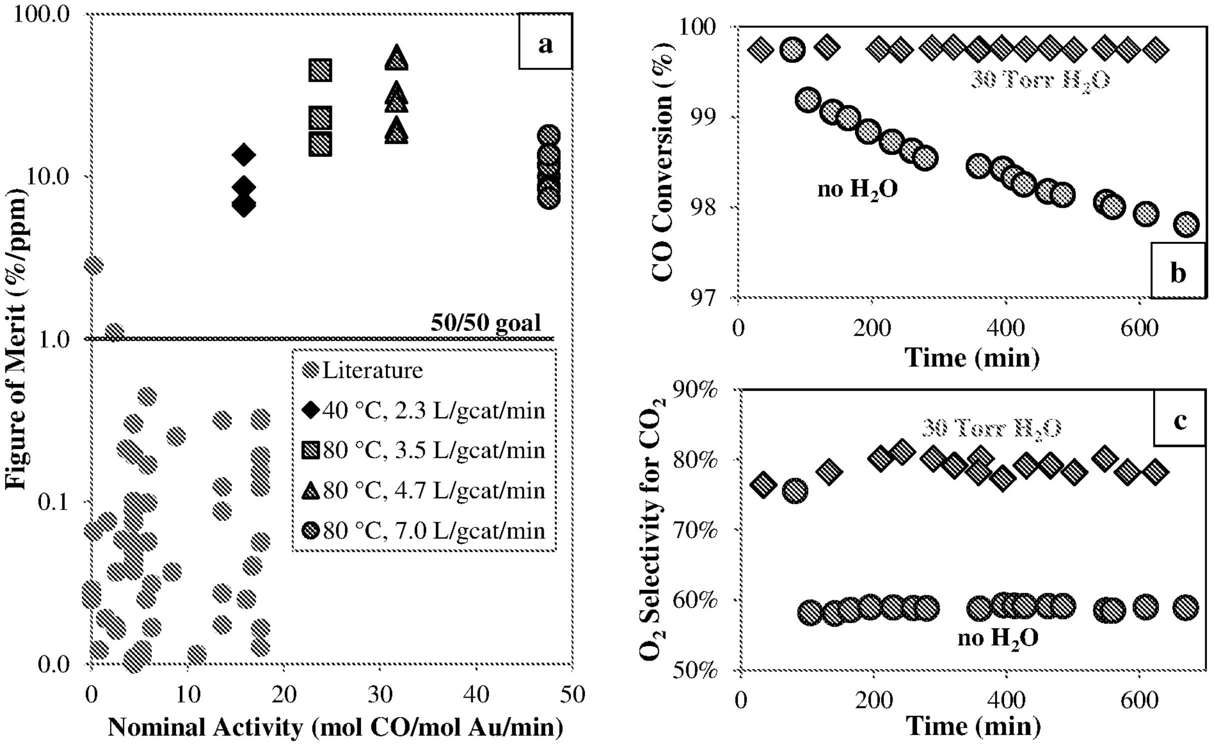
a
Figure of Merit (%/ppm)
100.0
10.0
1.0
0.1
0.0
0
10
20
30
40
50
Nominal Activity (mol CO/mol Au/min)
50/50 goal
Literature
40 °C, 2.3 L/gcat/min
80 °C, 3.5 L/gcat/min
80 °C, 4.7 L/gcat/min
80 °C, 7.0 L/gcat/min
b
CO Conversion (%)
100
99
98
97
0
200
400
600
Time (min)
30 Torr H_2O
no H_2O
c
O_2 Selectivity for CO_2
90%
80%
70%
60%
50%
0
200
400
600
Time (min)
30 Torr H_2O
no H_2O

FIG. 7

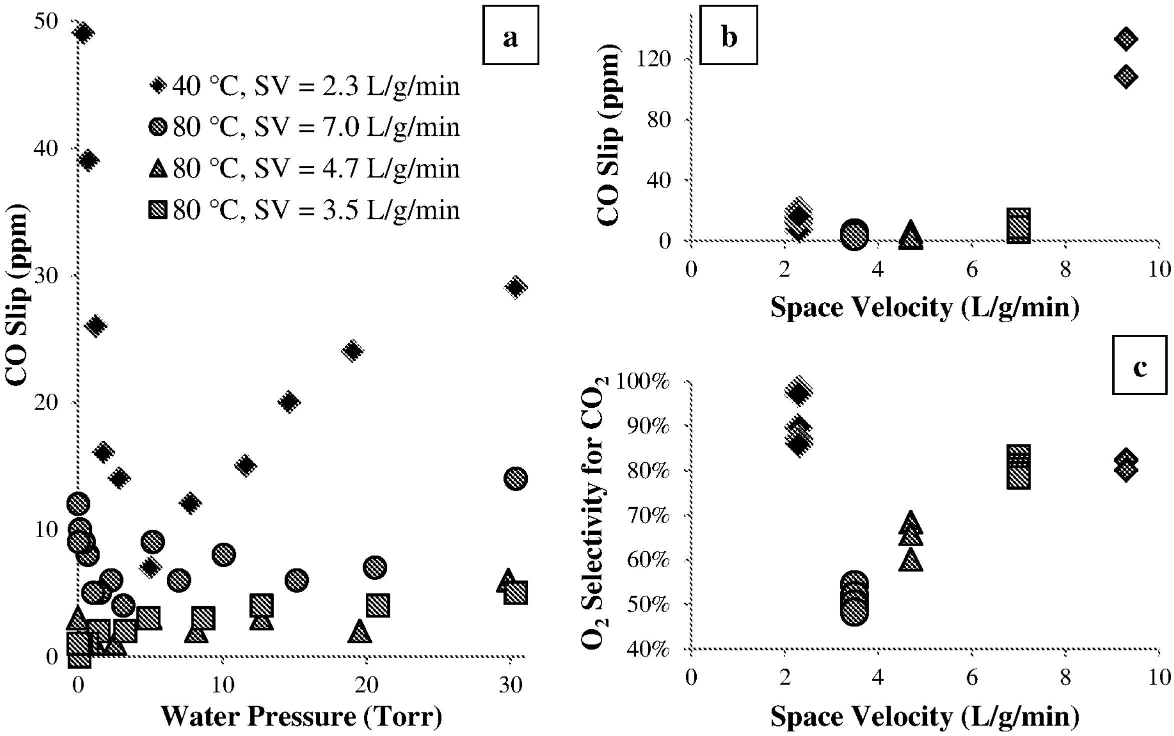
a
CO Slip (ppm)
50
40
30
20
10
0
0
10
20
30
Water Pressure (Torr)
40 °C, SV = 2.3 L/g/min
80 °C, SV = 7.0 L/g/min
80 °C, SV = 4.7 L/g/min
80 °C, SV = 3.5 L/g/min
b
CO Slip (ppm)
120
80
40
0
0
2
4
6
8
10
Space Velocity (L/g/min)
c
O_2 Selectivity for CO_2
100%
90%
80%
70%
60%
50%
40%
0
2
4
6
8
10
Space Velocity (L/g/min)

FIG. 8

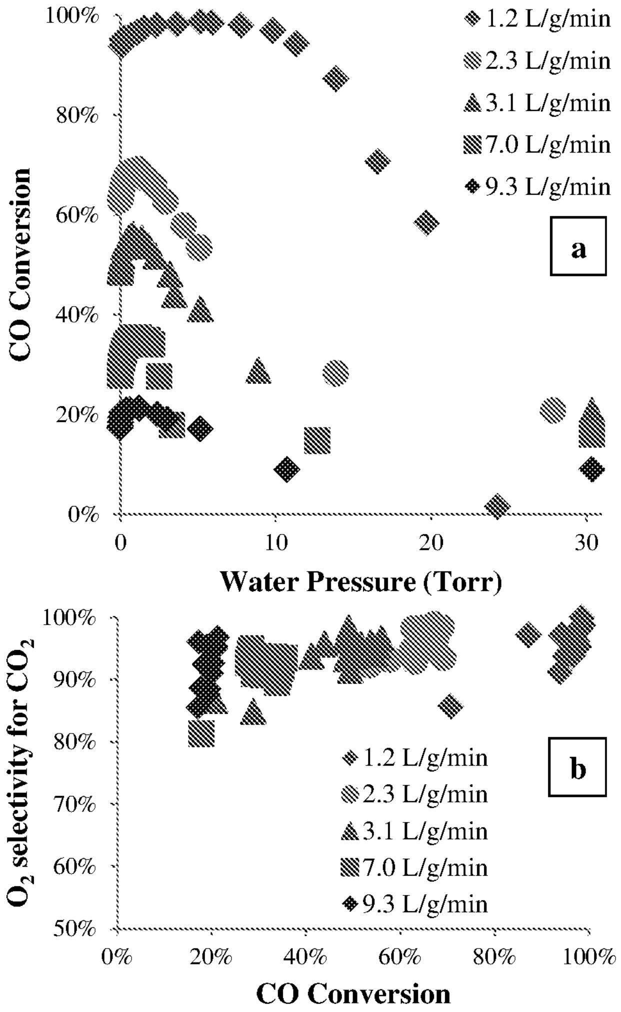
100%
80%
60%
40%
20%
0%
CO Conversion
0
10
20
30
Water Pressure (Torr)
1.2 L/g/min
2.3 L/g/min
3.1 L/g/min
7.0 L/g/min
9.3 L/g/min
a
100%
90%
80%
70%
60%
50%
O_2 selectivity for CO_2
0%
20%
40%
60%
80%
100%
CO Conversion
1.2 L/g/min
2.3 L/g/min
3.1 L/g/min
7.0 L/g/min
9.3 L/g/min
b

FIG. 9

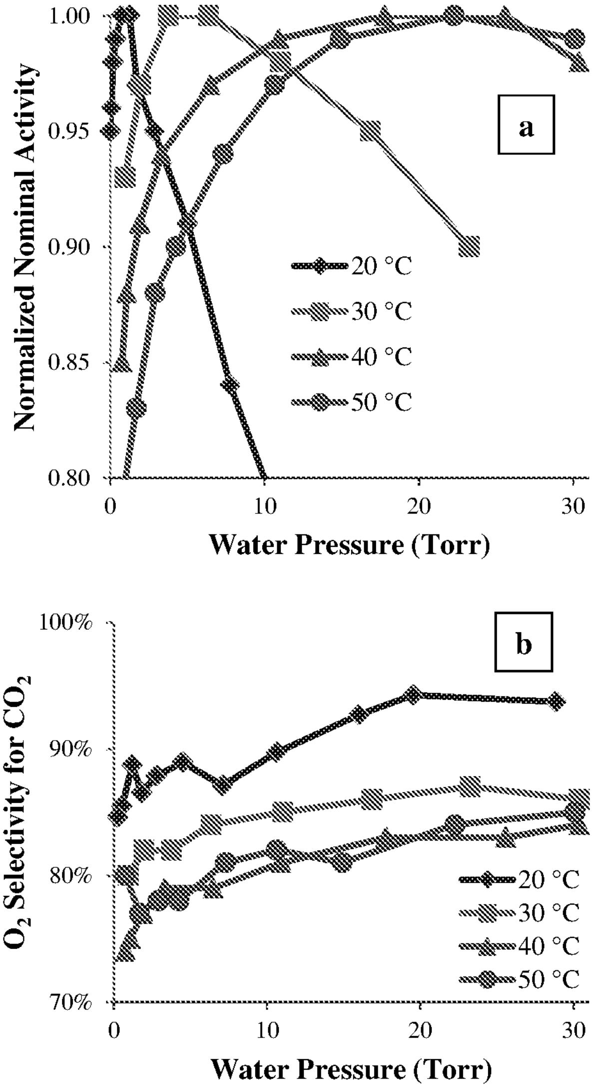
a
Normalized Nominal Activity
1.00
0.95
0.90
0.85
0.80
0
10
20
30
Water Pressure (Torr)
20 °C
30 °C
40 °C
50 °C
b
O_2 Selectivity for CO_2
100%
90%
80%
70%
0
10
20
30
Water Pressure (Torr)
20 °C
30 °C
40 °C
50 °C

FIG. 10

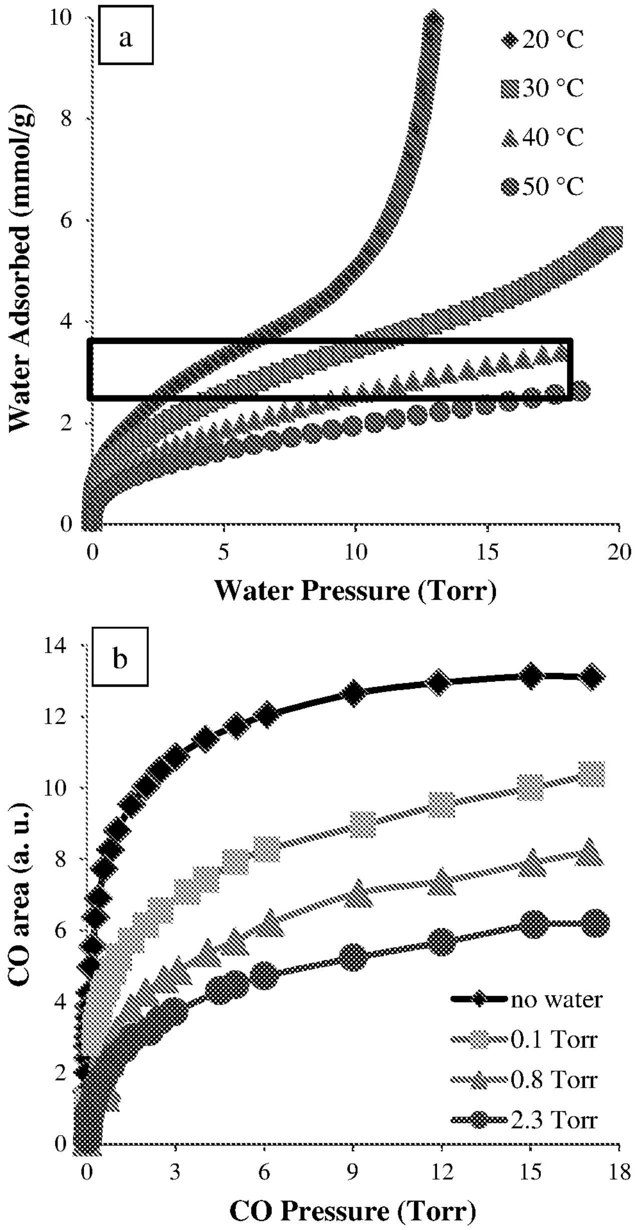
a
Water Adsorbed (mmol/g)
0
2
4
6
8
10
Water Pressure (Torr)
0
5
10
15
20
◆20 °C
▨30 °C
▲40 °C
●50 °C
b
CO area (a. u.)
0
2
4
6
8
10
12
14
CO Pressure (Torr)
0
3
6
9
12
15
18
no water
0.1 Torr
0.8 Torr
2.3 Torr

FIG. 11

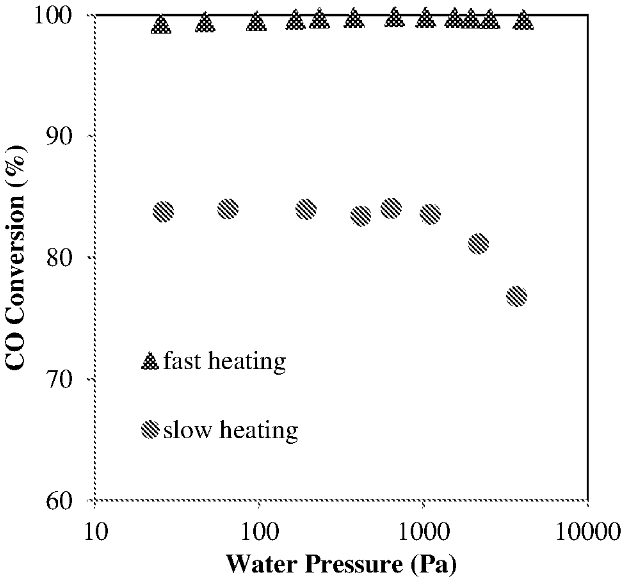
100
90
80
70
60
CO Conversion (%)
10
100
1000
10000
Water Pressure (Pa)
▲ fast heating
● slow heating

FIG. 12

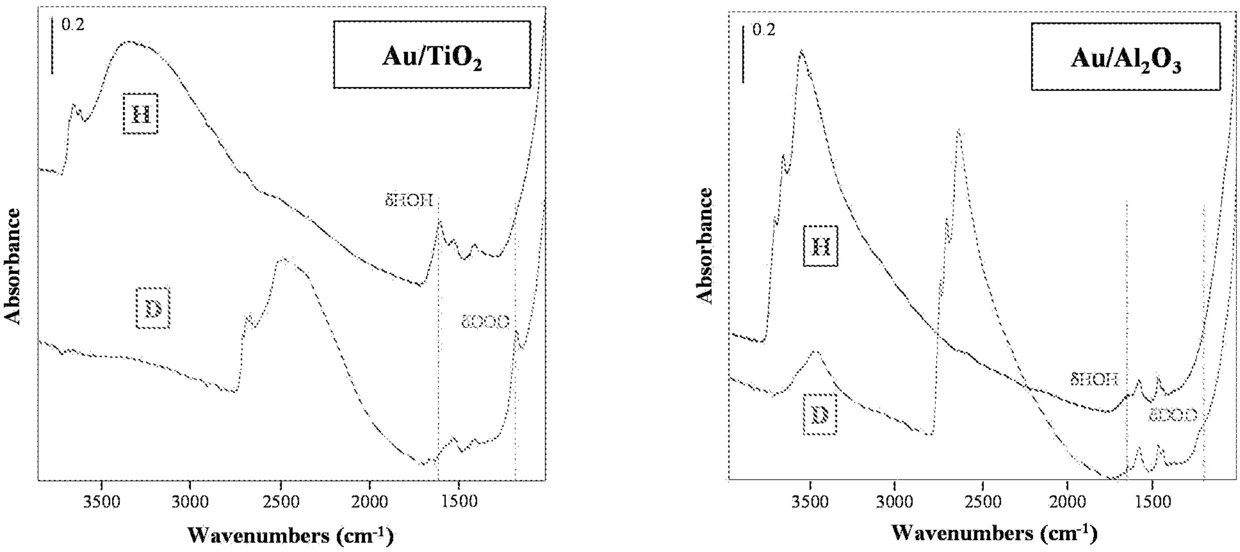
0.2
Au/TiO₂
H
D
δHOH
δDOD
Absorbance
3500
3000
2500
2000
1500
Wavenumbers (cm⁻¹)
0.2
Au/Al₂O₃
H
D
δHOH
δDOD
Absorbance
3500
3000
2500
2000
1500
Wavenumbers (cm⁻¹)

FIG. 13

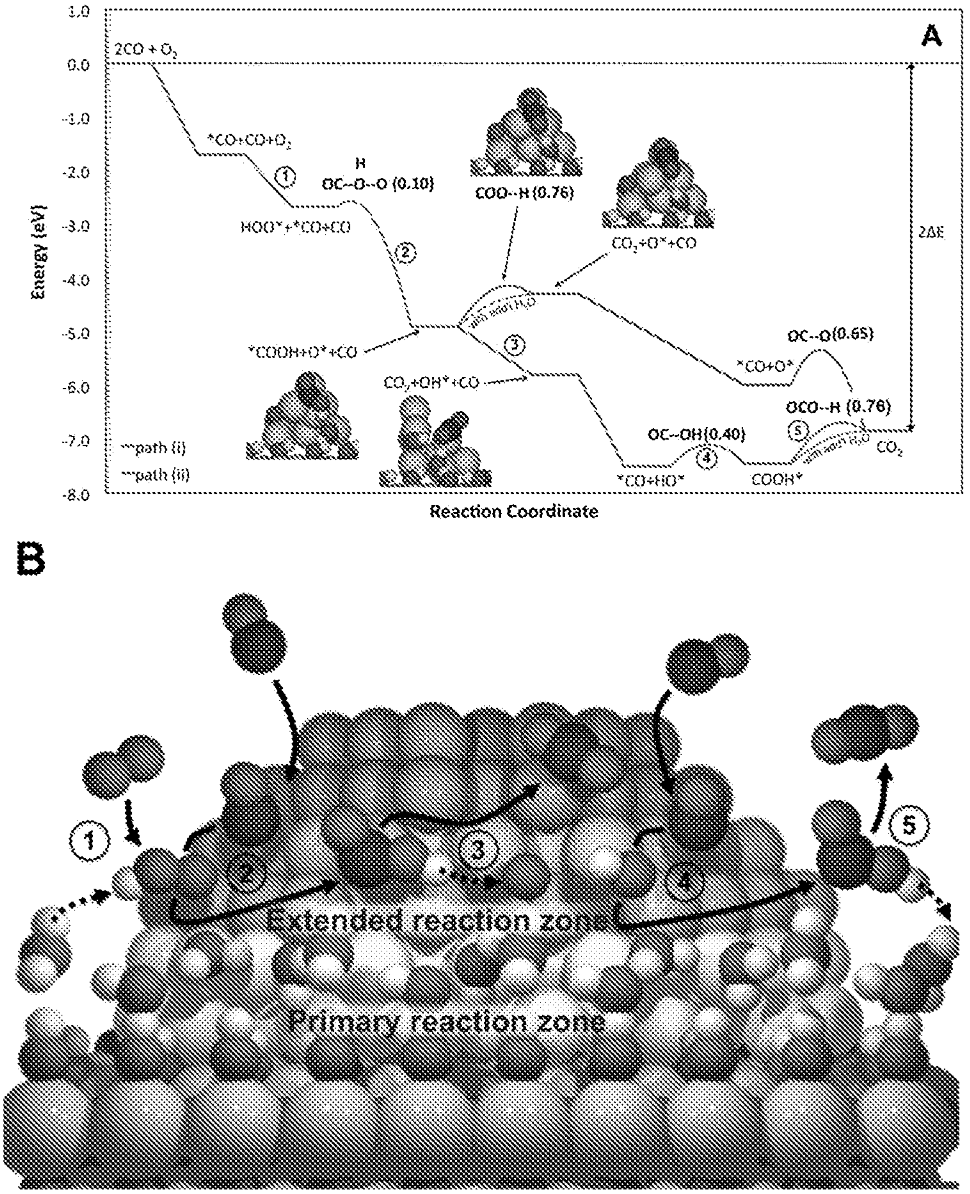
A
1.0
0.0
-1.0
-2.0
-3.0
-4.0
-5.0
-6.0
-7.0
-8.0
Energy (eV)
Reaction Coordinate
2CO + O$_2$
*CO+CO+O$_2$
①
H
OC--O--O (0.10)
HOO*+*CO+CO
②
COO--H (0.76)
CO$_2$+O*+CO
with add'l H$_2$O
COOH+O+CO
③
CO$_2$+OH*+CO
OC--O(0.65)
CO+O
OCO--H (0.76)
OC--OH(0.40)
④
⑤
with add'l H$_2$O
CO$_2$
CO+HO
COOH*
2ΔE
path (i)
path (ii)
B
①
②
③
④
⑤
Extended reaction zone
Primary reaction zone

FIG. 14

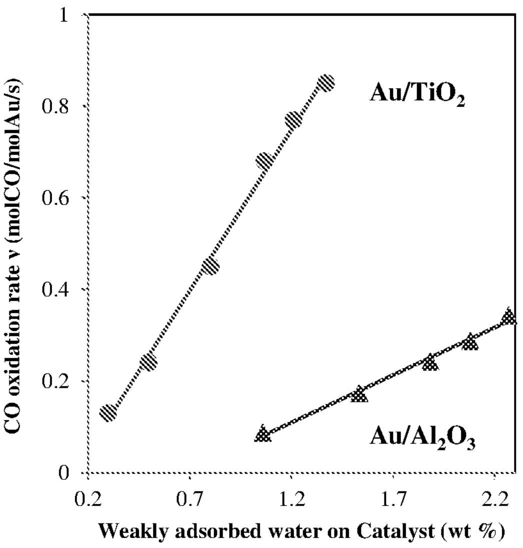
1
0.8
0.6
0.4
0.2
0
CO oxidation rate v (molCO/molAu/s)
0.2
0.7
1.2
1.7
2.2
Weakly adsorbed water on Catalyst (wt %)
Au/TiO$_2$
Au/Al$_2$O$_3$

FIG. 15

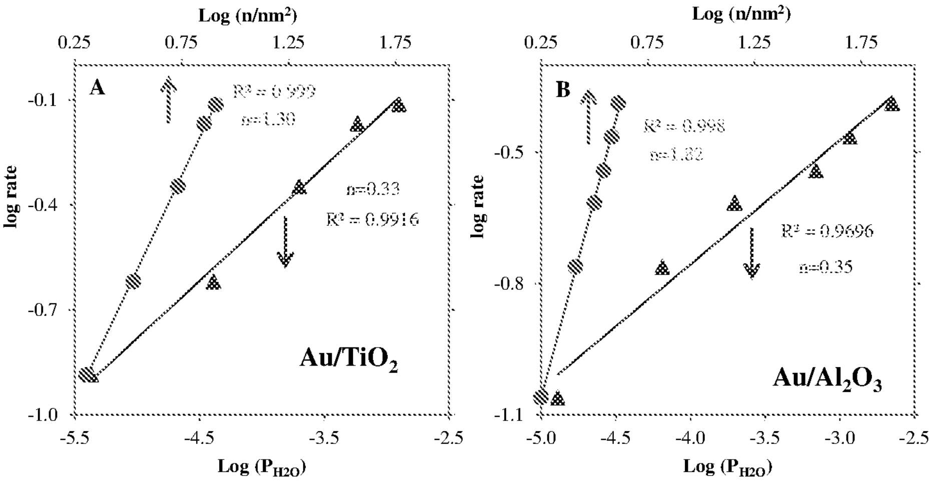
Log (n/nm^2)
0.25
0.75
1.25
1.75
A
R² = 0.999
n=1.30
n=0.33
R² = 0.9916
-0.1
-0.4
-0.7
-1.0
log rate
Au/TiO$_2$
-5.5
-4.5
-3.5
-2.5
Log (P$_{H2O}$)
Log (n/nm^2)
0.25
0.75
1.25
1.75
B
R² = 0.998
n=1.82
R² = 0.9696
n=0.35
-0.5
-0.8
-1.1
log rate
Au/Al$_2$O$_3$
-5.0
-4.5
-4.0
-3.5
-3.0
-2.5
Log (P$_{H2O}$)

FIG. 16

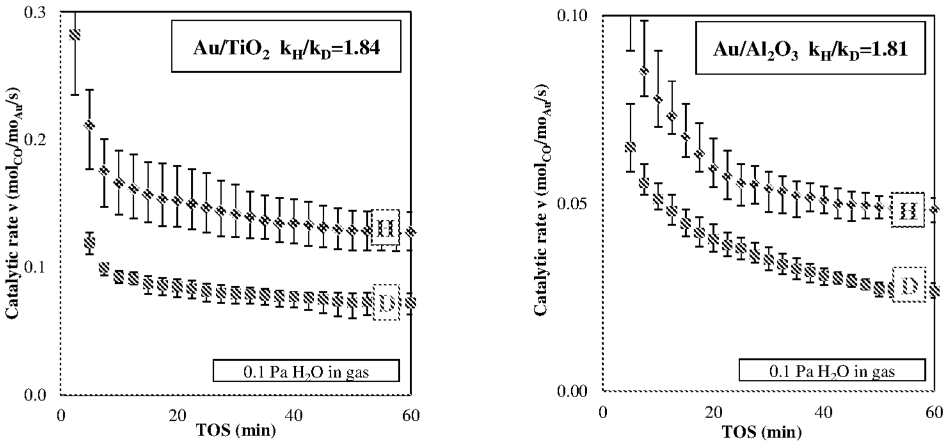
Au/TiO2 kH/kD=1.84
Catalytic rate v (molCO/moAu/s)
0.3
0.2
0.1
0.0
H
D
0.1 Pa H2O in gas
0
20
40
60
TOS (min)
Au/Al2O3 kH/kD=1.81
Catalytic rate v (molCO/moAu/s)
0.10
0.05
0.00
H
D
0.1 Pa H2O in gas
0
20
40
60
TOS (min)

FIG. 17

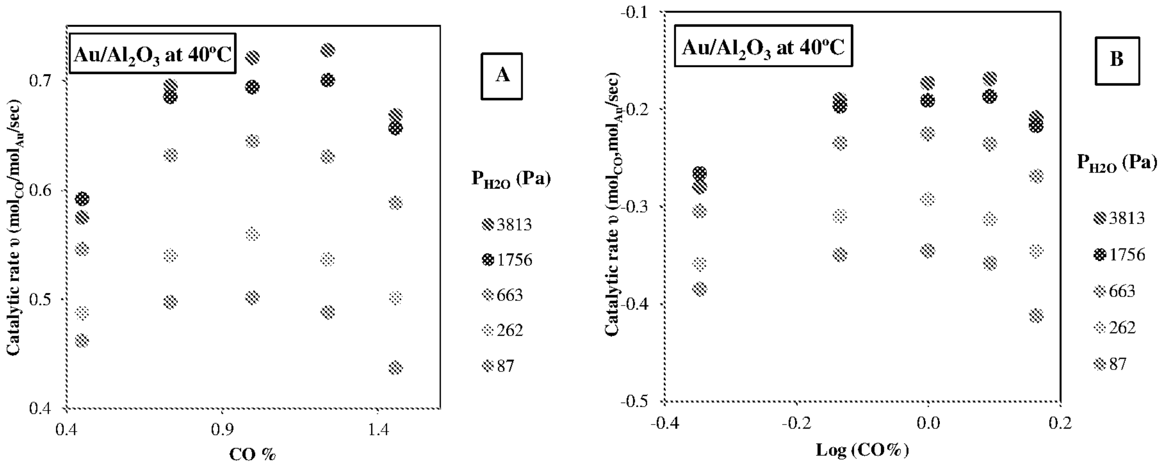
Au/Al2O3 at 40°C
A
Catalytic rate υ (molCO/molAu/sec)
0.7
0.6
0.5
0.4
0.4
0.9
1.4
CO %
PH2O (Pa)
3813
1756
663
262
87
Au/Al2O3 at 40°C
B
Catalytic rate υ (molCO.molAu/sec)
-0.1
-0.2
-0.3
-0.4
-0.5
-0.4
-0.2
0.0
0.2
Log (CO%)
PH2O (Pa)
3813
1756
663
262
87

FIG. 18

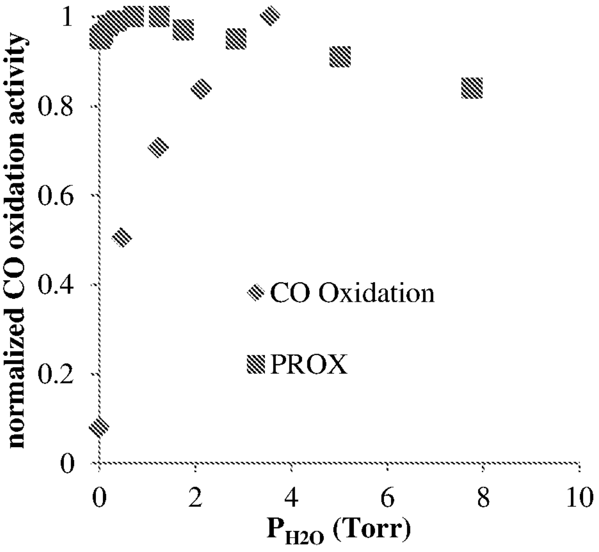
normalized CO oxidation activity
0
0.2
0.4
0.6
0.8
1
0
2
4
6
8
10
P_{H2O} (Torr)
CO Oxidation
PROX

FIG. 19.

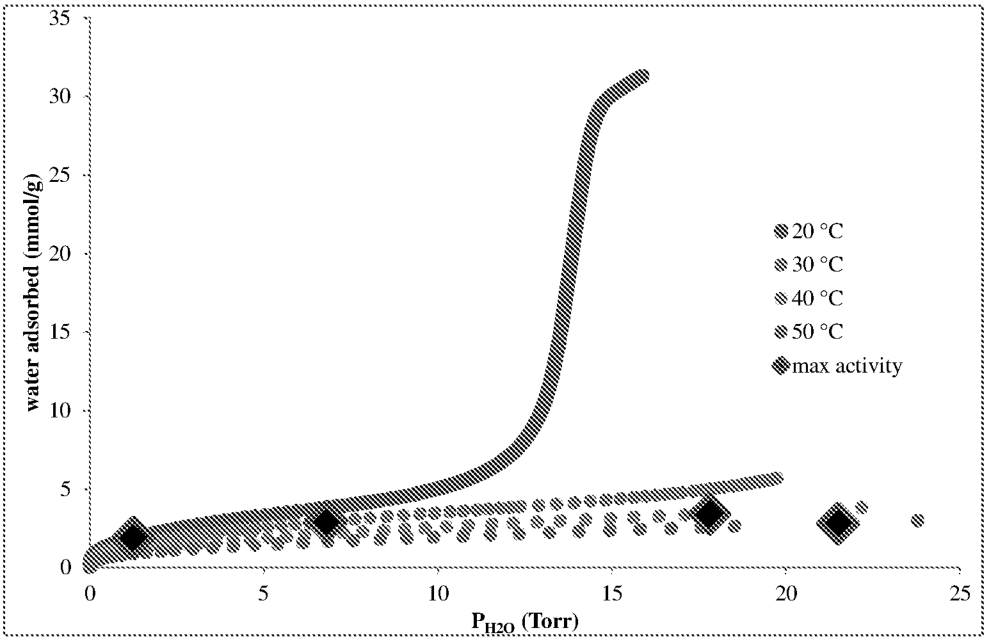
water adsorbed (mmol/g)
0
5
10
15
20
25
30
35
0
5
10
15
20
25
P_{H2O} (Torr)
20 °C
30 °C
40 °C
50 °C
max activity

FIG. 20

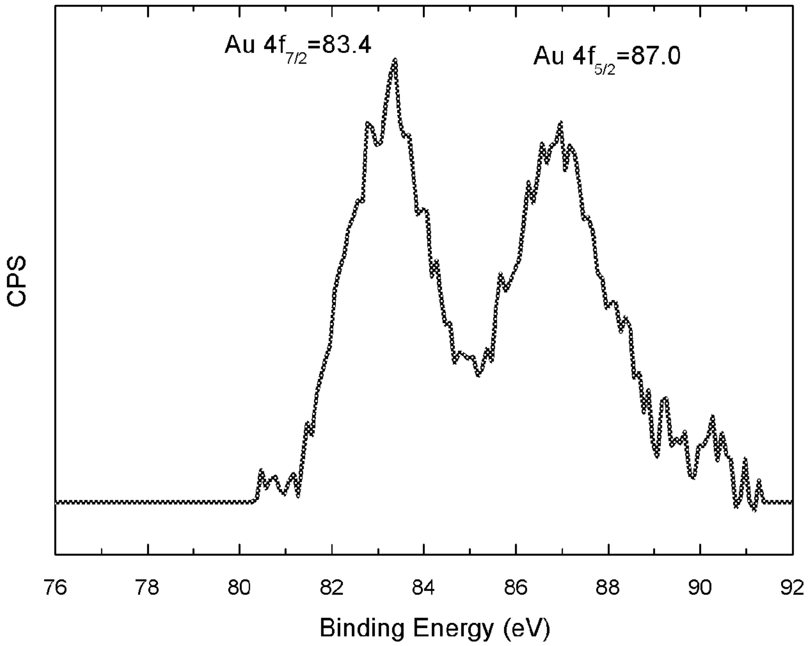
Au $4f_{7/2}$=83.4
Au $4f_{5/2}$=87.0
CPS
76
78
80
82
84
86
88
90
92
Binding Energy (eV)

FIG. 21

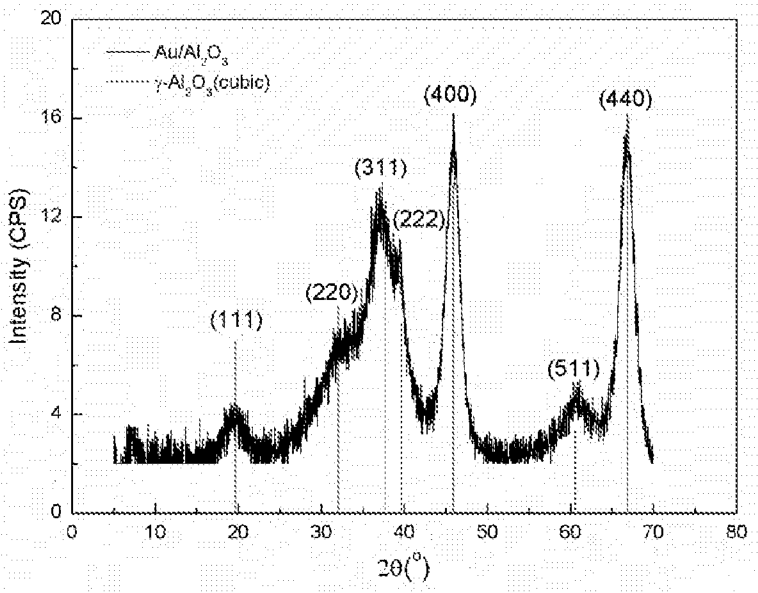
Au/Al_2O_3
γ-Al_2O_3(cubic)
(111)
(220)
(311)
(222)
(400)
(511)
(440)
Intensity (CPS)
0
4
8
12
16
20
0
10
20
30
40
50
60
70
80
2θ(°)

FIG. 22

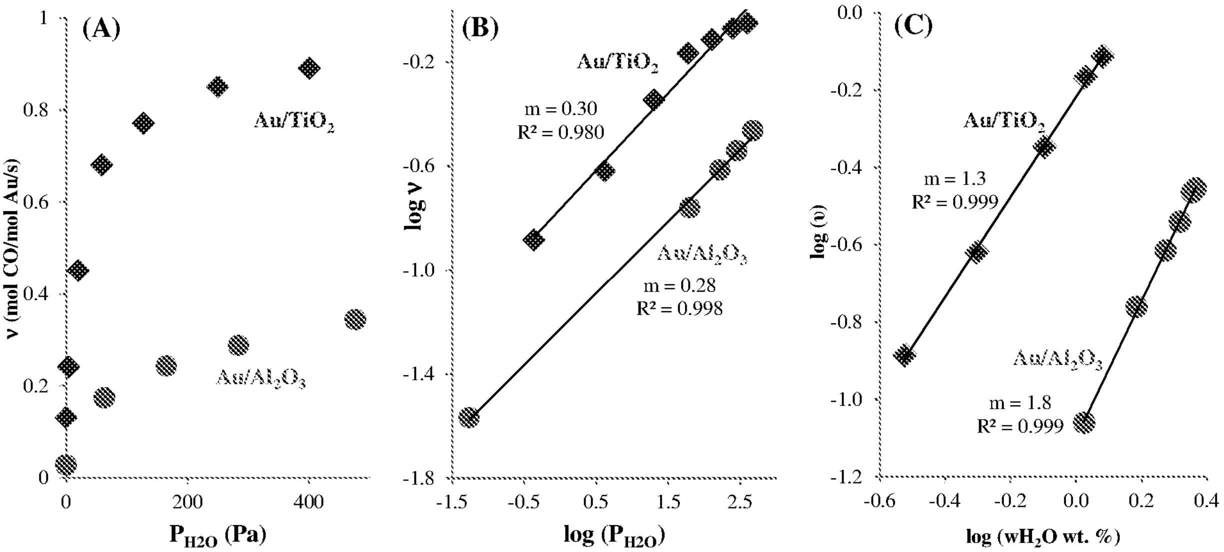
(A)
v (mol CO/mol Au/s)
1
0.8
0.6
0.4
0.2
0
0
200
400
P_{H2O} (Pa)
Au/TiO$_2$
Au/Al$_2$O$_3$
(B)
log v
-0.2
-0.6
-1.0
-1.4
-1.8
-1.5
-0.5
0.5
1.5
2.5
log (P_{H2O})
Au/TiO$_2$
m = 0.30
R² = 0.980
Au/Al$_2$O$_3$
m = 0.28
R² = 0.998
(C)
log (υ)
0.0
-0.2
-0.4
-0.6
-0.8
-1.0
-1.2
-0.6
-0.4
-0.2
0.0
0.2
0.4
log (wH$_2$O wt. %)
Au/TiO$_2$
m = 1.3
R² = 0.999
Au/Al$_2$O$_3$
m = 1.8
R² = 0.999

FIG. 23

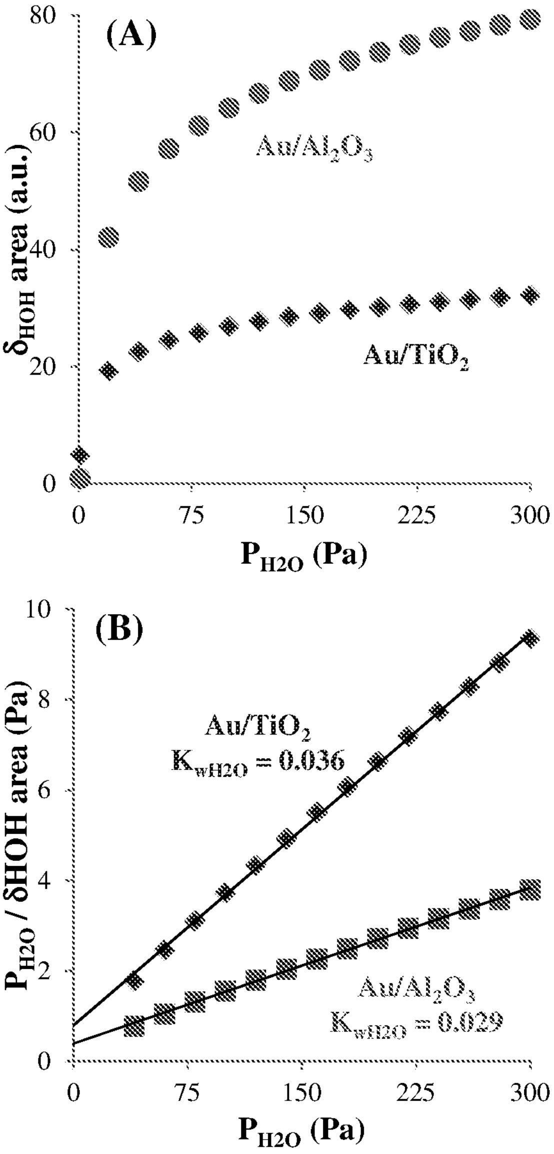
(A)
80
60
40
20
0
δ_{HOH} area (a.u.)
Au/Al$_2$O$_3$
Au/TiO$_2$
0
75
150
225
300
P_{H2O} (Pa)
(B)
10
8
6
4
2
0
P_{H2O} / δHOH area (Pa)
Au/TiO$_2$
K_{wH2O} = 0.036
Au/Al$_2$O$_3$
K_{wH2O} = 0.029
0
75
150
225
300
P_{H2O} (Pa)

FIG. 24

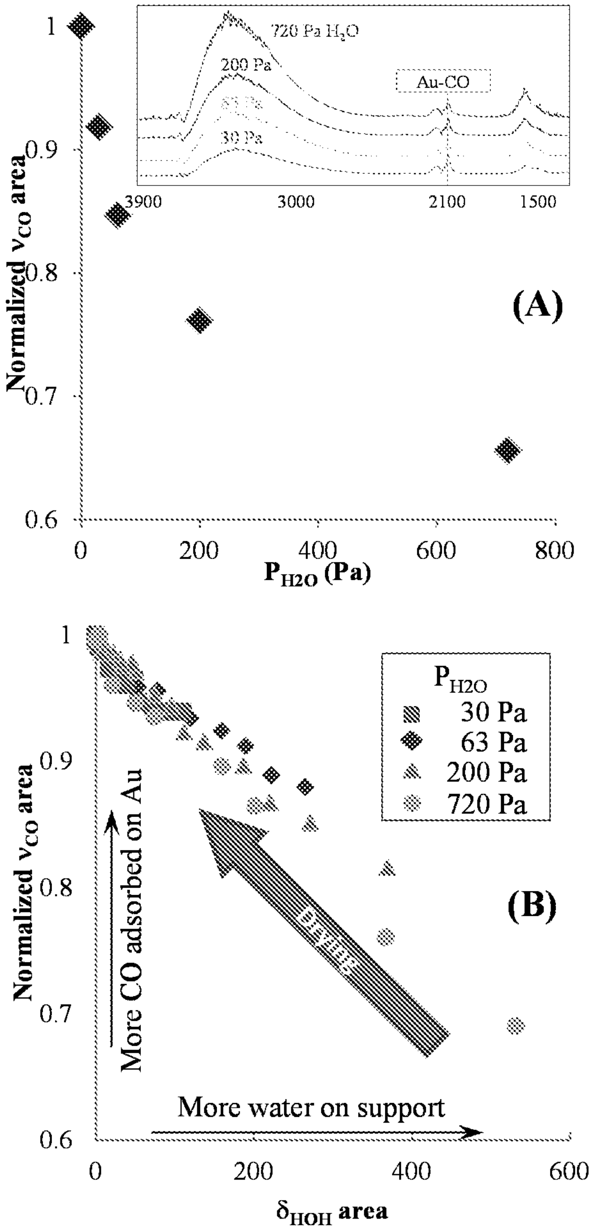
720 Pa H$_2$O
200 Pa
63 Pa
30 Pa
Au-CO
3900
3000
2100
1500
1
0.9
0.8
0.7
0.6
Normalized ν_{CO} area
0
200
400
600
800
P_{H2O} (Pa)
(A)
P_{H2O}
▨ 30 Pa
◆ 63 Pa
▲ 200 Pa
● 720 Pa
More CO adsorbed on Au
Drying
(B)
More water on support
δ_{HOH} area

FIG. 25

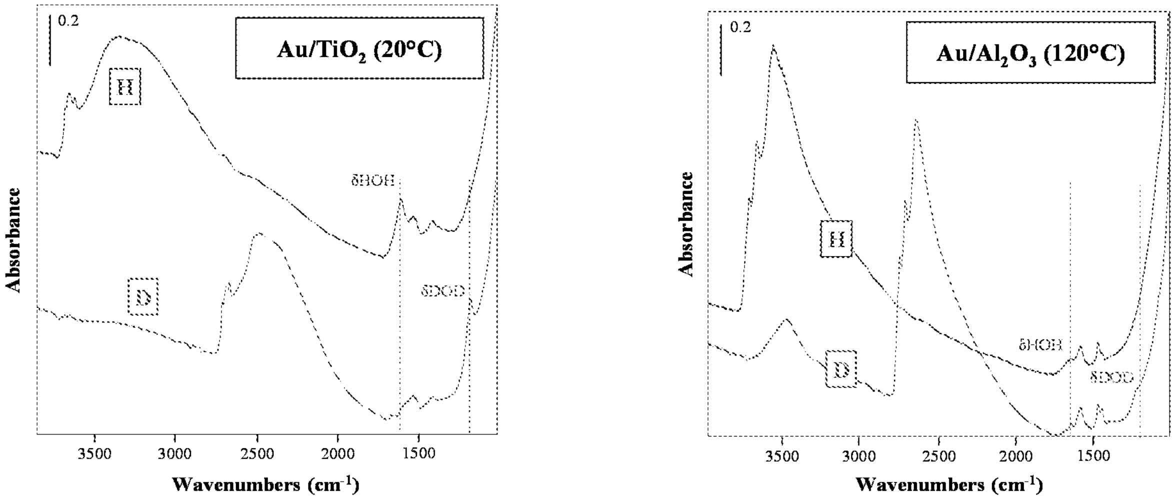
0.2
Au/TiO$_2$ (20°C)
H
D
δHOH
δDOD
Absorbance
3500
3000
2500
2000
1500
Wavenumbers (cm^{-1})
0.2
Au/Al$_2$O$_3$ (120°C)
H
D
δHOH
δDOD
Absorbance
3500
3000
2500
2000
1500
Wavenumbers (cm^{-1})

FIG. 26

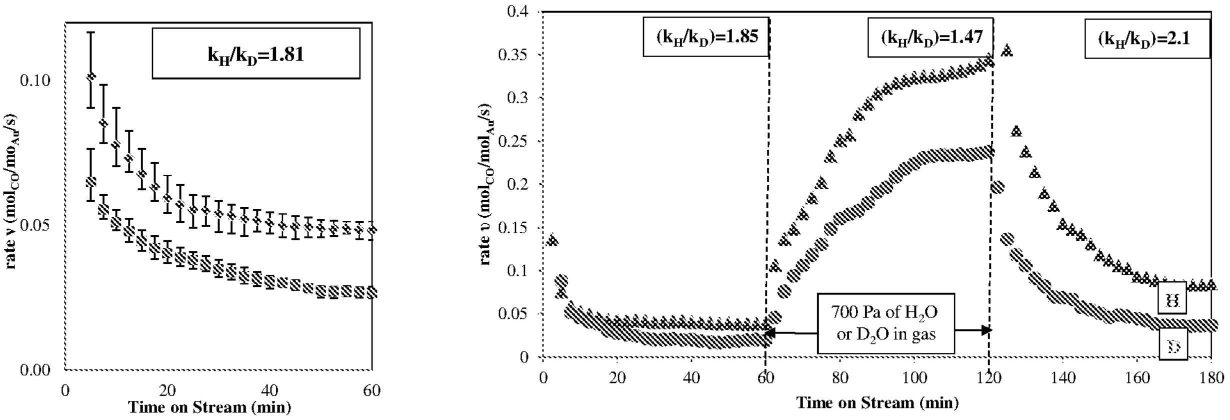
k$_H$/k$_D$=1.81
0.10
0.05
0.00
rate v (mol$_{CO}$/mo$_{Au}$/s)
0
20
40
60
Time on Stream (min)
0.4
0.35
0.3
0.25
0.2
0.15
0.1
0.05
0
rate υ (mol$_{CO}$/mol$_{Au}$/s)
(k$_H$/k$_D$)=1.85
(k$_H$/k$_D$)=1.47
(k$_H$/k$_D$)=2.1
700 Pa of H$_2$O or D$_2$O in gas
H
D
0
20
40
60
80
100
120
140
160
180
Time on Stream (min)

FIG. 27

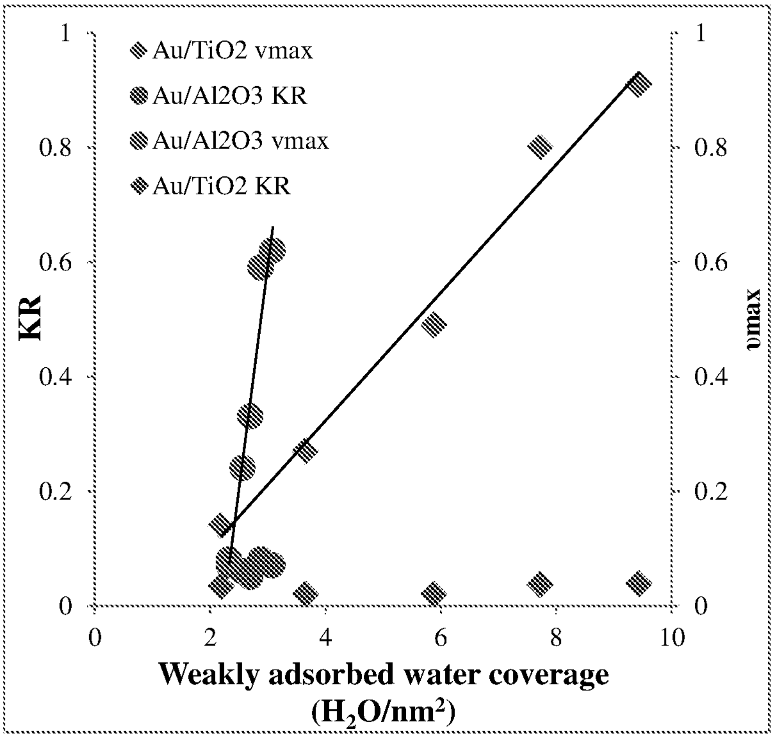
Au/TiO2 vmax
Au/Al2O3 KR
Au/Al2O3 vmax
Au/TiO2 KR
KR
vmax
0
0.2
0.4
0.6
0.8
1
0
2
4
6
8
10
Weakly adsorbed water coverage
(H2O/nm2)

FIG. 28

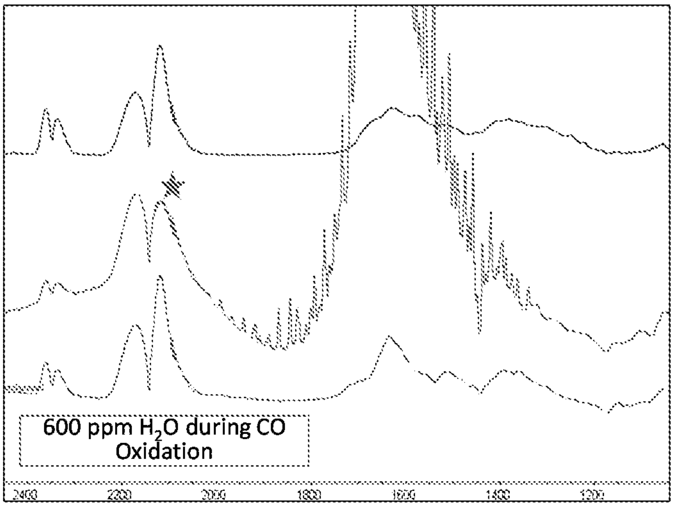
600 ppm H2O during CO Oxidation
2400
2200
2000
1800
1600
1400
1200

FIG. 29

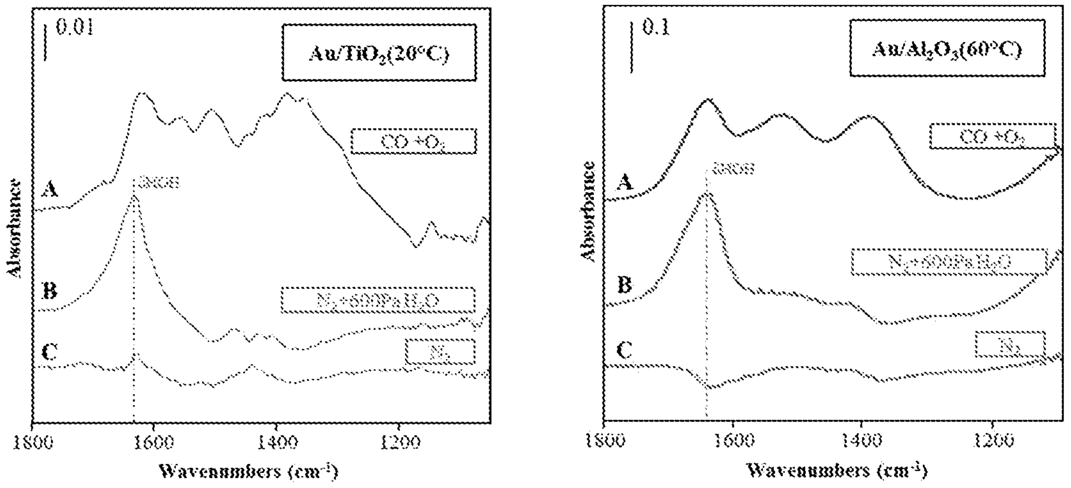

FIG. 30

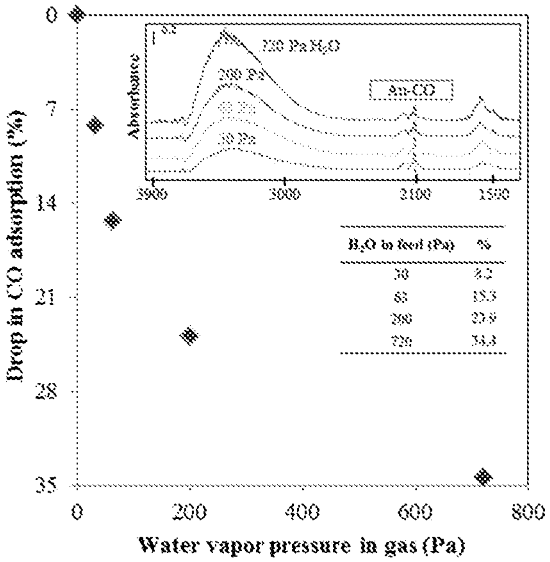

H$_2$O in feed (Pa)	%
30	8.2
63	15.3
200	23.9
720	34.3

FIG. 31

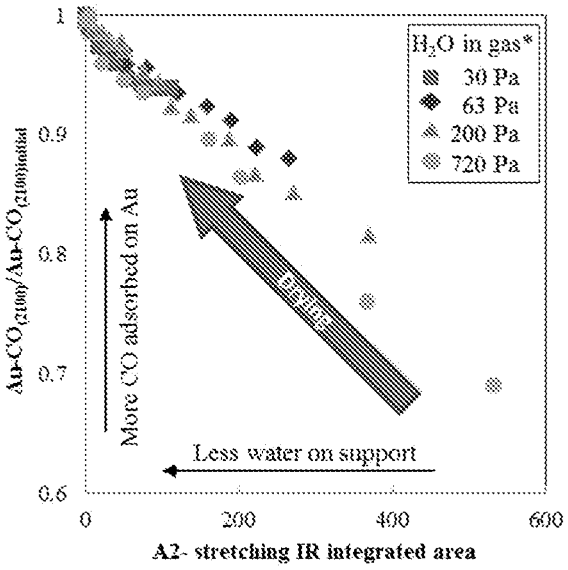
H_2O in gas*
30 Pa
63 Pa
200 Pa
720 Pa
Drying
More CO adsorbed on Au
Less water on support
$Au\text{-}CO_{(2100)}/Au\text{-}CO_{(2100)initial}$
1
0.9
0.8
0.7
0.6
0
200
400
600
A2- stretching IR integrated area

FIG. 32

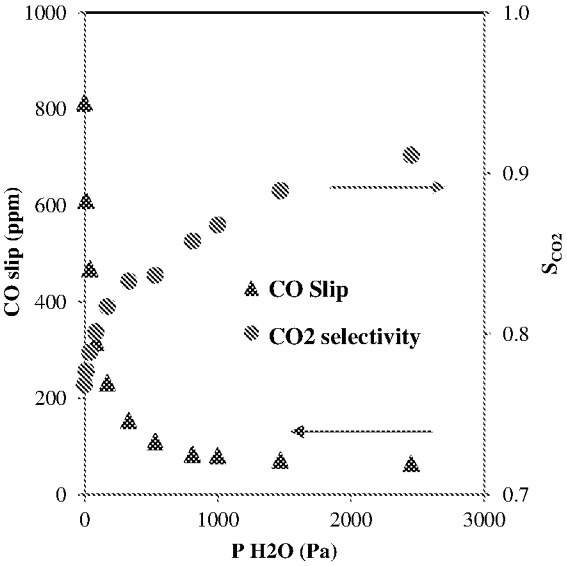
CO Slip
CO2 selectivity
CO slip (ppm)
1000
800
600
400
200
0
1.0
0.9
0.8
0.7
S_{CO2}
0
1000
2000
3000
P H2O (Pa)

FIG. 33

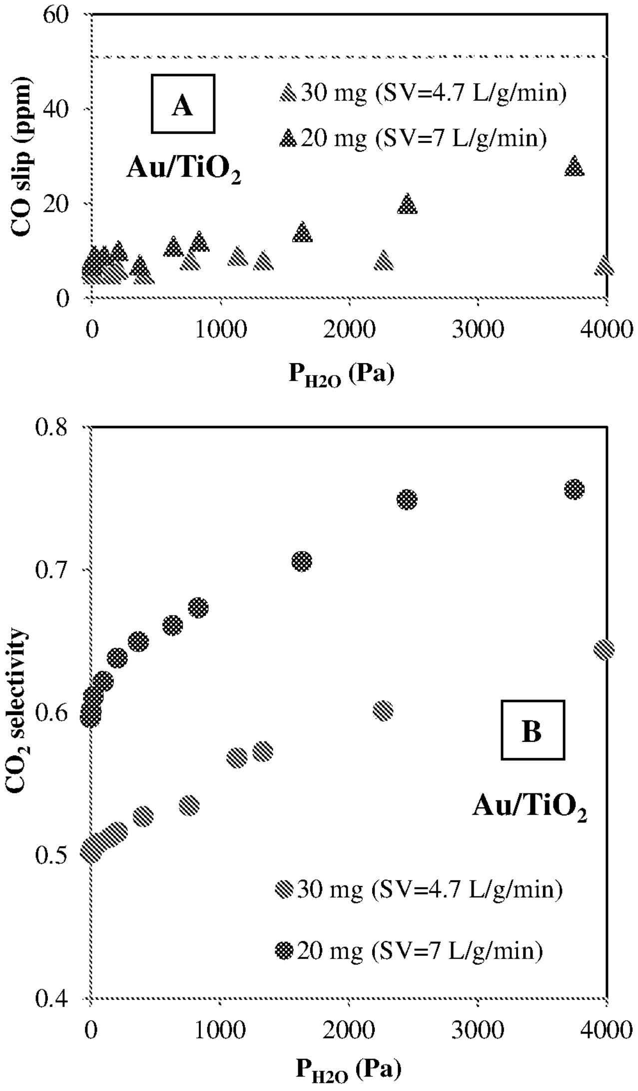
60
40
20
0
CO slip (ppm)
A
Au/TiO$_2$
▲30 mg (SV=4.7 L/g/min)
▲20 mg (SV=7 L/g/min)
0
1000
2000
3000
4000
P_{H2O} (Pa)
0.8
0.7
0.6
0.5
0.4
CO$_2$ selectivity
B
Au/TiO$_2$
●30 mg (SV=4.7 L/g/min)
●20 mg (SV=7 L/g/min)
0
1000
2000
3000
4000
P_{H2O} (Pa)

FIG. 34

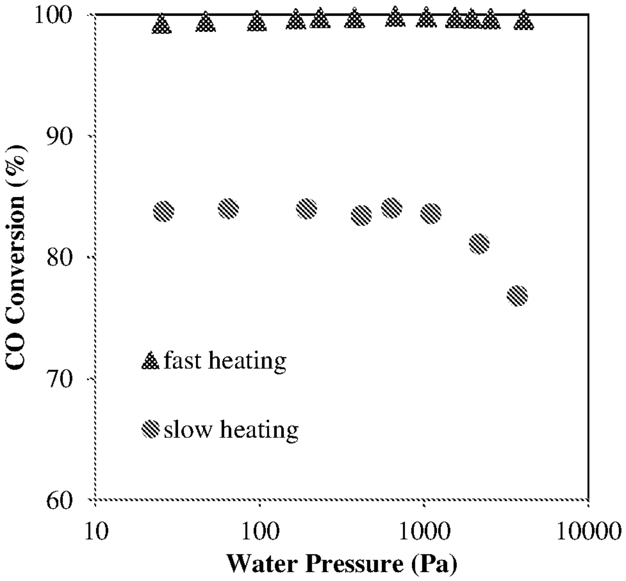
100
90
80
70
60
CO Conversion (%)
fast heating
slow heating
10
100
1000
10000
Water Pressure (Pa)

FIG. 35

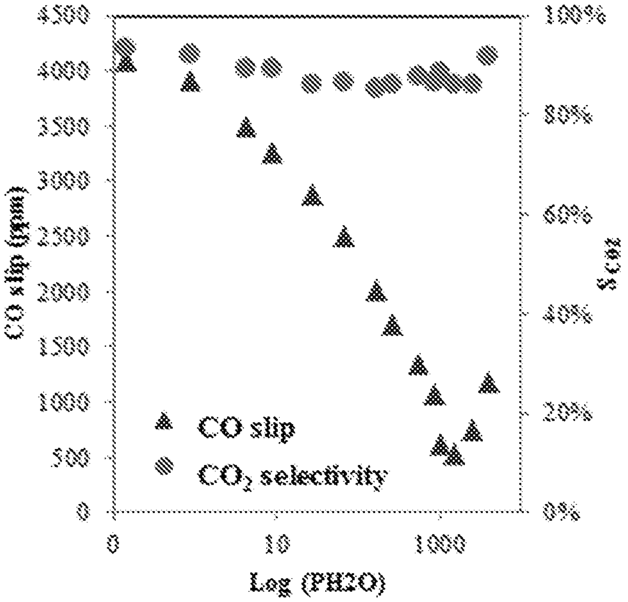
4500
4000
3500
3000
2500
2000
1500
1000
500
0
CO slip (ppm)
100%
80%
60%
40%
20%
0%
S_{CO2}
CO slip
CO_2 selectivity
0
10
1000
Log (PH2O)

FIG. 36

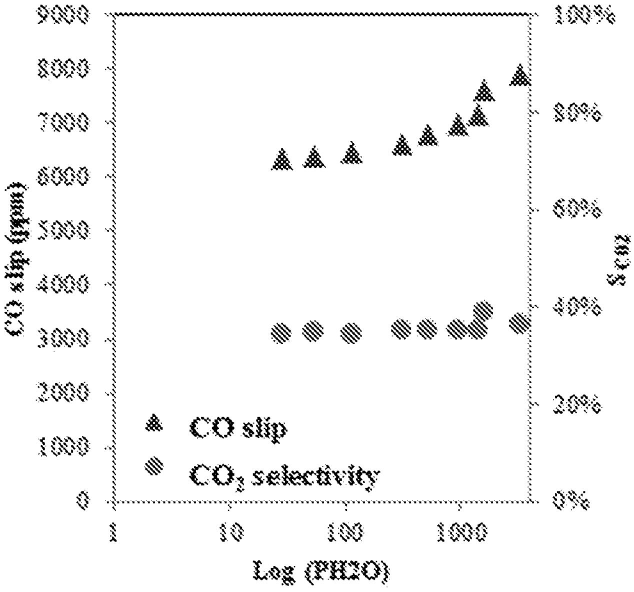
9000
8000
7000
6000
5000
4000
3000
2000
1000
0
CO slip (ppm)
100%
80%
60%
40%
20%
0%
S_{CO2}
1
10
100
1000
Log (PH2O)
CO slip
CO_2 selectivity

FIG. 37

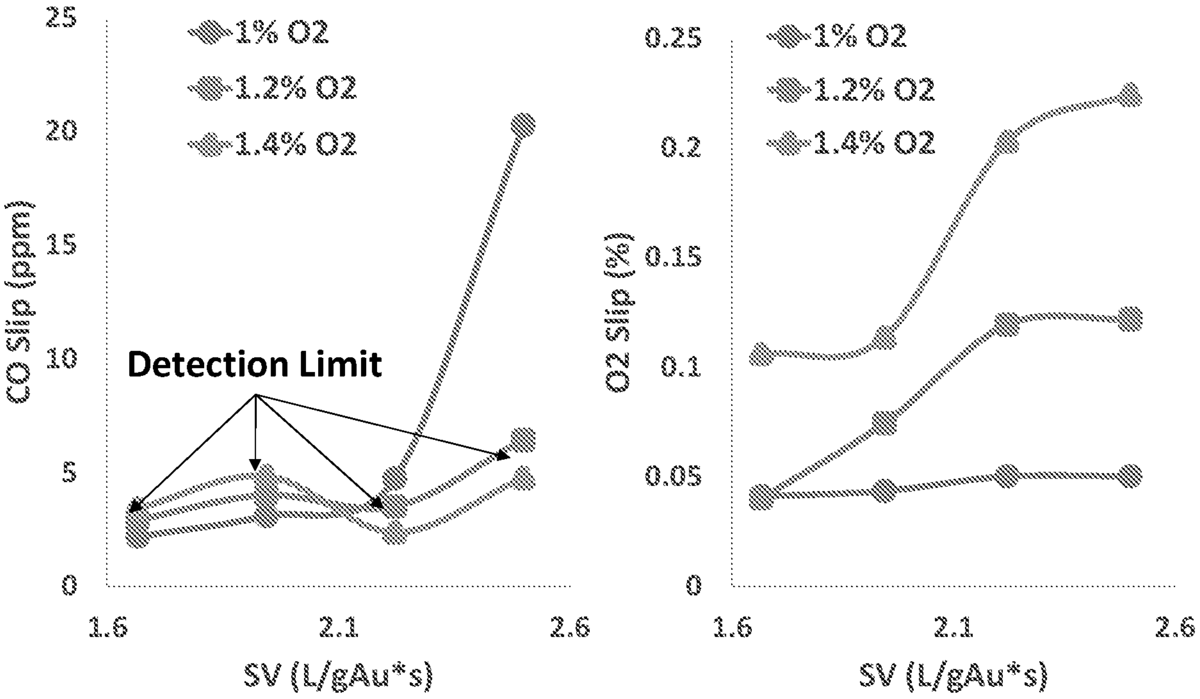
25
20
15
10
5
0
CO Slip (ppm)
1% O2
1.2% O2
1.4% O2
Detection Limit
1.6
2.1
2.6
SV (L/gAu*s)
0.25
0.2
0.15
0.1
0.05
0
O2 Slip (%)
1% O2
1.2% O2
1.4% O2
1.6
2.1
2.6
SV (L/gAu*s)

INTERNATIONAL SEARCH REPORT

International application No.
PCT/US2016/043783

A. CLASSIFICATION OF SUBJECT MATTER

IPC(8) - B01J 23/48; B01J 8/00; B01J 21/02; B01J 23/50; B01J 23/52; B01J 38/04 (2016.01)
CPC - B01J 23/48; B01J 8/00; B01J 21/02; B01J 23/50; B01J 23/52; B01J 38/04 (2016.11)
According to International Patent Classification (IPC) or to both national classification and IPC

B. FIELDS SEARCHED

Minimum documentation searched (classification system followed by classification symbols)
IPC(8) - B01J 8/00; B01J 21/02; B01J 23/48; B01J 23/50; B01J 23/52; B01J 38/04 (2016.01)
CPC - B01J 8/00; B01J 21/02; B01J 23/48; B01J 23/50; B01J 23/52; B01J 38/04 (2016.11)

Documentation searched other than minimum documentation to the extent that such documents are included in the fields searched
USPC - 423/239.1; 423/247; 423/655; 502/34; IPC(8) - B01J 8/00; B01J 21/02; B01J 23/48; B01J 23/50; B01J 23/52; B01J 38/04; CPC - B01J 8/00; B01J 21/02; B01J 23/48; B01J 23/50; B01J 23/52; B01J 38/04 (keyword delimited)

Electronic data base consulted during the international search (name of data base and, where practicable, search terms used)
Orbit, Google Patents, Google Scholar
Search terms used: catalyst, carbon monoxide, preferential oxidation, regeneration

C. DOCUMENTS CONSIDERED TO BE RELEVANT

Category*	Citation of document, with indication, where appropriate, of the relevant passages	Relevant to claim No.
X	SAAVEDRA et al., The critical role of water at the gold-titania interface in catalytic CO oxidation, Science, Vol. 345, Iss. 6204, 26 September 2014, Pgs. 1599-1602	1, 2, 4, 27, 28, 30, 35, 37-42, 45-49, 60
Y		3, 29, 31-33, 36, 43, 44, 50-59
Y	US 2012/0128562 A1 (FLYTZANI-STEPHANOPOULOS et al) 24 May 2012 (24.05.2012) entire document	3, 36, 56-59
Y	US 2004/0258598 A1 (YAO et al) 23 December 2004 (23.12.2004) entire document	29, 31-33
Y	US 2007/0129234 A1 (STOCKWELL) 07 June 2007 (07.06.2007) entire document	43, 44
Y	ZHU et al., In-situ regeneration of Au nanocatalysts by atmospheric-pressure air plasma: Significant contribution of water vapor, Applied Catalysis B: Environmental, Vol. 179, 08 May 2015, Pgs. 69-77	50-55

☐ Further documents are listed in the continuation of Box C. ☐ See patent family annex.

* Special categories of cited documents:
"A" document defining the general state of the art which is not considered to be of particular relevance
"E" earlier application or patent but published on or after the international filing date
"L" document which may throw doubts on priority claim(s) or which is cited to establish the publication date of another citation or other special reason (as specified)
"O" document referring to an oral disclosure, use, exhibition or other means
"P" document published prior to the international filing date but later than the priority date claimed
"T" later document published after the international filing date or priority date and not in conflict with the application but cited to understand the principle or theory underlying the invention
"X" document of particular relevance; the claimed invention cannot be considered novel or cannot be considered to involve an inventive step when the document is taken alone
"Y" document of particular relevance; the claimed invention cannot be considered to involve an inventive step when the document is combined with one or more other such documents, such combination being obvious to a person skilled in the art
"&" document member of the same patent family

Date of the actual completion of the international search
18 November 2016

Date of mailing of the international search report
09 DEC 2016

Name and mailing address of the ISA/US
Mail Stop PCT, Attn: ISA/US, Commissioner for Patents
P.O. Box 1450, Alexandria, VA 22313-1450
Facsimile No. 571-273-8300

Authorized officer
Blaine R. Copenheaver
PCT Helpdesk: 571-272-4300
PCT OSP: 571-272-7774

INTERNATIONAL SEARCH REPORT

International application No.
PCT/US2016/043783

Box No. II **Observations where certain claims were found unsearchable (Continuation of item 2 of first sheet)**

This international search report has not been established in respect of certain claims under Article 17(2)(a) for the following reasons:

1. ☐ Claims Nos.:
because they relate to subject matter not required to be searched by this Authority, namely:

2. ☐ Claims Nos.:
because they relate to parts of the international application that do not comply with the prescribed requirements to such an extent that no meaningful international search can be carried out, specifically:

3. ☒ Claims Nos.: 5-26, 66-105
because they are dependent claims and are not drafted in accordance with the second and third sentences of Rule 6.4(a).

Box No. III **Observations where unity of invention is lacking (Continuation of item 3 of first sheet)**

This International Searching Authority found multiple inventions in this international application, as follows:

See Extra Sheet

1. ☐ As all required additional search fees were timely paid by the applicant, this international search report covers all searchable claims.

2. ☐ As all searchable claims could be searched without effort justifying additional fees, this Authority did not invite payment of additional fees.

3. ☐ As only some of the required additional search fees were timely paid by the applicant, this international search report covers only those claims for which fees were paid, specifically claims Nos.:

4. ☒ No required additional search fees were timely paid by the applicant. Consequently, this international search report is restricted to the invention first mentioned in the claims; it is covered by claims Nos.:
1-4, 27-60

Remark on Protest

☐ The additional search fees were accompanied by the applicant's protest and, where applicable, the payment of a protest fee.

☐ The additional search fees were accompanied by the applicant's protest but the applicable protest fee was not paid within the time limit specified in the invitation.

☐ No protest accompanied the payment of additional search fees.

Continued from Box No. III Observations where unity of invention is lacking

This application contains the following inventions or groups of inventions which are not so linked as to form a single general inventive concept under PCT Rule 13.1. In order for all inventions to be examined, the appropriate additional examination fees need to be paid.

Group I: Claims 1-4 and 27-60 are drawn to a preferential CO oxidation reaction (PROX) catalyst, process of preparing, and a method thereof.

Group II: Claims 61-65 are drawn to a process for oxidizing CO.

Group III: Claims 106-115 are drawn to dual- and single-stage processes for using Au based catalysts or CO oxidation.

Group IV: Claim 116 is drawn to a pretreatment of Au based catalysts.

Group V: Claim 117 is drawn to catalyst regeneration.

The inventions listed in Groups I-V do not relate to a single general inventive concept under PCT Rule 13.1, because under PCT Rule 13.2 they lack the same or corresponding special technical features for the following reasons:

The special technical features of Group I, a preferential CO oxidation reaction (PROX) catalyst, process of preparing, and a method thereof, are not present in Groups II-V; and the special technical features of Group II, a process for oxidizing CO, are not present in Groups I and III-V; and the special technical features of Group III, dual- and single-stage processes for using Au based catalysts or CO oxidation, are not present in Groups I, II, IV and V; and the special technical features of Group IV, a pretreatment of Au based catalysts, are not present in Groups I-III and V; and the special technical features of Group V, catalyst regeneration, are not present in Groups I-IV.

The Groups I-V share the technical features of a preferential CO oxidation reaction (PROX) catalyst, comprising: a plurality of Au or Ag particles having a size ranging from about 0.5 to about 20 nm; a hydrophilic support in contact with the particles; and about 0.1 to about 10 monolayers of water on a surface of the support; and a preferential CO oxidation reaction (PROX) catalyst, prepared by process comprising: removing one or more of an adsorbed carbonate, bicarbonate, carboxylate, organic carbonate, or a mixture of two or more thereof from a surface of a supported catalyst, the supported catalyst comprising a plurality of Au or Ag particles having a size ranging from about 0.5 to about 20 nm and a hydrophilic support in contact with the particles; and simultaneously or thereafter adsorbing about 0.1 to about 10 monolayers of water on a surface of the support. However, these shared technical features do not represent a contribution over the prior art.

Specifically, "The critical role of water at the gold-titania interface in catalytic CO oxidation" to Saavedra et al. teach of a preferential CO oxidation reaction (PROX) catalyst (Saavedra Pg. 1599 Col. 1, Para. 3, We performed an experimental and computational study to better understand how water, surface hydroxyls, and the metal-support interface interact during CO oxidation over Au/TiO2 catalysts), comprising: a plurality of Au or Ag particles having a size ranging from about 0.5 to about 20 nm (Saavedra Pg. 1599, Col. 3, Para. 2, This model substantially simplifies the real system, using a small Au cluster and a single water molecule to represent 3-nm particles); a hydrophilic support in contact with the particles (Saavedra Pg. 1599, Col. 3, Para. 2, We explored potential mechanistic roles of O-H bonds with density functional theory (DFT) studies using a 10-atom gold nanocluster residing on four layers of TiO2(110) support); and about 0.1 to about 10 monolayers of water on a surface of the support (Saavedra Pg. 1560, Col. 2, Para. 1, Tile adsorption isotherm quasi-saturated around 700 Pa (1.7 weight %, 13 molecules/nm2) , corresponding to roughly 1.5 monolayers of water on titania, suggesting a bilayer adsorption structure typical for water); and a preferential CO oxidation reaction (PROX) catalyst (Saavedra Pg. 1599 Col. 1, Para. 3, We performed an experimental and computational study to better understand how water, surface hydroxyls, and the metal-support interface interact during CO oxidation over Au/TiO2 catalysts), prepared by process comprising: removing one or more of an adsorbed carbonate, bicarbonate, carboxylate, organic carbonate, or a mixture of two or more thereof from a surface of a supported catalyst (Saavedra Pg. 1601, Col. 3, Para. 2, Closing the catalytic cycle requires the direct reaction between *OH and *CO (till = 0.10 eV, Ea = 0.4-0 eV, SM 6.4) to yield *COOH, followed by *COOH decomposition, which returns the proton and restores the active site. The second pathway is initiated by an endothermic proton transfer from *COOH to an adsorbed water molecule (simultaneously transferring a proton to the support); Pg. 1601, Col. 3, Para. 3, This step is the likely RDS because it involves a proton transfer (*COOH to water)), the supported catalyst comprising a plurality of Au or Ag particles having a size ranging from about 0.5 to about 20 nm (Saavedra Pg. 1599, Col. 3, Para. 2, This model substantially simplifies the real system, using a small Au cluster and a single water molecule to represent 3-nm particles) and a hydrophilic support in contact with the particles (Saavedra Pg. 1599, Col. 3, Para. 2, We explored potential mechanistic roles of O-H bonds with density functional theory (DFT) studies using a 10-atom gold nanocluster residing on four layers of TiO2(110) support); and simultaneously or thereafter adsorbing about 0.1 to about 10 monolayers of water on a surface of the support (Saavedra Pg. 1560, Col. 2, Para. 1, Tile adsorption isotherm quasi-saturated around 700 Pa (1.7 weight %, 13 molecules/nm2) , corresponding to roughly 1.5 monolayers of water on titania, suggesting a bilayer adsorption structure typical for water; Pg. 1601, Col. 3, Para. 2, Closing the catalytic cycle requires the direct reaction between *OH and *CO (till = 0.10 eV, Ea = 0.4-0 eV, SM 6.4) to yield *COOH, followed by *COOH decomposition, which returns the proton and restores the active site. The second pathway is initiated by an endothermic proton transfer from *COOH to an adsorbed water molecule (simultaneously transferring a proton to the support); Pg. 1601, Col. 3, Para. 3, This step is the likely RDS because it involves a proton transfer (*COOH to water)).

The inventions listed in Groups I-V therefore lack unity under Rule 13 because they do not share a same or corresponding special technical feature.